
[All ETDs from UAB](#)

[UAB Theses & Dissertations](#)

2014

Engineering Fibroblast-Remodeled Electrospun Matrices for Full-Thickness Skin Regeneration

Paul Bonvallet
University of Alabama at Birmingham

Follow this and additional works at: <https://digitalcommons.library.uab.edu/etd-collection>

Recommended Citation

Bonvallet, Paul, "Engineering Fibroblast-Remodeled Electrospun Matrices for Full-Thickness Skin Regeneration" (2014). *All ETDs from UAB*. 1210.
<https://digitalcommons.library.uab.edu/etd-collection/1210>

This content has been accepted for inclusion by an authorized administrator of the UAB Digital Commons, and is provided as a free open access item. All inquiries regarding this item or the UAB Digital Commons should be directed to the [UAB Libraries Office of Scholarly Communication](#).

ENGINEERING FIBROBLAST-REMODELED ELECTROSPUN MATRICES FOR
FULL-THICKNESS SKIN REGENERATION

by

PAUL PIERRE BONVALLET

SUSAN L. BELLIS, ADVISOR
MARCAS M. BAMMAN, COMMITTEE CHAIR
STEVEN J. THOMAS
JOANNE E. MURPHY-ULLRICH
LISA M. SCHWIEBERT

A DISSERTATION

Submitted to the graduate faculty of The University of Alabama at Birmingham,
in partial fulfillment of the requirements for the degree of
Doctor of Philosophy

BIRMINGHAM, ALABAMA

2014

ENGINEERING FIBROBLAST-REMODELED ELECTROSPUN MATRICES FOR FULL-THICKNESS SKIN REGENERATION

PAUL P. BONVALLET

CELLULAR AND MOLECULAR PHYSIOLOGY

ABSTRACT

Skin is often severely damaged, resulting in the need for surgical intervention. There are many limitations to current therapies, therefore a synthetic skin graft would be invaluable for skin regeneration. The focus of the current study is on developing engineered scaffolds with embedded dermal fibroblasts that can be remodeled into native skin tissue upon implantation. To achieve this goal we created electrospun scaffolds composed of collagen I and polycaprolactone (PCL), and then introduced pores to allow fibroblast infiltration. In initial experiments performed to optimize pore size and collagen to PCL concentration, we determined that a 160 μm pore diameter, and 70:30 ratio of collagen to PCL, were ideal parameters based on favorable fibroblast responses and mechanical properties. Fibroblasts grown in these scaffolds exhibited proper morphology, rapid proliferation, and importantly, the cells secreted and filled the pores with native matrix molecules, including collagen I and fibronectin. These molecules are important for scaffold remodeling into human skin. Upon implantation, the scaffolds must support the formation of an epidermal layer: therefore, we evaluated keratinocyte growth on the scaffolds and determined that keratinocytes proliferate and stratify into an epithelial layer upon fibroblast embedded scaffolds. Scaffolds also exhibited a low rate of contraction ($< 19\%$), which is comparable, and possibly less than, the contraction rates of

current clinical graft products. Furthermore, porous scaffolds composed of 70:30 collagen I/PCL have degradation rates in the 3-4 week range, an appropriate time frame for degradation in vivo. Also, when placed in full-thickness rat skin wound defects these porous electrospun scaffolds enhance the skin wound healing effect as seen from H&E stained sections. Porous scaffolds had a significantly higher degree of more normal appearing dermal matrix than scaffolds not containing large induced pores. Additionally, porous electrospun scaffolds pre-seeded with fibroblasts prior to implantation further enhanced skin regenerative properties, with healed tissues resembling normal unwounded skin with a high degree of basket weave matrix, hair follicle development, and blood vessel infiltration. In conclusion, microporous electrospun scaffolds with embedded fibroblasts are promising new substrates for skin regeneration.

Keywords: electrospun scaffolds, skin regeneration, tissue engineering, collagen and PCL matrices, fibroblast embedded skin matrices, pre-seeded scaffolds

ACKNOWLEDGMENTS

First and foremost I would like to acknowledge my family for providing me with a strong foundation and pushing me to be the person I am today. Without their support and guidance, none of this would have been possible. I would also like to acknowledge my Uncle John for first introducing me to a laboratory environment and affording me the opportunity to do research in High School. Thank you for taking me under your wing and opening my eyes to something that I would not have considered otherwise. I would also like to thank my lab mates for creating a great environment to perform research. You recognized that hard work and collaboration was important for excelling in our respective fields, but also ensured that we enjoyed ourselves along the way. I would also like to thank my committee for taking time out of their busy schedules in order to provide guidance and insight into my project, allow me to shadow in the operating room, and ensuring that I develop as a research scientist. I would also like to thank all of the friends that I have made along the way. Each and every one of you have truly made graduate school an experience that will never be forgotten.

Finally, I would like to thank my advisor Dr. Susan Bellis. Dr. Bellis is the reason I came to UAB. She has been such a great role model, showing us that hard work and perseverance has its rewards. She is truly one of the greatest minds in her respective research fields. I have developed as a well-rounded scientist as a result of her mentoring. Her graduate students' best interest is always a priority and I can't express how fortunate we are to have such an amazing mentor. Thank you for all that you have done throughout this journey.

TABLE OF CONTENTS

	Page
ABSTRACT.....	ii
ACKNOWLEDGMENTS	iv
LIST OF TABLES	vii
LIST OF FIGURES	viii
INTRODUCTION	1
Human Integumentary System.....	1
Cells of the Epidermis.....	3
Keratinocytes	3
Melanocytes	4
Merkel Cells.....	4
Langerhans Cells.....	5
Cells of the Dermis	5
Fibroblasts.....	5
Mesenchymal Stem Cells.....	6
Macrophages	6
Extracellular Matrix in the Skin.....	7
Collagen	7
Fibronectin	8
Elastin	8
Vitronectin	8
Laminins	9
Hyaluronan.....	9
Dermal and Epidermal Signaling.....	9
Wound Healing	10
Hemostasis and Inflammation Phase	11
Proliferation Phase	12
Remodeling Phase.....	12
Current Skin Graft Therapies.....	12
Limitations of Commercially Available Skin Substitutes	15
Engineered Skin Biomaterials.....	16
Hydrogels.....	17
Emulsion Freeze-Drying.....	18
3D Printing.....	18
Electrospinning	18
Enhanced Wound Healing Benefit of Scaffolds Pre-Seeded with Cells.....	21
Strategies for Improving Electrospun Skin Scaffolds.....	22
Incorporation of Cell Ligands	22

Increasing Porosity.....	22
Research Objectives.....	23
MICROPOROUS DERMAL-LIKE ELECTROSPUN SCAFFOLDS PROMOTE ACCELERATED SKIN REGENERATION	29
MICROPOROUS DERMAL-MIMETIC ELECTROSPUN SCAFFOLDS PRE-SEEDED WITH FIBROBLASTS PROMOTE TISSUE REGENERATION IN FULL- THICKNESS SKIN WOUNDS.....	69
CONCLUSIONS	93
GENERAL LIST OF REFERENCES	106
APPENDIX A: IACUC Approval	114

LIST OF TABLES

Tables		Page
INTRODUCTION		
1	Cells of the Epidermis.....	25
2	Cells of the Dermis	26
MICROPOROUS DERMAL-LIKE ELECTROSPUN SCAFFOLDS PROMOTE ACCELERATED SKIN REGENERATION		
1	Tensile testing of porous and non-porous scaffolds	67
3	Number of newly formed hair follicles.....	68

LIST OF FIGURES

Figures	Page
INTRODUCTION	
1 Electrospinning Apparatus.....	27
2 Fibroblasts do not Migrate Through Normal Electrospun Scaffolds.....	28
MICROPOROUS DERMAL-LIKE ELECTROSPUN SCAFFOLDS PROMOTE ACCELERATED SKIN REGENERATION	
1 Fibroblast growth and proliferation on electrospun scaffolds composed of varying ratios of collagen I and PCL	56
2 Fibroblast viability on 70:30 col/PCL scaffolds	57
3 Infiltrating fibroblasts fill 160 μ m, but not 250 μ m, pores with matrix	58
4 Extracellular matrix is deposited into the pores of 70:30 col/PCL scaffolds, but not 50:50 col/PCL scaffolds.....	59
5 Contraction of 70:30 col/PCL scaffolds with or without 160 μ m pores and fibroblasts.....	60
6 Keratinocytes proliferate and form a stratified epidermal layer on the surface of fibroblast-remodeled scaffolds.....	61
7 70:30 col/PCL scaffolds degrade more rapidly than 50:50 col/PCL scaffolds.....	62
8 More rapid wound closure is observed for critical size defects implanted with porous scaffolds	63
9 Scaffolds with micropores promote more effective tissue regeneration.....	64
10 4x images of wound healing at 7, 14 and 21 days following implantation	65
11 20x images of wound healing over a 21 day time period show the structure of the matrix	66

MICROPOROUS DERMAL-MIMETIC ELECTROSPUN SCAFFOLDS PRE-SEEDED WITH FIBROBLASTS PROMOTE TISSUE REGENERATION IN FULL- THICKNESS SKIN WOUNDS

1	Fibroblast viability on 70:30 col/PCL scaffolds	86
2	Contraction of porous 70:30 col/PCL scaffolds containing seeded fibroblasts.....	87
3	Extracellular matrix is deposited into the 160 μ m pores of 70:30 col/PCL scaffolds	88
4	Collagen and fibronectin are deposited into 160 μ m pores within scaffolds.....	89
5	Pre-seeded scaffolds promote more effective tissue regeneration	90
6	Scaffolds pre-seeded with fibroblasts promote formation of ECM with a high degree of basket-weave structure, resembling unwounded skin tissue	91
7	Images (10X) of wound healing over a 21-day time period show the structure of the matrix in each treatment group	92

CONCLUSION

1	Electrospinning and Electrospraying	104
2	Mechanical Press for Creating Large Pores.....	105

INTRODUCTION

Human Integumentary System

The human integumentary system is a complex system that comprises skin tissue as well as its subsidiaries; hair, nails, nerve endings, and glands. Skin tissue is the largest organ of the body, making up approximately 12-15% of the total body weight. It is a complex tissue because it serves numerous functions including physical protection, storage center for water and lipids, temperature regulation, touch and pain sensation, and insulation. There are many features which make skin tissue a unique organ, but consequently make it challenging to engineer a scaffold that will stimulate ideal regeneration.

Skin tissue is composed of 2 layers, the dermis and epidermis. The epidermis is the outermost layer that is primarily composed of keratinocytes, melanocytes, Merkel cells, and Langerhans cells. It acts as the first line of defense against trauma and a barrier against invading organisms. The keratinocytes are stratified, meaning there are separate layers of keratinocytes with varying function. Each layer serves a different function and represents the polarity of the epidermis. The basal layer, or bottom layer adhered to the basement membrane, is composed of proliferating cells. The basal layer gives rise to the outer layers of keratinocytes. As keratinocytes age, they delaminate, forming layers of various differentiated keratinocytes. The layers include the stratum spinosum, stratum granulosum, stratum lucidum, and stratum corneum. In the stratum spinosum, the

keratinocytes become connected through desmosomes, which form a contact between adjacent cells. Also in this layer, the keratinocytes exit the cell cycle and lose their nuclei. In the stratum granulosum, keratinocytes develop tight junctions which regulate the passage of ions, cells, and molecules from one cell to the next and also allow for the communication from one cell to the next [1]. The tight junctions serve as a barrier function to prevent the loss of water as demonstrated by Kirschner et al where they describe a claudin-1, tight junction specific protein, knockdown results in lethal water loss [2]. The stratum lucidum is a thin layer of dead keratinocytes that is only present in thicker skin such as on the palms of the hands and on the soles of feet. At the outermost surface of skin is where the stratum corneum resides. The stratum corneum contains 10 to 30 layers of terminally differentiated keratinocytes which are constantly being shed. These epidermal layers interact with an integrated network of cellular junctions and cytoskeletal elements in order to regulate cell signaling, polarization and form a physical barrier from the external environment [3].

Between the dermis and epidermis is a thin connecting layer, termed the basement membrane. It is connected to the dermis through anchoring fibrils. The basement membrane is rich in collagens type IV and VII as well as perlecan, nidogen, and laminins which are synthesized by fibroblasts and keratinocytes. The function of the basement membranes is to provide a barrier between the dermis and epidermis and provide a structure in which keratinocytes can adhere and proliferate [4].

Underlying the epidermis is the dermis which is comprised of an abundance of extracellular matrix (ECM) proteins, cells such as fibroblasts, and various growth factors. All of these components interact in an ongoing mutually beneficial manner in order to

regenerate tissue as well as maintain a normal functioning dermis. This ongoing interaction is termed dynamic reciprocity [5-7]. There are also many other structures that are present in the dermis such as blood vessels, lymph vessels, glands, hair follicles, and nerve endings. The dermis can be subdivided into 2 main layers; the papillary and reticular dermis. The papillary dermis is directly beneath the basement membrane and is connected to the epidermis through the fingerlike projections of the stratum basale. The papillary dermis contains loose woven bundles of ECM fibrils. The papillary layer provides nutrients to the epidermis and has an extensive blood vessel system that can control temperature. The reticular dermis is the innermost layer and is denser than the papillary dermis. This layer contains thick collagen fibers which give strength to the skin.

Beneath the skin there is one more layer that provides support for the skin tissue, but is not considered part of the skin. This layer is known as the hypodermis. It is attached to the dermis by elastin and collagen fibers. The hypodermis is primarily composed of fat cells which serve to act as an insulating layer, conserving heat in the body as well as serving as an energy source. It also provides an extra layer of protection against physical trauma and contains many blood vessels, nerves, and lymph vessels.

Cells of the Epidermis

Keratinocytes

Keratinocytes compose a majority of the epidermis. They synthesize various forms of keratin, the most abundant protein of the epidermis. The different layers of the epidermis can be defined in terms of their keratin composition. Each layer has a different

stage of keratin present within. Typically the basal keratinocytes express keratins K5 and K14 while the more differentiated keratinocytes express K1 and K10 [8].

The epidermis is known to be self-renewing because of its constant generation of new keratinocytes simultaneously with the shedding of the most apical keratinocytes. This process creates polarized layers throughout the epidermis. Keratinocytes initially proliferate at the basal layer, giving rise to the terminally differentiated suprabasal cells. These suprabasal cells transition to the surface of the skin and undergo many transcriptional stages. The keratinocytes also flatten and elongate as they transition to the apical surface [9].

Melanocytes

Melanocytes are the cells that cause pigmentation in skin by the production of melanin, also known as melanogenesis. This process typically occurs in the basal layer of the epithelium. Melanocytes contain tyrosinase, a crucial enzyme for melanin synthesis. Melanocytes arise from melanoblasts which are unpigmented and lack functional tyrosinase. Fully differentiated melanocytes also contain tyrosinase related proteins 1 and 2 which also assist in the production of melanin [10]. Different forms of melanin exist. The different forms, in combination with various concentrations of melanin, give rise to skin tones [11].

Merkel cells

Merkel cells are receptor cells contained in the stratum basale which have a role in the sensation of light touch. This light touch sensation is important for tactile discrimination between objects, shapes, and textures. Merkel cells are found in complex with neuritis, which leads to the physical sensation [12, 13].

Langerhans cells

Langerhans cells are typically found in the stratum spinosum and are the antigen-presenting immune dendritic cells of skin tissue. They are the immune system's first line of defense against invading pathogens, microbes, and other foreign organisms. These cells present invading antigens to lymph nodes where native T cells can activate the cutaneous immune system [14]. They express langerin, a lectin receptor that has a role in the uptake of several pathogens. They are potent inducers of the T cell response to foreign invasions [15].

Cells of the epidermis can be found in Table 1.

Cells of the Dermis

Fibroblasts

Fibroblasts are the most predominant cell type present in dermal tissue. They play a large role in the secretion of extracellular matrix proteins, growth factors, cytokines, and matrix metalloproteinases. Combinations of these factors all affect the wound healing response [16]. The fibroblasts control the remodeling process from the initial stages of wound healing to the final, fully regenerated dermal tissue. Initially, they secrete proteases to break down the fibronectin rich environment which is responsible for closing the wound and acting as a provisional matrix for the recruitment of cells and growth factors. Over time, the fibroblasts secrete other proteins such as collagens, hyaluronan, and elastin as the wound healing progresses [17].

Fibroblasts can differentiate into myofibroblasts, which express α -actin filaments. These filaments allow the myofibroblasts to pull on the extracellular matrix that the cells are adhered to, resulting in contraction of the wound area. The myofibroblasts become bipolar allowing them to orient along a line of tension. This contraction of myofibroblasts is thought to result in the overall contraction of the wound bed ultimately causing the wound to close, but if excess contraction occurs, scar formation and sub-optimal wound healing may result [18, 19].

Mesenchymal Stem Cells

Mesenchymal stem cells (MSCs) are multipotent progenitor cells that have a potent role in the wound healing process. They secrete growth factors which are responsible for many aspects of wound healing and regeneration. These growth factors can recruit cells such as fibroblasts and regulate their secretion of ECM and fibroblast growth factors [20, 21]. MSCs have been shown to have an advantageous effect on the aesthetic and functional results of skin tissue in a pig burn model [22].

Macrophages

In normal skin tissue, levels of macrophages are low. However, in the wound healing process, an influx of macrophages occurs in order to assist in the phagocytosis of invading foreign organisms as well as break down damaged tissue. Macrophages are typically recruited to the wound site by other cells such as mesenchymal stem cells and fibroblasts. Cells present in the wound area recruit macrophages by releasing cytokines and chemokines [23]. Under normal conditions, tissue-resident macrophages serve to monitor for invading pathogens [24]. They migrate into the wound site early on in the

wound healing process and remain present throughout the process in order to organize other cells. They are also involved in fibrosis that can lead to scar formation [25].

Cells of the Dermis can be found in Table 2.

Extracellular Matrix in the Skin

Extracellular matrix has both direct and indirect effects on its surrounding environment. It can bind and adhere directly to growth factors and cytokines and can in turn release them to influence cell behavior. ECM can also have indirect effects through the cells that it binds to [5]. The bound cells will then release growth factors and cytokines, which may then influence wound healing. Many different ECM proteins are present in the skin tissue, which all have a role in the various stages of the wound healing process. The major ECM proteins of the skin include various collagens, fibronectin, elastin, vitronectin, laminin, and hyaluronan.

Collagen

An array of extracellular matrix proteins resides in dermal tissue. Collagen is a triple helical structure consisting of three polypeptide chains twisted around each other. The helix structure is held together by hydrogen bonds. The strands consist of the three basic amino acids glycine, proline, and hydroxyproline. Various other amino acids are incorporated into the strands which give the collagen a specific function [26]. Collagen I composes approximately 80-85% of the total dermis while collagen III constitutes approximately 10-15%. Fetal skin wounds typically heal without scarring. This is thought to be a result of the large amount of col III in fetal skin. As aging occurs, the ratio of col I:col III increases [27]. In normal skin wound healing, there is a large amount of collagen

III deposition into the granulation tissue early on. As the healing process progresses, this col III is broken down and replaced with col I. Along with col I and III, the basement membrane contains collagen IV, VII, and XVII.

Fibronectin

Fibronectin deposition occurs early in the wound healing process and plays a major role in the organization of new tissue. It is secreted initially by platelets flowing in from the surrounding broken blood vessels followed by macrophages and fibroblasts. It serves as a support structure for cells to adhere to and allows them to migrate throughout the wounded area. It also has roles in coating tissue debris to be broken down and in angiogenesis. In a healthy wound healing response, fibronectin is broken down and cleared from the wound area. If fibronectin presence remains in the wound bed, delayed wound healing typically occurs [28].

Elastin

Elastin is an insoluble protein that is present in the dermis of skin and is secreted by cells such as fibroblasts and smooth muscle cells. These cells secrete tropoelastin molecules that are then cross-linked outside the cell to make elastin fibers [29]. The purpose of elastin in skin is to give skin elasticity and allow it to recoil when stretched. Aging individuals undergo a structural and composition transformation in the elastin fibers that results in skin with reduced elasticity. This can also occur in pathologic conditions [30].

Vitronectin

Vitronectin is a glycoprotein that is commonly found in the ECM and blood. It serves to bind to the $\alpha v \beta 3$ receptor of cells through its RGD (Arg-Gly-Asp) sequence

[31]. Vitronectin can also regulate the proteolytic degradation of the ECM, participate in the immune response, as well as assist in clot formation [32].

Laminins

Laminins are also in the glycoprotein family that are primarily found in the basement membrane separating the dermal and epidermal layer. Laminins are heterotrimers composed of α , β , and γ chains. Laminins bind to each other, forming sheets. They also form interactions with cell surface receptors, acting as a foundation to organize tissue cells [33].

Hyaluronan

Hyaluronan is a hydrophilic polysaccharide that is commonly found in many tissues throughout the body. Its ability to bind to large quantities of water makes it ideal for control of tissue hydration. It also has roles in cell attachment, mitosis, migration, tumor development, and inflammation. Hyaluronan has a role in wound healing. Initially it assists in providing a temporary scaffold for provisional wound healing. Nutrients and cells can migrate into the wound and adhere to this provisional matrix. It also assists in keratinocyte stratification into an epithelial layer. Receptors for hyaluronan include CD44, intercellular adhesion molecule-1 (ICAM-1) and HA-mediated motility (RHAMM) [34, 35]. Hyaluronan has also been shown to play a role in the reduction of scar formation, especially in fetal wounds [36].

Dermal and Epidermal Signaling

The cells of the skin communicate with each other under both normal conditions and in the wound healing process. Both keratinocytes and fibroblasts secrete growth

factors and cytokines in order to communicate with the surrounding tissue and cells. Keratinocytes can stimulate fibroblasts to either differentiate or synthesize and secrete growth factors and as a result, fibroblasts will affect the proliferation and stratification of keratinocytes [37]. It has been shown that without the presence of fibroblasts, keratinocytes cannot stratify into a functional epidermis [38]. The cross-talk between keratinocytes and fibroblasts is primarily with four major signaling molecules: platelet-derived growth factor (PDGF), transforming growth factor- β (TGF- β), interleukin-1, and keratinocyte growth factor (KGF) [39].

PDGF and TGF- β present in the wound bed serve as a chemoattractant for fibroblasts. TGF- β 1 has a role in the increase in fibroblast proliferation. Once in the wound, fibroblasts and macrophages release TGF- β . If too much TGF- β 1 remains in the wound bed, scarring usually occurs. This is because TGF- β stimulates collagen secretion by fibroblasts.

Interleukin-1 is secreted by keratinocytes and has numerous roles in communicating with fibroblasts. It is also a direct up regulator of fibroblast proliferation. It has a role in regulating extracellular matrix secretion from fibroblasts. For example, interleukin-1 downregulates collagen secretion from fibroblasts. Interleukin-1 also has a role in influencing fibroblasts to release KGF (also is referred to as FGF7). KGF has been shown to organize the regeneration of the epidermis by increase its thickness, crowding and elongating the basal cell layer, and inducing proliferation of keratinocytes [40].

Wound Healing

Wound healing is a complex process that occurs in skin because skin is a self-healing organ. It involves many processes all happening in a highly orchestrated manner. Cells, growth factors, cytokines, and ECM all have individual roles in a series of events that occur in the wound healing process. The process is typically broken down into four different phases: hemostasis, inflammation, proliferation, and remodeling phases [41].

Hemostasis and inflammation phase

The initiation of wound healing begins immediately after damage is created to the skin tissue. When the tissue is damaged, blood vessels are severed which is crucial for the initial stages of wound healing to occur. Immediately, the vessels and capillaries undergo vasoconstriction in order to stop the bleeding. This vasoconstriction is followed by vasodilation, which allows for the release of blood and platelets into the wound bed [42]. Platelets assist in the formation of a fibrin plug that finalizes the initial stage of hemostasis. Platelets release various growth factors in the wound bed to further initiate the wound healing process. They release PDGF, FGFs, Epidermal growth factors (EGFs), TGF- β , along with many other factors responsible for the closing of the initial wound and cell recruitment. Following plug formation, the inflammation stage of wound healing begins. Cells such as macrophages and neutrophils infiltrate in order to phagocytize bacteria and debride the wounded tissue. Macrophages serve to digest foreign organisms as well as break down wound debris. They also release many chemotactic and cell instructive factors such as TGF- β , tumor necrosis factor- α (TNF- α), interleukins, vascular endothelial growth factor (VEGF), metalloproteinases (MMPs), and tissue inhibitors of metalloproteinases (TIMPs). A lot of these factors are responsible for initiating the proliferation phase of wound healing [42].

Proliferation phase

The proliferation phase occurs when dermal fibroblasts and epidermal keratinocytes infiltrate and proliferate to form granulation tissue. Fibroblasts and macrophages begin secreting more factors to recruit more fibroblasts to the site. Fibroblasts secrete large amounts of collagen III along with other ECM proteins such as fibronectin to create a provisional matrix. Fibroblasts also differentiate into myofibroblasts which express contractile filaments that serve to pull the wound margins closer to together in order to reduce the wound size.

Keratinocytes in surrounding healthy skin tissue begin to proliferate and migrate over the fibrin clot from signals released during the inflammatory phase. Keratinocytes secrete proteases in order to move through and break down the clot [43].

Remodeling phase

The proliferation and remodeling phases are overlapping. The remodeling phase begins near the end of the proliferation phase when collagen III is deposited and collagen I is broken down. Cross-linking occurs amongst the collagen I fibrils, which adds to the stability and strength. The newly remodeled collagen tends to form a 'basket weave,' pattern. This phase is a continuous cycle that can last for up to 20 years [44, 45].

These interacting factors make skin regeneration a complex process, consequently making it difficult to create therapeutic interventions.

Current Skin Graft Therapies

It is estimated that there are over 11 million severe burn wounds every year that will need medical attention and intervention. Of those, approximately 300,000 will result

in death [46]. Skin grafting is the predominant method for assisting in the regeneration of large skin defect areas. Other injuries to skin that require grafting include diabetic ulcers, chemical burns, physical trauma, necrotizing fasciitis, skin ulcers, unstable scar replacement, and infection [47, 48]. Grafting provides a protective barrier that allows for the repair of tissue while ultimately restoring the functional properties of normal skin. Autografts from the patient are taken from a healthy area of skin tissue by the use of a dermatome. After removal from the body, the grafts can be stretched out with the use of a mesher, allowing the autograft to cover a larger burn area. However, the meshed material often results in abnormal appearing skin once it has healed [49]. Autografts are the gold standard treatment; however, limited donor site availability along with secondary wound site creation are major limitations. Clinically, allografts and xenografts are also used. Therefore, surgeons typically use a commercially available graft. There is a plethora of graft products currently on the market such as Alloderm, Integra, Oasis, Dermagraft, Apligraf and Primatrix that can be used for the regeneration of skin tissue. They are advantageous because they eliminate the need for autologous skin, assist in skin wound healing, and have limited immunogenicity. Recently, groups have been investigating the incorporation of other off the shelf products to accompany these skin grafts. These off the shelf therapies include products such as human amniotic membrane (Mimedx, NuTech) or porcine urinary bladder matrix (ACell). These products are used because they have an abundant quantity of ECM proteins, cytokines, and growth factors which all have been shown to have added benefits in skin wound healing.

Alloderm was one of the first acellular dermal matrices on the market. It is an aseptically processed cadaveric skin tissue that has been specially prepared by the use of

detergents to remove the epidermis and other cells that could lead to host rejection or graft failure. The donor skin is screened for possible pathogens, and is freeze-dried in order to maintain the ECM structure. Alloderm is advantageous because it maintains the natural ECM structure that is crucial for skin regeneration, it has been shown to increase joint mobility, and reduces scar formation when compared to no graft at all [50-52].

Dermagraft is a polyglactin mesh that has been seeded with human foreskin fibroblasts. These foreskin fibroblasts secrete matrix to fill out the mesh with ECM along with growth factors and cytokines. These meshes are cryopreserved in order to maintain cell viability and matrix structure. The fibroblasts are from a certified cell bank that performs extensive testing in order to insure cell viability and that there are no harmful pathogens. Dermagraft is FDA approved for the treatment of diabetic foot ulcers [53].

Integra is a porous cross-linked bovine tendon collagen matrix that also contains glycosaminoglycans. It also contains an outer semi-permeable silicone layer that prevents water loss and acts as a temporary epidermis. This silicone layer is removed after the dermis is vascularized and is typically replaced with a thin autograft [54]. Integra is approved by the FDA to treat full-thickness or deep partial-thickness burn wounds as well as the repair of scar contractures.

Apligraf is constructed by seeding fibroblast cells onto a bovine type I collagen matrix. Over time a neodermis is produced by the fibroblasts in which a layer of keratinocytes is seeded onto. These seeded keratinocytes stratify into a stratified epidermis. Apligraf is FDA approved to heal both diabetic foot ulcers as well as venous leg ulcers [55].

Primatrix is a fetal bovine derived scaffold that contains ECM proteins valuable for the wound healing process. Because of its fetal bovine source, it is naturally rich in collagen type III, known for its scarless wound healing. It is approved for full and partial-thickness skin wounds. Interestingly, the Primatrix integrates with the native tissue when implanted, is remodeled, but doesn't degrade over time [56, 57].

Limitations of commercially available skin substitutes

The commercially available skin substitutes mentioned above along with numerous others used in the clinic all have several limitations. These limitations include integration failure, scarring, lack of vascularization, poor mechanical properties, low adherence to the wound bed, high costs, and some can initiate an immune response [58, 59]. The challenge of blood inflow and vascularization into the graft material often times poses challenges to wound healing. It is crucial that blood can flow into the scaffolds with ease and that vessels can grow throughout the scaffolds in order to accelerate the wound healing process by bringing the proper nutrients to and from the wound bed. Cells can also have a tough time invading the depths of these scaffolds, making it difficult for these products to integrate. Many of these problems stem from the lack of porosity within these substitutes. It has been shown that scaffolds containing a higher degree of porosity can promote tissue ingrowth and vessel formation more quickly than similar substitutes with a smaller degree of porosity [60]. With a higher degree of blood inflow and cell migration, the grafts will initially have a faster take rate and the resultant skin tissue will resemble more normal unwounded tissue versus scar tissue. Current therapies also lack crucial mechanical properties necessary for proper skin regeneration. They typically have

insufficient mechanical properties and not on the scale of normal human skin tissue. Graft contraction is also a common issue because it results in poor graft take, immobile skin, and scarring [61]. Another limitation of current therapies is the composition of scaffolds. Because skin wound healing is such a complex process, it requires many different factors in order to heal properly. Most of the current therapies only address certain phases of the wound healing process because of their limited material composition and do not supply the proper environment for the whole process to occur, resulting in healed skin tissue that is sub-optimal.

Engineered Skin Biomaterials

For the reasons listed above, creating an ideal substitute has proven to be difficult. Current skin tissue engineering research efforts are focusing on designing scaffolds with an improved architecture and composition. As discussed previously, most of the current therapies utilize collagen I as the base component. Collagen I provides biological cues for the recruitment and survival of cells and mimics native skin tissue [62]. However, collagen used in grafting materials often degrades at a rapid rate. In order to prevent this fast degradation, the collagen is typically cross-linked, which has its own disadvantages. The cross-linking reagent glutaraldehyde often remains in the collagen which can have toxic effects on cells. Also, it is difficult to control the degree of cross-linking that can occur which often leads to small pore sizes. Finally, cross-linking may result in scaffolds that break down too slowly, which is disadvantageous to wound healing. In order to control the degradation rates of collagen and avoid using cross-linking reagents, groups

are combining collagen I with biodegradable synthetic polymers which increase the tensile strength and decrease the scaffold contractility.

Research efforts have also focused on incorporating other ECM proteins, glycosaminoglycans (GAGs), proteoglycans, growth factors, and cytokines into scaffolds to further assist in the wound healing process. Some of the ECM proteins in skin tissue that groups are incorporating into scaffolds are elastin, fibronectin, and various collagens. GAGs such as hyaluronan are hydrophilic capable of absorbing 1000 times its volume in water, keeping the wound bed moist. Growth factors such as vascular endothelial growth factor (VEGF), platelet derived growth factor (PDGF), transforming growth factor β (TGF- β), and various fibroblast growth factors (FGFs) have all been shown to play a role in the wound healing process [5]. By incorporating various combinations of these elements researchers have begun to develop more advanced biomimetic matrices. These biologics increase the amount of biochemical cues present in the matrix; resulting in a material that more closely resembles native skin tissue. A 3D support structure must be created that allows for cellular localization, adhesion, and differentiation ultimately leading to the regrowth of functional tissue. These scaffolds must allow the cells to maintain a normal phenotype; therefore, must resemble the native ECM environment. This structure must also have appropriate mechanical properties and prevent wound contraction [63]. To incorporate these different elements into one scaffold, a number of different methods are used.

Hydrogels

Hydrogels are highly absorbent cross-linked polymers that are mostly liquid, but behave as a solid due to cross-linking. Various proteins such as collagen and hyaluronan

can be incorporated into these scaffolds to provide a more favorable environment for skin cells. Hydrogels are typically used for an in vitro model for skin cells and not used as grafting material due to their mechanical properties [64]. Hydrogels are advantageous as graft dressings because of their moist environment [65]. In vitro, skin cells have shown favorable responses to hydrogels [66].

Emulsion freeze-drying

Emulsion freeze-drying is a technique that mixes together both natural and synthetic polymers, synthetic polymers, and water. This method is useful because it allows for the mixture of various materials [67]. Freeze-dried scaffolds can provide a 3D microstructure with pores, controlled degradation rates, and appropriate mechanical properties [68].

3D printing

Three-dimensional (3D) printing has shown great promise in the field of tissue engineering in order to regenerate organs and tissues. It is a novel free-form fabrication method that allows you to design complex constructs in the form in which it is desired. 3D printers are capable of printing a wide range of materials such as polymers, ECM proteins, and cells [69]. 3D printed constructs can combine these various materials and custom tailor them to the patient. Patients with severe burn wounds can undergo imaging in order to analyze the thickness and size of burns. After imaging, a model of the newly desired tissue can be constructed by engineers that will fit the burn wound perfectly. Once a model has been constructed, it can be printed out, sterilized, and then used in the clinic.

Electrospinning

Electrospinning is not a new concept. It was originally developed in the textile industry; however, it has recently been more widely used as a method for engineering biocompatible scaffolds [70, 71]. Electrospinning is a process that creates nanofibrous meshes that mimic the native extracellular matrix architecture [72]. Briefly, a composite solution of polymers and natural biomaterials is mixed with an organic solvent such as hexafluoroisopropanol, creating a viscous solution. That solution is then pumped from a syringe with a metal needle by the use of a syringe pump. Concurrently, the metal tip of the needle is given a highly positive charge while a metal plate is grounded a given distance from the tip of the needle (Fig 1) [73]. Naturally, the solution from the syringe forms at the tip of the needle in a cone shape, defined as a Taylor cone. At the very leading edge of this cone, a fiber is created that whips around in the air until it lands on the grounded collecting plate [74]. As the fiber travels across the defined distance, the organic solvent evaporates and the fiber elongates. On the collecting plate, the fibers collect in a random pattern in the nano to micro scale range which is similar to native collagen and ECM proteins.

Electrospun scaffolds are unique because they can be tailored to meet specific demands. By varying parameters such as the voltage, solution flow rate, viscosity of the solution, needle size, and collector distance from the needle, the fibrous mesh can be altered. Electrospun scaffolds have a high surface-to-volume ratio which is beneficial for cell adhesion, proliferation, migration, and differentiation [75]. Electrospun scaffolds also have interconnected pores throughout the scaffold which allow for nutrient transport and waste removal of cells. Another unique advantage of these scaffolds is that they can incorporate a wide variety of materials. Many groups have focused on combining

multiple materials in order to meet the specific needs of skin tissue. For example groups typically use a synthetic polymer such as polycaprolactone (PCL), poly lactic-co-glycolic acid (PLGA), and polyurethanes in order to increase strength and degradation rates of scaffolds. Other natural materials such as elastin, fibronectin, hyaluronan, and various collagens are included with the synthetic polymers in order to add a biologic element that creates a favorable cell environment. It is possible to have individual fibers composed of 100% polymer and 100% natural materials in one scaffold, but that is not ideal because the natural fibers would more than likely degrade at a faster rate than the synthetic materials, resulting in a 100% synthetic scaffold after a short amount of time. For this reason, the various materials are dissolved together, resulting in a homogenous fiber. In this study we hypothesized that electrospinning a solution of collagen I and polycaprolactone will create a biomimetic nanofibrous matrix for skin tissue regeneration.

While electrospun scaffolds have many advantageous features for skin tissue engineering, there has been one major limitation reported in literature. While these meshes have high porosity with interconnected pores, the average pore sizes throughout the scaffold are on the nano scale inhibiting cell infiltration. This is a result of layers of fibers being laid down on top of preexisting layers during the electrospinning process. This results in nanopores that are much smaller than fibroblasts; therefore, fibroblasts don't migrate throughout the thickness of the scaffolds when seeded on the surface. In Fig 2, fibroblasts expressing red nanocrystals can be seen on the surface of electrospun col/PCL scaffolds (green). Because of the lack of infiltration, many groups have focused on increasing the porosity of these electrospun scaffolds [76-79]. These methods include

salt leaching particles, ice crystals, varied patterned collector plate setups, increased needle diameter, laser porosity creation, and sacrificial fibers. While some of these methods have some advantages, none of them are cost-effective, reproducible, or can be made on a large scale. Also, some of these methods only work for synthetic materials and can not be performed with natural polymers. Consequently, this creates a void in the field for engineering a more effective method for increasing porosity within scaffolds.

Enhanced wound healing benefit of scaffolds pre-seeded with cells

Recent literature has brought to light the added benefit of pre-seeding scaffolds with cells prior to implantation in the patient. Groups have demonstrated that seeding human dermal fibroblasts on scaffolds for at least 24 hours prior to implantation has resulted in faster healing, more normal skin tissue than just scaffolds alone [80, 81]. Researchers have showed advantageous effects by including umbilical cord blood stem cells and somatic stem cells loaded into porous matrices [82, 83]. Others have demonstrated that co-culturing keratinocytes and fibroblasts has an added benefit and resulted in healing with minimal scar tissue [84]. An environment supporting dynamic reciprocity is produced when cells are incorporated into scaffolds that mimic the native ECM because the cells will in turn secrete growth factors and cytokines back in to the matrix. By having skin cells already present in the scaffold, they can assist the wounded tissue through the wound healing stages [85]. Keratinocytes provide a barrier function while fibroblasts secrete an abundance of ECM proteins, GAGs, growth factors, and cytokines [86]. The concentration of collagen in the healing wound is reduced significantly when fibroblasts are pre-seeded in scaffolds. This is thought to be the reason for the decrease in

scar tissue formation in healed rabbit skin wounds [81]. We hypothesized in our research that incorporating fibroblasts into our scaffolds would jump start the wound healing response and have multiple effects throughout. We believe the secreted matrix will create an environment similar to native skin tissue. The fibroblasts will also secrete growth factors and cytokines which in turn will stimulate the proper cells and factors to enter the wound site at the appropriate times.

Strategies for Improving Electrospun Skin Scaffolds

Incorporation of Cell Ligands

Electrospun scaffolds containing solely synthetic polymers and limited porosity have favorable mechanical properties; however, they have a deficiency of biological cues crucial for the recruitment, adhesion, and proliferation of cells and lack space for cells to migrate and secrete ample amounts of ECM. By incorporating natural cellular ligands in these scaffolds, while including the synthetic polymers, a composite material can be constructed that maintains mechanical properties while mimicking the native ECM environment. Numerous different proteins have been investigated for their ability to enhance cell behavior in skin tissue such as gelatin, hyaluronan, elastin, and collagens. For this study, the goal was to create a biomimetic skin scaffold. For this reason we incorporated the largest element of skin tissue, collagen I. Collagen I composes approximately 70-80% of normal skin tissue [87].

Increasing Porosity

As mentioned previously, the limitation of small pore sized in electrospun scaffolds needs to be addressed. Therefore one of the goals of this research was to

increase the porosity within these scaffolds. The criteria we had for increasing porosity included cost-effectiveness, reproducibility, variability of pore sizes, marketable, and scalable.

Research Objectives

To address the issue of limited effective skin grafts, the primary objective of this dissertation was to develop a biomimetic electrospun scaffold to support rapid and effective skin regeneration. In order to make a scaffold for skin regeneration we combined collagen I and PCL, an FDA approved biodegradable polymer into a nanofibrous mesh by the use of electrospinning.

Initially we investigated various electrospinning apparatus setups along with scaffold modifications in order to increase scaffold porosity. There are many different methods reported in literature. We used some of these methods reported in literature and developed some on our own. A few of the setups included vertical electrospinning, sacrificial fibers, layer-by-layer electrospinning and electrospraying fibroblasts, and a microneedle press to manually create pores post-scaffold construction.

Our second objective was to assess the fibroblast and keratinocyte responses to scaffolds composed of different ratios of col:PCL as well as various pore sizes. It is important to maintain a high degree of collagen I in scaffolds, but a synthetic polymer is needed to increase the tensile strength, contraction rates, and degradation rates of these scaffolds because 100% collagen I scaffolds degraded within 24 hours of being placed in media. We performed many experiments to verify the highest ratio of collagen:PCL we could make a successful skin substrate that exhibited a favorable cellular response while still maintaining mechanical properties in a range ideal for skin tissue regeneration. To do

this we did tensile testing, contraction studies with and without seeded cells, fluorescent imaging of cells over time, proliferation assays, and in vivo degradation experiments. To assess cell response to micropore size, we seeded fibroblasts on the surface of microporous scaffolds and let them grow, proliferate, and secrete ECM over various time points. We assessed the migration of the cells along with the secretion of ECM proteins over time by staining, immunoblotting, and measuring fluorescence levels.

Our third objective was to assess the micropore effect of scaffolds when implanted in vivo. To do this we created full-thickness defects in the back skin of rats and implanted porous, non-porous, and sham wounds. By harvesting and staining the tissues we were able to determine the effect of pores on wound healing.

Our final objective was to compare microporous scaffolds seeded with fibroblasts for 1 and 4 days prior to implantation to porous scaffolds not containing any cells. We also created a sham wound for comparison purposes. Again, by harvesting the tissue and staining we were able to assess the effect that pre-seeded scaffolds had on the wound healing response.

Table 1: Cells of the Epidermis.

Keratinocytes	<ul style="list-style-type: none"> • Synthesize keratin. • Polarized layers with proliferating cells at the basal layer and terminally differentiated cells at the apical surface.
Melanocytes	<ul style="list-style-type: none"> • Produce melanin, giving the skin pigmentation
Merkel Cells	<ul style="list-style-type: none"> • Receptor cells for sensation
Langerhans Cells	<ul style="list-style-type: none"> • Antigen-presenting immune cells • Potent inducers of T-cell response.

Table 2: Cells of the Dermis.

Fibroblasts	<ul style="list-style-type: none">• Most predominant cell in dermal tissue.• Secrete ECM, growth factors, cytokines.• Control the remodeling process.
Mesenchymal Stem Cells	<ul style="list-style-type: none">• Secrete many growth factors that play a role in the wound healing process.
Macrophages	<ul style="list-style-type: none">• In wound healing, macrophages phagocytize foreign matter and break down damaged tissue.

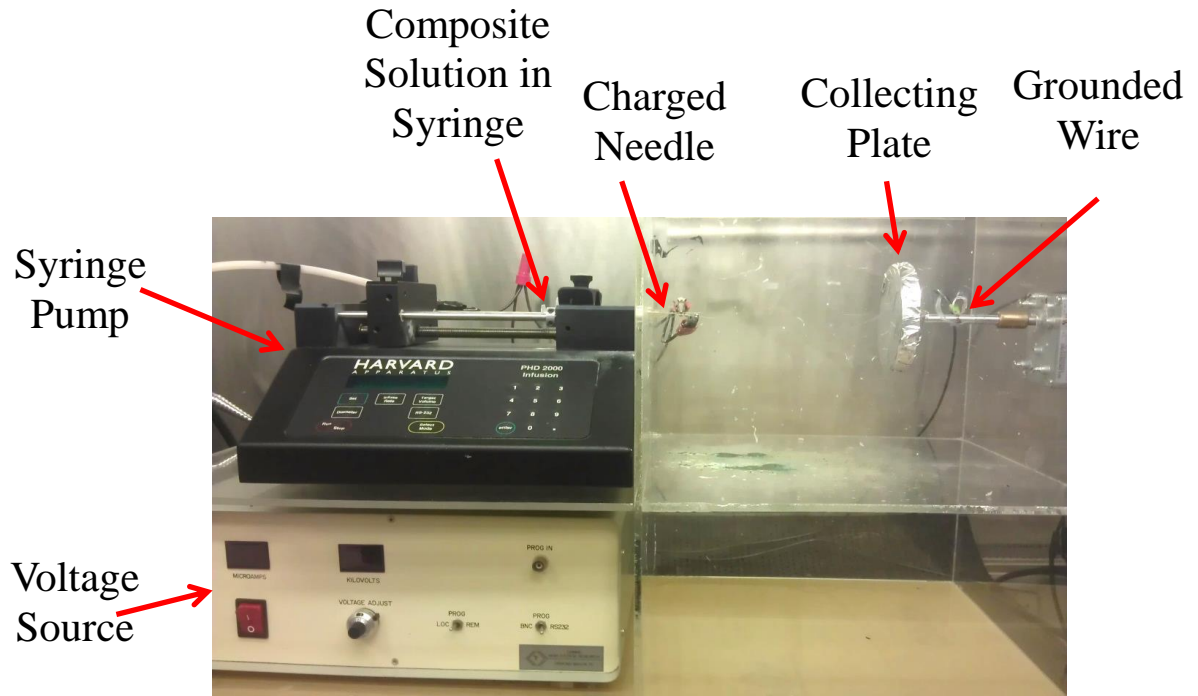


Fig 1. Electrospinning apparatus. Pictured are the components of a standard electrospinning apparatus set up. The voltage source is used to charge the needle in which the scaffold solution is pumped out at a constant rate by the use of a syringe pump. The solution travels across a given distance to a grounded collecting plate where it collects into a nanofibrous mesh.

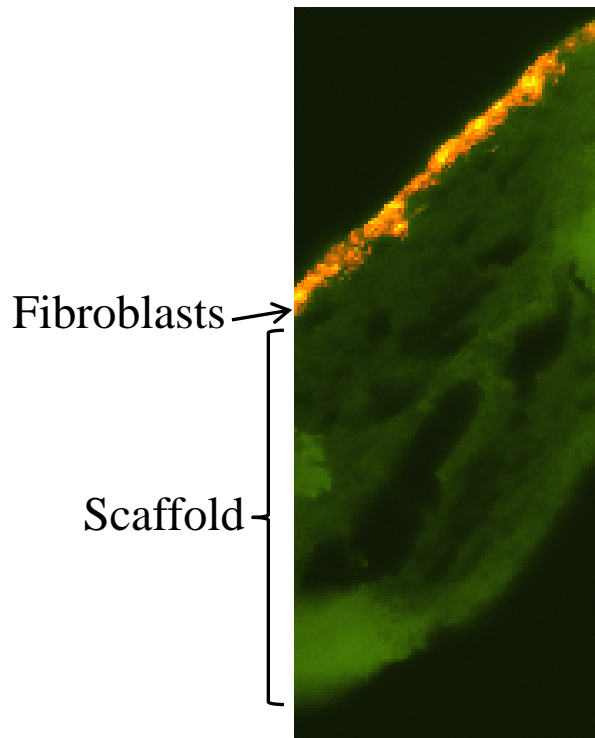


Fig 2. Fibroblasts do not migrate through normal electrospun scaffolds. A cross-section of a scaffold shows fibroblasts (red) don't migrate throughout the thickness of scaffolds (green) due to the limited porosity of scaffolds created during the electrospinning process.

MICROPOROUS DERMAL-LIKE ELECTROSPUN SCAFFOLDS PROMOTE
ACCELERATED SKIN REGENERATION

by

PAUL P. BONVALLET, BONNIE K. CULPEPPER, JENNIFER L. BAIN, MATTHEW
J. SCHULTZ, STEVEN J. THOMAS, SUSAN L. BELLIS

Tissue Engineering Part A, 2014 March; Epub ahead of print

Copyright
2014

by

Bonvallet et al.

Used by permission

Format adapted for dissertation

Abstract

The goal of this study was to synthesize skin substitutes that blend native extracellular matrix molecules (ECM) with synthetic polymers that have favorable mechanical properties. To this end, scaffolds were electrospun from collagen I (col) and polycaprolactone (PCL), and then pores were introduced mechanically to promote fibroblast infiltration, and subsequent filling of the pores with ECM. A 70:30 col/PCL ratio was determined to provide optimal support for dermal fibroblast growth, and a pore diameter, 160 μm , was identified that allowed fibroblasts to infiltrate and fill pores with native matrix molecules including fibronectin and collagen I. Mechanical testing of 70:30 col/PCL scaffolds with 160 μm pores revealed a tensile strength of 1.4 MPa, and the scaffolds also exhibited a low rate of contraction (<19%). Upon implantation, scaffolds must support epidermal regeneration; we therefore evaluated keratinocyte growth on fibroblast-embedded scaffolds with matrix-filled pores. Keratinocytes formed a stratified layer on the surface of fibroblast-remodeled scaffolds, and staining for CK-10 revealed terminally differentiated keratinocytes at the apical surface. When implanted, 70:30 col/PCL scaffolds degraded within 3-4 weeks, an optimal time frame for degradation in vivo. Finally, 70:30 col/PCL scaffolds with or without 160 μm pores were implanted into full-thickness critical size skin defects. Relative to nonporous scaffolds or sham wounds, scaffolds with 160 μm pores induced accelerated wound closure, and stimulated regeneration of healthy dermal tissue, evidenced by a more normal-appearing matrix architecture, blood vessel in-growth, and hair follicle development. Collectively these results suggest that microporous electrospun scaffolds are effective substrates for skin regeneration.

Introduction

Skin is often damaged as a result of physical insult, burns, diabetic ulcers, and other traumatic events. Frequently the wound can heal on its own, however large wounds require surgical intervention. Current treatments for skin repair include the use of autograft, allograft, or xenograft tissues. Autografted skin is the gold standard therapy, however the amount of donor skin is in limited supply, and the quality of donor skin is sometimes compromised. Allograft and xenograft tissues are substitutes for autograft, however these materials present disadvantages such as graft rejection, scar formation, contraction and potential disease transmission [1, 2]. Accordingly, intensive research is aimed at developing synthetic skin-mimetic materials that serve as temporary supports, while simultaneously inducing the regeneration of native skin tissue [3, 4].

Many engineered skin substitutes incorporate molecules found within the native extracellular matrix (ECM). ECM is critical for the guidance of cells and proper tissue formation during the wound healing process. Collagen I is an abundant dermal ECM molecule, and is widely used in regenerative scaffolds. However, collagen-based materials often have inadequate tensile properties due to collagen's fast degradation rate and poor mechanical characteristics [5]. In order to circumvent this issue, collagen I is either chemically cross-linked, or mixed with synthetic polymers that add mechanical strength and flexibility. Poly (ϵ -caprolactone) (PCL) is an FDA-approved degradable polymer that is commonly blended with collagen I to create scaffolds with a tunable degradation rate and increased tensile strength [6]. While many methods can be used to generate collagen/PCL composites, electrospinning is emerging as a promising technology. Electrospinning offers a simple method for producing scaffolds that can be

tailored to mimic the biochemistry and three-dimensional structure of native ECM [7]. Electrospun scaffolds composed of PCL and collagen I support cell adhesion and proliferation, possess favorable biomechanical characteristics, have a high surface to volume ratio, and are composed of a nanofibrous structure with interconnected pores, similar to native ECM [8-10].

One of the main limitations of electrospun scaffolds is that the pores created by the nanofibrous mesh have small diameters that impede cell infiltration, hindering scaffold remodeling and wound healing [11-13]. A number of reports have highlighted the importance of porosity within skin-mimetic materials in facilitating fibroblast, endothelial and stem cell infiltration, nutrient transport for better graft survival, and neovascularization [14-16]. On the other hand, if pores are too large, cells may have a difficult time filling the void with ECM. Excessive porosity or large pore diameters may also compromise scaffold mechanical properties. The most effective pore diameter for tissue regeneration is likely to be influenced by other scaffold properties such as the presence of integrin ligands for cell attachment and migration (e.g. collagen), scaffold stiffness, and degradation characteristics (e.g., amenability to endogenous enzymatic or hydrolytic processes).

The goal of the current study was to develop an electrospun scaffold that integrates a number of features critical for effective tissue repair including: a cell-instructive biochemical composition; suitable mechanical properties and degradation rate, and pores of sufficient size to allow cell infiltration and scaffold remodeling. Electrospun scaffolds composed of collagen I/PCL blends with varying pore diameters were evaluated for fibroblast-directed ECM deposition. Pores were created mechanically, based on an

adaptation of a device used in the cosmetics field to stimulate skin regeneration. Specifically, a paddle-like device composed of numerous micro-diameter needles (Dermastamp) creates small injuries in the facial skin, which consequently promotes wound healing. Modeling this process, pores were created in electrospun scaffolds with micro-diameter needles, and a pore size that supported ECM deposition was identified. Microporous scaffolds implanted into full-thickness skin wounds were found to promote more rapid skin regeneration than standard electrospun scaffolds. Compared with other technologies for increasing scaffold pore size, the generation of a commercial press device with a defined needle diameter offers a technically straightforward and cost-effective strategy for introducing well-controlled and reproducible pores in sheets of electrospun materials.

Materials and Methods

Preparation of electrospun scaffolds. 100% PCL, 50:50 col/PCL, and 70:30 col/PCL scaffolds were synthesized by dissolving collagen I and PCL into hexafluoroisopropanol (HFP) solvent (Sigma), resulting in a solid weight of 7.5% of the total solution weight. Calf skin collagen I was purchased from MP Biomedicals and 100,000 Da PCL was purchased from Scientific Polymer Products. Solutions were taken up into a 3 cc syringe with a 27 gauge needle, and a syringe pump (Harvard Apparatus) was used to eject the solution at a constant 2 mL/hr rate towards an aluminum foil covered collecting plate that rotated at 20 rotations/min. Scaffolds were placed in a desiccator for 24 hours to remove any residual HFP. Individual scaffolds were punched from the larger electrospun sheet using a Humboldt Boring Machine (Fisher). Scaffolds were placed in CellCrowns

(Scaffdex) and micropores were created mechanically using either an acupuncture needle (scaffolds with 160 μm pores) or a Dermastamp device (scaffolds with 250 μm pores, Dermastamp purchased from Alibaba.com). For cell culture studies, scaffolds were sterilized by soaking in 70% ethanol prior to use.

Cell Culture. Immortalized J2 mouse fibroblasts were a generous gift from Dr. Louise Chow (UAB). GFP-expressing J2 cells were generated by stable transduction with lentivirus particles obtained from the UAB Virology Core facility. GFP-J2 fibroblasts were cultured in DMEM supplemented with 10% fetal bovine serum (FBS) and 1% penicillin/streptomycin/ amphotericin solution (Invitrogen). Primary human fibroblasts and keratinocytes harvested from neonatal foreskin were obtained from the Skin Cell Culture Core facility at UAB. Human fibroblasts were cultured in fibroblast basal medium supplemented with insulin, FBS, Fibroblast Growth Factor (FGF), gentamicin, and amphotericin (Lonza). Keratinocytes were cultured in serum free keratinocyte medium supplemented with L-glutamine, epidermal growth factor (EGF), and bovine pituitary extract (BPE) (Gibco).

Cell growth on scaffolds. GFP expressing J2 fibroblasts were seeded onto scaffolds held in place by CellCrowns and allowed to grow for 3 or 10 days. Scaffolds were then removed from the CellCrowns, placed on microscope slides, and rinsed with PBS. Cells were fixed in 4% paraformaldehyde for 15 minutes and permeabilized in 0.2% Triton-X 100 for 15 minutes. All steps were followed by 3 washes in PBS. The samples were coverslipped and imaged by confocal microscopy.

To quantitatively evaluate cell proliferation, 5×10^4 GFP-expressing J2 fibroblasts were seeded onto scaffolds and allowed to grow for varying time points ranging from 1-21 days. The samples were then rinsed in PBS, frozen in liquid nitrogen, and pulverized using a cryo-pulverizer. Cells were lysed in 50 mM Tris buffer (pH 7.4) containing 150 mM NaCl, 1% Triton X-100, 1% deoxycholate, 0.1% SDS, 5mM EDTA, and 0.5% Igepal. Lysates were then homogenized and centrifuged at 15,000xg for 20 minutes at 4°C, and supernatants were collected for analysis. Solution fluorescence of the lysates (reflecting GFP) was measured using a BioRad Versafluor fluorometer. For western blotting, lysates were mixed with NuPAGE lithium dodecyl sulfate (LDS) and sample reducing agent (Invitrogen) and resolved in a BioRad precast gel at 100V. The proteins were transferred overnight to a polyvinylidene fluoride (PVDF) membrane at 4°C. The membrane was blocked with 10% bovine serum albumin for an hour. An anti-GFP monoclonal antibody (Roche) and an HRP conjugated secondary antibody (Cell Signaling) were used. Imaging was performed on a BioRad ChemiDoc imaging system.

Cell viability on scaffolds. Human fibroblasts (lacking any fluorescent tag) were seeded on the surface of scaffolds and allowed to grow for 1, 7, 14, and 21 days. Scaffolds containing fibroblasts were then submerged in a live/dead cell imaging solution for 15 minutes that stains live cells green and dead cells red (Life Technologies). The scaffolds were subsequently imaged on a Nikon confocal microscope. Cell counting was performed by automatic detection using the Volocity image analysis software program in order to determine the number of live and dead cells.

Scanning electron microscopy (SEM) of scaffolds. Scaffolds were dried in a desiccator for 24 hours, and then gold plated and imaged using a Philips XL-30 SEM with an accelerating voltage of 10kV.

Cell invasion into pores and matrix deposition. Human fibroblasts were pre-loaded for 24 hours with red fluorescent nanocrystals (Qtracker 655, Invitrogen), and then seeded onto scaffolds and cultured for 10 days. Scaffolds were subsequently cut into strips, embedded in optimal cutting temperature (OCT) gel, frozen, and sectioned with a cryostat. Nuclei were stained with Hoechst. Matrix deposition was evaluated by phase contrast imaging using a dissecting microscope, or scaffolds were stained for specific matrix molecules. Collagen was stained using a Picrosirius Red kit (Polysciences Inc), and fibronectin was detected using an anti-fibronectin antibody (Abcam), followed by Alexa-488 conjugated secondary antibody (Molecular Probes). Fibronectin and collagen deposition was validated by immunoblotting (primary antibodies from Abcam).

Keratinocyte stratification on fibroblast-remodeled scaffolds. Human fibroblasts were seeded on the scaffold surface and allowed to grow for 10 days. At this time point, human keratinocytes were seeded onto the fibroblast-embedded scaffolds and allowed to adhere for 24 hours. Scaffolds were then placed on top of a wire mesh and media was filled to the level of the scaffold, positioning the keratinocyte layer at the air-media interface. Scaffolds were grown at the air-liquid interface for 10 days, and were then OCT embedded, frozen, and sectioned. Sections were stained with hematoxylin and eosin. In addition, scaffolds were immunostained for cytokeratin 10 (Abcam).

Mechanical testing. Human foreskin fibroblasts were seeded onto 70:30 col/PCL scaffolds with or without mechanically generated pores and cultured for 7, 14, and 21 days. At each time point, the diameters of the scaffolds were measured with calipers. The difference in diameter from the original diameter was measured, and the percent contraction was calculated. The procedure was reproduced without seeded fibroblasts in order to compare contraction of scaffolds with or without cells.

Tensile strength and strain were measured for scaffolds of varying col/PCL ratios, with or without 160 μm pores. The scaffolds were first soaked in PBS to ensure adequate hydration, and then samples were analyzed using a MTS 858 mini Bionix mechanical test machine applying a displacement strain rate of 5 mm/min, time interval of 100 Hz, a 100 N load cell, and using MTS pneumatic controller grips. A dog-bone shaped die was used to cut scaffolds. Scaffold thickness and grip distance were measured and taken into account prior to testing.

Degradation of scaffolds in vivo. All animal procedures were performed under the guidelines approved by the Institutional Animal Care and Use Committee (IACUC) at the University of Alabama at Birmingham. Three 15-mm diameter full-thickness wounds were created in the backskin of a Sprague Dawley rat (i.e., each rat received a total of 3 wounds placed linearly on the backskin). One of the wounds was implanted with a 70:30 col/PCL scaffold, another with a 50:50 col/PCL scaffold, and the third was covered with gauze (sham) (n=5 rats). Scaffolds were stained with DiI dye (Invitrogen) prior to implantation. At 7, 14, and 26 days, tissues were harvested, OCT embedded, and

sectioned. Fluorescent pictures were taken and the areas of remaining scaffold were measured using NIS Elements BR software.

Wound closure and histology. As described above, each rat received three 15 mm diameter full thickness wounds on the backskin. One wound was implanted with a 70:30 col/PCL scaffold containing 160 μ m pores; the second wound was implanted with a 70:30 col/PCL scaffold lacking micropores, and third wound was covered with gauze as a sham control (n=5). Top-view photos of the rat backskin containing the 3 side-by-side wounds were taken at 7, 14, and 21 days, and unhealed wound areas were measured by Image J analysis. Tissues were harvested at these same time points, paraffin-embedded, sectioned and stained with hematoxylin and eosin (H&E). Representative images were taken to highlight blood vessel formation, hair follicle development, and dermal matrix architecture. In addition, whole field H&E stained sections were taken with an Olympus VS120, and the junction between the normal and abnormal-appearing tissue was designated. The area of abnormal dermal tissue area was measured by Image J analysis.

Results

Fibroblast growth on scaffolds with varying ratios of collagen and PCL. Pilot studies were performed on electrospun scaffolds with varying collagen I/PCL ratios to identify a base formulation that supported fibroblast adhesion to the scaffold surface and subsequent cell proliferation. Four formulations were examined: (1) 100% collagen I; (2) 70% collagen I and 30% PCL (70:30 col/PCL); (3) 50% collagen I and 50% PCL (50:50 col/PCL); and (4) 100% PCL. Scaffolds composed of 100% collagen I degraded within

24 hours and were not investigated further. The three other scaffold formulations were seeded with GFP-expressing dermal fibroblasts, and cells were visualized by confocal microscopy (Fig 1A). All three scaffolds supported some degree of cell attachment and survival, although at 10 days there appeared to be a greater number of cells on scaffolds composed of 70:30 col/PCL. Fibroblasts on the 70:30 col/PCL scaffolds displayed a well-spread morphology, and numerous mitotic figures were present (Fig 1B), confirming active cell proliferation. Based on these data, further analyses of the 70:30 col/PCL scaffolds were performed. To quantitatively assess cell survival and proliferation, scaffolds with GFP-expressing fibroblasts were homogenized at varying time intervals and the fluorescence of the cell lysates (representing the GFP-expressing cell fraction) was measured by fluorometry (Fig 1C). Cell lysates were also immunoblotted for GFP (Fig 1D). A substantial increase in relative cell number was observed from 1-10 days, after which cell number stabilized. Stabilization is likely due to cells reaching confluence on the scaffold surface.

We next evaluated cell viability on 70:30 col/PCL scaffolds by seeding primary human fibroblasts (not expressing GFP) onto scaffolds, and then staining for both live (green) and dead (red) cells after 1, 7, 14, and 21 days. We observed minimal cell death over the 21 day time interval, and cells appeared to reach confluence between 7 and 14 days (Fig 2A), consistent with results in Fig 1. The respective numbers of live and dead cells were quantified from multiple fields (Fig 2B), which confirmed a low rate of cell death at each time point.

Optimization of scaffold pore size. Having determined that 70:30 col/PCL scaffolds provided good support for fibroblast growth, pores with diameters of either 250 or 160 μm were introduced into the scaffolds using microneedles (Fig 3). Human dermal fibroblasts loaded with fluorescent nanocrystals were seeded onto the scaffolds and allowed to migrate and proliferate for 10 days. A confluent monolayer of fibroblasts formed on the surface of scaffolds with 250 and 160 μm diameter pores, indicating that sufficient fibroblast-mediated matrix deposition occurred to allow bridging across the top of the pores (Fig 3C&F). However, it was evident that the 160, but not 250, μm pores were filled with matrix. We also compared the capacity of fibroblasts to fill the pores of scaffolds with varying col/PCL ratios. Fibroblasts were grown on either 70:30 or 50:50 col/PCL scaffolds with 160 μm pores, and at 7 days minimal pore-filling was observed (Fig 4A). However, at 14 days there was obvious matrix deposition within the 70:30, but not 50:50, scaffolds. Magnified images at 14 days demonstrate that the newly-deposited matrix was fibrous in nature. These results indicate that both the col/PCL ratio and pore diameter are important parameters for fibroblast-directed matrix deposition.

Infiltrating fibroblasts fill scaffold pores with ECM. Fibronectin is a major constituent in provisional wound-healing matrices [17], therefore immunostaining for fibronectin was performed on the fibroblast-remodeled 70:30 col/PCL scaffolds with 160 μm pores. As shown in Fig 4B, a substantial amount of fibronectin was present throughout the pores. Scaffolds were also stained with picrosirius red, a dye selective for fibrillar forms of collagen (e.g., collagens I and III) which are abundantly secreted by fibroblasts. Extensive collagen deposition was observed (Fig 4C). The deposition of collagen I and

fibronectin was further validated by immunoblotting homogenates prepared from fibroblast-embedded scaffolds (Fig 4D).

Scaffold mechanical properties. We next examined the effect of introducing pores on the mechanical properties of the scaffolds. Scaffolds with varying col/PCL ratios, with or without introduced pores, were analyzed for tensile strength and strain (Table 1).

Comparable tensile strength and strain were observed for 70:30 and 50:50 col/PCL scaffolds, although both had lower values than 100% PCL. The addition of 160 μ m pores had little effect on tensile strength for 100% PCL and 50:50 col/PCL scaffolds, however strength of the microporous 70:30 col/PCL substrates was diminished to 1.4 MPa. Nonetheless, this value seems reasonable for therapeutic applications given that native skin exhibits a tensile strength of 5-30 MPa [18].

Wound contraction is a natural part of healing; however, excessive contraction of dermal substitutes used for large wounds can lead to scarring, pain, and joint immobility. To address this issue, 70:30 col/PCL scaffolds with or without micropores were incubated in media over a 21 day time period and contraction was evaluated by measuring scaffold diameter (Fig 5). Contraction occurred within the first 2 weeks for both scaffold types, and then stabilized. Scaffolds with micropores exhibited a maximal contraction of 18% within 21 days, while scaffolds without micropores had a 19% contraction. We subsequently evaluated contraction for scaffolds seeded with fibroblasts. Fibroblast-containing scaffolds without micropores had a maximal contraction rate of 17%, whereas microporous fibroblast-embedded scaffolds exhibited 13% contraction. These results demonstrate that the introduction of micropores into electrospun scaffolds

does not increase the degree of scaffold contraction. Although one cannot directly compare with rates of scaffold contraction in vivo, the values observed for the microporous electrospun scaffolds seem acceptable, given that some clinical products have a contraction rate of up to 50% when grafted [19, 20].

Fibroblast-remodeled scaffolds support keratinocyte growth and stratification. Re-epithelialization of the skin is a critical step in wound healing, and maturation of the epidermis is known to be dependent on a healthy supportive dermal layer [21]. Hence, we examined the capacity of fibroblast-embedded scaffolds to support keratinocyte growth. 70:30 col/PCL scaffolds with 160 μm pores were seeded with dermal fibroblasts, and the constructs were cultured for 10 days to allow matrix deposition. Keratinocytes were then seeded onto the surface of the scaffolds and the substrates were grown at the air/media interface for an additional 10 days. H&E staining (Fig 6A) suggested that keratinocytes proliferated and formed a stratified epidermal layer on top of the microporous scaffold surface. Conversely, keratinocytes grown on microporous 70:30 col/PCL scaffolds without embedded fibroblasts did not proliferate or stratify (Fig 6B). To better characterize the effects of the fibroblast-remodeled scaffolds on maturation of the keratinocyte layer, fibroblast-embedded constructs with an overlying keratinocyte layer (prepared as in panel A), were immunostained for expression of cytokeratin 10 (CK-10), a marker for well-differentiated keratinocytes. CK-10 expression was found selectively in the apical surface of the keratinocyte layer, consistent with normal keratinocyte differentiation (Fig 6C). Thus, keratinocytes grown on fibroblast-remodeled scaffolds recapitulate the normal cellular distribution and morphology of native epidermis.

Scaffold degradation and integration in vivo. Scaffolds are initially utilized as a support and infrastructure for the guidance of new tissue development. However, as more mature skin tissue forms, scaffolds should degrade within 3-4 weeks to avoid hindering complete tissue healing [22]. To measure scaffold degradation rate, 50:50 and 70:30 col/PCL scaffolds (acellular) were pre-stained with a red fluorescent dye, and implanted into full-thickness skin wounds created in the backskin of rats. Fluorescent and phase contrast images were taken of cross-sections from wounded tissues. NIS Elements BR software was used to quantify the area of scaffold remaining in the wound site. As shown in Fig 7, the 70:30 col/PCL scaffolds degraded more rapidly than 50:50 col/PCL scaffolds, with 70:30 col/PCL scaffolds exhibiting nearly complete degradation by 26 days. As well, there appeared to be faster integration of 70:30 col/PCL scaffolds into the native tissue. These results suggest that 70:30 col/PCL scaffolds are incorporated into newly formed skin tissue and degrade within an optimal time interval for a skin substitute.

Porous scaffolds promote faster wound closure than scaffolds lacking micropores. The studies above suggested that 70:30 col/PCL scaffolds with 160 μm pores provided the best balance between biochemical composition, biomechanics and biodegradability, and a permissive pore diameter for fibroblast infiltration and cell-directed matrix synthesis. We thus examined the efficacy of the scaffolds in stimulating wound healing. Three full-thickness critical-size wounds were created in the backskin of a rat. One was implanted with a 70:30 col/PCL scaffold with 160 μm pores, another with a 70:30 col/PCL scaffold lacking micropores, and the third wound was covered with gauze (sham). Images were

taken of the surface of the skin to monitor the rate of wound closure (n=5, representative image shown in Fig 8A). Wound closure was quantified at 7 and 14 days by measuring the area of unhealed tissue. Data were normalized by comparing the area of the scaffold-containing wound to the area of the corresponding sham wound for each animal. At 7 days following implantation, the amount of unhealed tissue associated with scaffolds lacking micropores, relative to the sham, was 97%, indicating that these scaffolds had a minimal effect on wound healing (“no-pores:sham ratio”, Fig 8B). In contrast, the amount of unhealed tissue present in wounds with porous scaffolds, relative to sham, was 67% at 7 days (“pores:sham ratio”, Fig 8B). Strikingly, the no-pores:sham ratio of unhealed tissue remained at 97% at 14 days (Fig 8C), underscoring the poor performance of electrospun scaffolds with insufficient porosity. For the wounds with microporous scaffolds, the unhealed tissue area had decreased further to 40% at 14 days (relative to shams) (Fig 8C).

Microporous scaffolds facilitate regeneration of more normal-appearing skin tissue. Scaffolds were implanted into full-thickness critical size skin wounds, and tissues were harvested for histology at 7, 14 and 21 days. H&E staining of the sham wounds showed a dense matrix, absent of follicles or other structures, consistent with scar tissue formation. For the wounds implanted with scaffolds with or without micropores, as well as the shams, the junction between the normal-appearing skin and abnormal scar-like tissue was designated (Fig 9A), and the area of abnormal tissue was quantified (Fig 9B). The area of abnormal tissue was significantly smaller at every time point in wounds implanted with

70:30 scaffolds with 160 μm pores as compared with scaffolds lacking micropores, or the shams.

We also examined higher-magnification images to better assess the quality of the newly-formed tissue. Defects implanted with 70:30 col/PCL scaffolds with 160 μm pores supported the rapid formation of an overlying epidermal layer with finger-like projections into the dermis, which function to strengthen the bond between the two layers of skin (Fig 10). It also appeared that microporous scaffolds facilitated earlier infiltration of new blood vessels when compared with defects implanted with standard electrospun scaffolds or the shams. Another notable feature was the architecture of the matrix. The newly-formed matrix within defects implanted with the microporous scaffolds had a loose, wavy appearance, similar to native skin (Fig 11). Conversely, the matrix within defects implanted with scaffolds lacking micropores or shams was markedly more compact. Finally, regenerated hair follicles were more numerous in wounds implanted with the microporous scaffolds (Figs 10, 11 & Table 2). These collective results suggest that electrospun scaffolds with micropores not only accelerate wound healing, but also stimulate greater regeneration of tissue approximating normal skin.

Discussion

There are numerous commercial skin graft products, along with many in the research phase, intended for use in the regeneration of damaged tissue [6, 23, 24]. However, an ideal skin graft material has yet to be developed [2]. Allogeneic or xenograft materials can elicit clinical challenges such as rejection, contraction, bleeding and infection, scar formation, and poor tissue formation [1, 2], whereas synthetic skin

substitutes often lack sufficient biologic information for effective scaffold integration. An optimal bioengineered skin equivalent must assimilate a number of critical features such as appropriate three-dimensional architecture, tensile properties, degradation kinetics, and cell-instructive biochemical cues [6].

Electrospinning is emerging as a promising approach for synthesizing regenerative scaffolds due to the: 1) relatively low cost and simplicity of this technology, 2) high capacity for blending multiple types of molecules within an ECM-like nanofibrous architecture, and 3) tunable control of scaffold biomechanics and degradation rate. A wealth of literature has highlighted the suitability of electrospun scaffolds to serve as supports for cells integral to tissue repair, such as dermal fibroblasts or mesenchymal stem cells [3, 25-29]. However the small pores created by the electrospinning process restrict cell infiltration and scaffold remodeling. In the current study, scaffolds were electrospun with varying ratios of collagen I and PCL to identify a formulation, 70:30 col/PCL, that provided the best support for fibroblast growth, while maintaining sufficient tensile strength, low contractility and a suitable degradation rate. Subsequently, pores were created mechanically, and an optimal pore diameter, 160 μm , was identified that enabled fibroblast infiltration and complete filling of the pores with fibroblast-secreted ECM molecules including fibronectin and collagen I. Functionality of fibroblast-remodeled 70:30 col/PCL porous scaffolds was evidenced by the finding that keratinocytes cultured on the scaffold surface differentiated and formed a stratified epidermal layer.

When implanted into critical-size full-thickness skin defects, 70:30 col/PCL scaffolds with 160 μm pores stimulated more rapid and effective wound healing

compared with scaffolds lacking micropores or sham wounds. Wound closure was accelerated in defects with the porous scaffolds, and the quality of the regenerated tissue was more similar to native skin. Additionally, a greater number of newly-generated hair follicles was observed within wounds grafted with microporous scaffolds. Given that stem cells are required for the regeneration of hair follicles [30], these data imply that stem cells were recruited from the surrounding unwounded skin tissue into the defect site. As well, in the first week after wounding, greater neovascularization was apparent in tissues with implanted microporous scaffolds. Taken together, these results underscore the importance of pore size for proper tissue healing. Similar to our studies, Xiao et al. reported that pores created in acellular dermal matrix (ADM) from bovine skin were essential for the imbibition of plasma from the wound bed to the outer surface. The ADM was suggested to act as an inducer for the formation of a “neodermis” by the infiltration of fibroblasts and blood vessels [14].

Another advantage of scaffolds with mechanically-generated pores is the feasibility for large-scale production. The use of a press-like device with microneedles is amenable to commercialization (as suggested by the Dermastamp device), and pores created in this manner have a homogeneous and well-defined size and spacing. A number of alternative electrospinning protocols have been developed to increase scaffold pore size [12, 31-35], however these have primarily been successful with scaffolds composed solely of synthetic polymers. These variant protocols become more challenging when the scaffolds incorporate biologic molecules, which is noteworthy given the extensive evidence pointing to the importance of biologic molecules for optimal cell survival and signaling [32, 36, 37]. Moreover, it may be difficult to achieve good reproducibility of

pore size and distribution when these alternate protocols are scaled-up for commercial distribution. An additional benefit of the mechanically-generated pores is that they are introduced following the synthesis of electrospun sheets. This approach would synergize with one of the key advantages of electrospinning, namely, the capacity to tailor scaffold biochemical composition to match tissue-specific ECMs. Mechanically-created pores can be introduced into any type of electrospun formulation. For example, through the use of co-spinning from multiple syringes, additional fibers composed of molecules such as elastin can be incorporated [38, 39], while co-axial spinning can be employed to deliver various growth factors and chemokines [40, 41]. The mechanical generation of pores is compatible with these developing technologies, and also offers a simpler and better-controlled strategy for increasing pore size when compared with methods such as the use of sacrificial fibers or particles.

In conclusion, 70:30 col/PCL scaffolds with 160 μm pores support dermal fibroblast infiltration and ECM deposition, and also serve as favorable substrates for keratinocyte proliferation and stratification. When implanted into full-thickness skin wounds, the microporous scaffolds promote faster and better healing than scaffolds lacking micropores. These results not only establish the critical importance of scaffold pore diameter (even for scaffolds with uncrosslinked, cleavable collagen I), but also highlight a practical method for producing effective regenerative skin substitutes.

Acknowledgements

This research was supported by a grant from the Skin Diseases Research Center at the University of Alabama, Birmingham (NIH P30 AR050948). Mr. Bonvallet was supported

by predoctoral fellowships funded by the NIH T32 training grant GM 008111-25, National Center for Advancing Translational Research of the NIH TL1TR000167, and the Howard Hughes Medical Institute through the Med into Grad Initiative 56005705. Ms. Culpepper was supported by NIH/NIDCR predoctoral fellowship 1F31DE021613. The authors are grateful for assistance from the UAB Skin Cell Culture Core Facility, supported by NIH grant# P30 AR050948, the High Resolution Imaging Core Facility, the Experimental Biomechanics Core, and the Virology Core Facility.

Disclosure Statement

The authors of this article have nothing to disclose.

References

1. Chern PL, Baum CL, Arpey CJ. Biologic dressings: current applications and limitations in dermatologic surgery. *Dermatol Surg*; 35:891. 2009.
2. Priya SG, Jungvid H, Kumar A. Skin tissue engineering for tissue repair and regeneration. *Tissue Eng Part B Rev*; 14:105. 2008.
3. Jayarama Reddy V, Radhakrishnan S, Ravichandran R, Mukherjee S, Balamurugan R, Sundarrajan S, Ramakrishna S. Nanofibrous structured biomimetic strategies for skin tissue regeneration. *Wound Repair Regen*; 21:11. 2012.
4. Atala A, Kasper FK, Mikos AG. Engineering complex tissues. *Sci Transl Med*; 4:160rv12. 2012.
5. Grover CN, Cameron RE, Best SM. Investigating the morphological, mechanical and degradation properties of scaffolds comprising collagen, gelatin and elastin for use in soft tissue engineering. *J Mech Behav Biomed Mater*; 10:62. 2012.
6. Zhong SP, Zhang YZ, Lim CT. Tissue scaffolds for skin wound healing and dermal reconstruction. *Wiley Interdiscip Rev Nanomed Nanobiotechnol*; 2:510. 2010.
7. Kumbar SG, James R, Nukavarapu SP, Laurencin CT. Electrospun nanofiber scaffolds: engineering soft tissues. *Biomed Mater*; 3:034002. 2008.
8. Venugopal J, Ramakrishna S. Biocompatible nanofiber matrices for the engineering of a dermal substitute for skin regeneration. *Tissue Eng*; 11:847. 2005.

9. Powell HM, Boyce ST. Engineered human skin fabricated using electrospun collagen-PCL blends: morphogenesis and mechanical properties. *Tissue Eng Part A*; 15:2177. 2009.
10. Cipitria A, Skelton A, Dargaville TR, Dalton PD, Hutmacher DW. Design, fabrication and characterization of PCL electrospun scaffolds-a review. *Journal of Materials Chemistry*; 21:9419. 2011.
11. Kelleher CM, Vacanti JP. Engineering extracellular matrix through nanotechnology. *J R Soc Interface*; 7 Suppl 6:S717. 2010.
12. Zhong S, Zhang Y, Lim CT. Fabrication of large pores in electrospun nanofibrous scaffolds for cellular infiltration: a review. *Tissue Eng Part B Rev*; 18:77. 2012.
13. Rnjak-Kovacina J, Weiss AS. Increasing the pore size of electrospun scaffolds. *Tissue Eng Part B Rev*; 17:365. 2011.
14. Xiao SC, Xia ZF, Ben DF, Tang HT, Wang GQ, Zhu SH, Yu WR. The role of pores in acellular dermal matrix substitute. *Ann Burns Fire Disasters*; 19:192. 2006.
15. Wang HM, Chou YT, Wen ZH, Wang ZR, Chen CH, Ho ML. Novel biodegradable porous scaffold applied to skin regeneration. *PLoS One*; 8:e56330. 2013.
16. Chiu Y-C, Cheng M-H, Engel H, Kao S-W, Larson JC, Gupta S, Brey EM. The role of pore size on vascularization and tissue remodeling in PEG hydrogels. *Biomaterials*; 32:6045. 2011.
17. Kondo T, Ishida Y. Molecular pathology of wound healing. *Forensic Science International*; 203:93. 2010.

18. Li WJ, Laurencin CT, Caterson EJ, Tuan RS, Ko FK. Electrospun nanofibrous structure: a novel scaffold for tissue engineering. *J Biomed Mater Res*; 60:613. 2002.
19. Stephenson AJ, Griffiths RW, La Hausse-Brown TP. Patterns of contraction in human full thickness skin grafts. *Br J Plast Surg*; 53:397. 2000.
20. Harrison CA, Gossiel F, Layton CM, Bullock AJ, Johnson T, Blumsohn A, MacNeil S. Use of an in vitro model of tissue-engineered skin to investigate the mechanism of skin graft contraction. *Tissue Engineering*; 12:3119. 2006.
21. Moulin V, Auger FA, Garrel D, Germain L. Role of wound healing myofibroblasts on re-epithelialization of human skin. *Burns*; 26:3. 2000.
22. Franco R, Nguyen T, Lee B-T. Preparation and characterization of electrospun PCL/PLGA membranes and chitosan/gelatin hydrogels for skin bioengineering applications. *Journal of Materials Science: Materials in Medicine*; 22:2207. 2011.
23. Philandrianos C, Andrac-Meyer L, Mordon S, Feuerstein JM, Sabatier F, Veran J, Magalon G, Casanova D. Comparison of five dermal substitutes in full-thickness skin wound healing in a porcine model. *Burns*; 38:820. 2012.
24. van der Veen VC, Boekema BK, Ulrich MM, Middelkoop E. New dermal substitutes. *Wound Repair Regen*; 19 Suppl 1:s59. 2011.
25. Rnjak-Kovacina J, Wise SG, Li Z, Maitz PK, Young CJ, Wang Y, Weiss AS. Tailoring the porosity and pore size of electrospun synthetic human elastin scaffolds for dermal tissue engineering. *Biomaterials*; 32:6729. 2011.

26. Rnjak J, Li Z, Maitz PK, Wise SG, Weiss AS. Primary human dermal fibroblast interactions with open weave three-dimensional scaffolds prepared from synthetic human elastin. *Biomaterials*; 30:6469. 2009.
27. Gholipour-Kanani A, Bahrami SH, Samadi-Kochaksaraie A, Ahmadi-Tafti H, Rabbani S, Kororian A, Erfani E. Effect of tissue-engineered chitosan-poly(vinyl alcohol) nanofibrous scaffolds on healing of burn wounds of rat skin. *IET Nanobiotechnol*; 6:129. 2012.
28. Kim HL, Lee JH, Lee MH, Kwon BJ, Park JC. Evaluation of electrospun (1,3)-(1,6)-beta-D-glucans/biodegradable polymer as artificial skin for full-thickness wound healing. *Tissue Eng Part A*; 18:2315. 2012.
29. Lu LX, Zhang XF, Wang YY, Ortiz L, Mao X, Jiang ZL, Xiao Z, Huang NP. Effects of hydroxyapatite-containing composite nanofibers on osteogenesis of mesenchymal stem cells in vitro and bone regeneration in vivo. *ACS Appl Mater Interfaces*; 5:319. 2012.
30. Yang CC, Cotsarelis G. Review of hair follicle dermal cells. *J Dermatol Sci*; 57:2. 2010.
31. Blakeney BA, Tambralli A, Anderson JM, Andukuri A, Lim DJ, Dean DR, Jun HW. Cell infiltration and growth in a low density, uncompressed three-dimensional electrospun nanofibrous scaffold. *Biomaterials*; 32:1583. 2011.
32. Phipps MC, Clem WC, Grunda JM, Clines GA, Bellis SL. Increasing the pore sizes of bone-mimetic electrospun scaffolds comprised of polycaprolactone, collagen I and hydroxyapatite to enhance cell infiltration. *Biomaterials*; 33:524. 2012.

33. Zhu X, Cui W, Li X, Jin Y. Electrospun fibrous mats with high porosity as potential scaffolds for skin tissue engineering. *Biomacromolecules*; 9:1795. 2008.
34. Nam J, Huang Y, Agarwal S, Lannutti J. Improved cellular infiltration in electrospun fiber via engineered porosity. *Tissue Eng*; 13:2249. 2007.
35. Leong MF, Rasheed MZ, Lim TC, Chian KS. In vitro cell infiltration and in vivo cell infiltration and vascularization in a fibrous, highly porous poly(D,L-lactide) scaffold fabricated by cryogenic electrospinning technique. *J Biomed Mater Res A*; 91:231. 2009.
36. Phipps MC, Clem WC, Catledge SA, Xu Y, Hennessy KM, Thomas V, Jablonsky MJ, Chowdhury S, Stanishevsky AV, Vohra YK, Bellis SL. Mesenchymal stem cell responses to bone-mimetic electrospun matrices composed of polycaprolactone, collagen I and nanoparticulate hydroxyapatite. *PLoS One*; 6:e16813. 2011.
37. Ravichandran R, Sundarrajan S, Venugopal JR, Mukherjee S, Ramakrishna S. Advances in polymeric systems for tissue engineering and biomedical applications. *Macromol Biosci*; 12:286. 2012.
38. Han J, Lazarovici P, Pomerantz C, Chen X, Wei Y, Lelkes PI. Co-electrospun blends of PLGA, gelatin, and elastin as potential nonthrombogenic scaffolds for vascular tissue engineering. *Biomacromolecules*; 12:399. 2011.
39. Almine JF, Bax DV, Mithieux SM, Nivison-Smith L, Rnjak J, Waterhouse A, Wise SG, Weiss AS. Elastin-based materials. *Chem Soc Rev*; 39:3371. 2010.
40. Ji W, Sun Y, Yang F, van den Beucken JJ, Fan M, Chen Z, Jansen JA. Bioactive electrospun scaffolds delivering growth factors and genes for tissue engineering applications. *Pharm Res*; 28:1259. 2011.

41. Sahoo S, Ang LT, Goh JC, Toh SL. Growth factor delivery through electrospun nanofibers in scaffolds for tissue engineering applications. *J Biomed Mater Res A*; 93:1539. 2010.

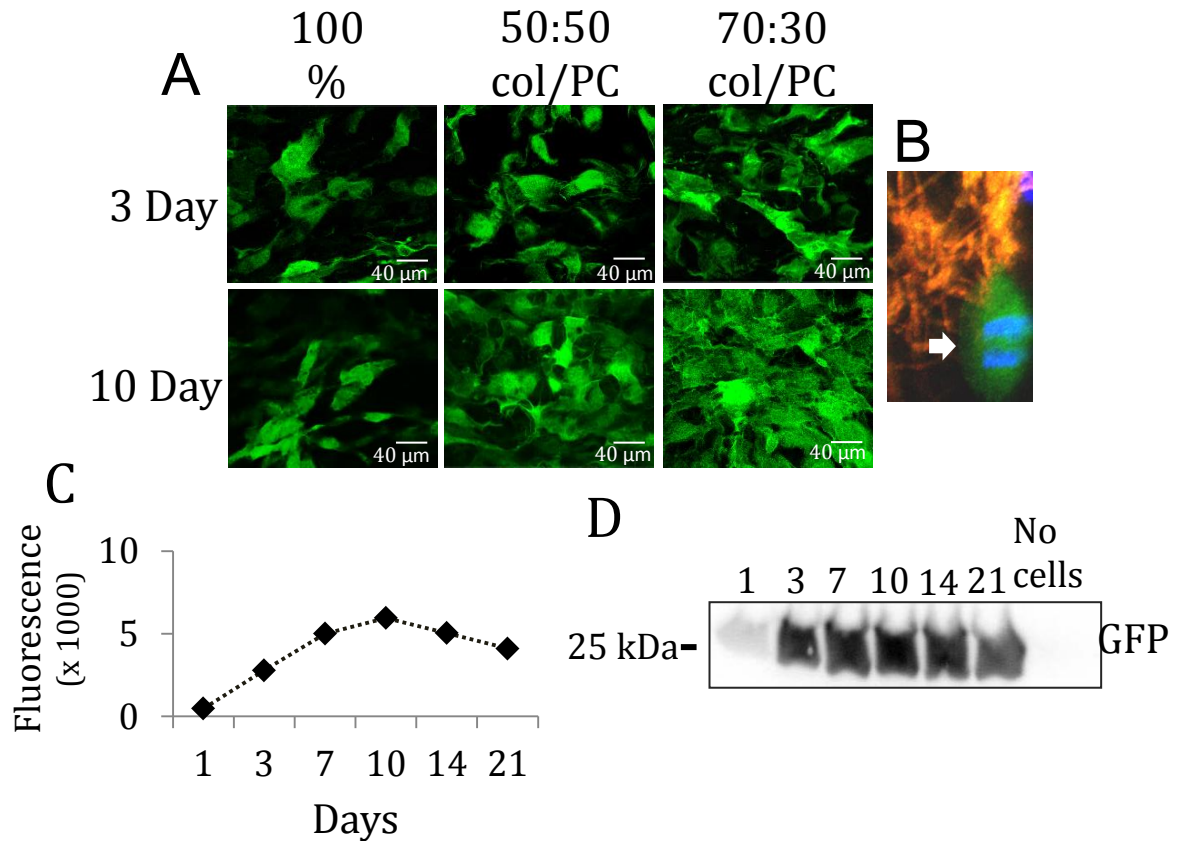


Figure 1: Fibroblast growth and proliferation on electrospun scaffolds composed of varying ratios of collagen I and PCL. A) GFP-expressing J2 fibroblasts were seeded onto scaffolds and allowed to grow for 3 or 10 days. Shown in the figure are representative images of cells grown on scaffolds of 100% PCL, 50% collagen I:50%PCL (50:50 col/PCL) and 70% collagen I:30%PCL (70:30 col/PCL). Scale bar = 40 μ m. B) Mitotic fibroblasts were apparent on 70:30 col/PCL scaffolds (arrow). In this experiment, the electrospun scaffold was stained with DiI dye to label scaffold fibers red. C) GFP-expressing J2 fibroblasts were grown on 70:30 col/PCL scaffolds over a 21 day time interval, and cell lysates were prepared at designated time points. Fluorometer readings were taken from lysates. D) Western Blot for GFP using lysates from the same samples used for fluorescence readings. As a negative control, homogenates were prepared from scaffolds lacking seeded fibroblasts ("no cells"). Each sample represents a pooled group of lysates from 6 distinct scaffolds, and two independent experiments were performed.

Note: From "Microporous Dermal-Like Electrospun Scaffolds Promote Accelerated Skin Regeneration" by P.P. Bonvallet, B.K. Culpepper, J.L. Bain, M.J. Schultz, S.J. Thomas, S.L. Bellis, 2014, Tissue Engineering Part A, Epub ahead of print. Copyright 2014 by Bonvallet et al. Reprinted with permission.

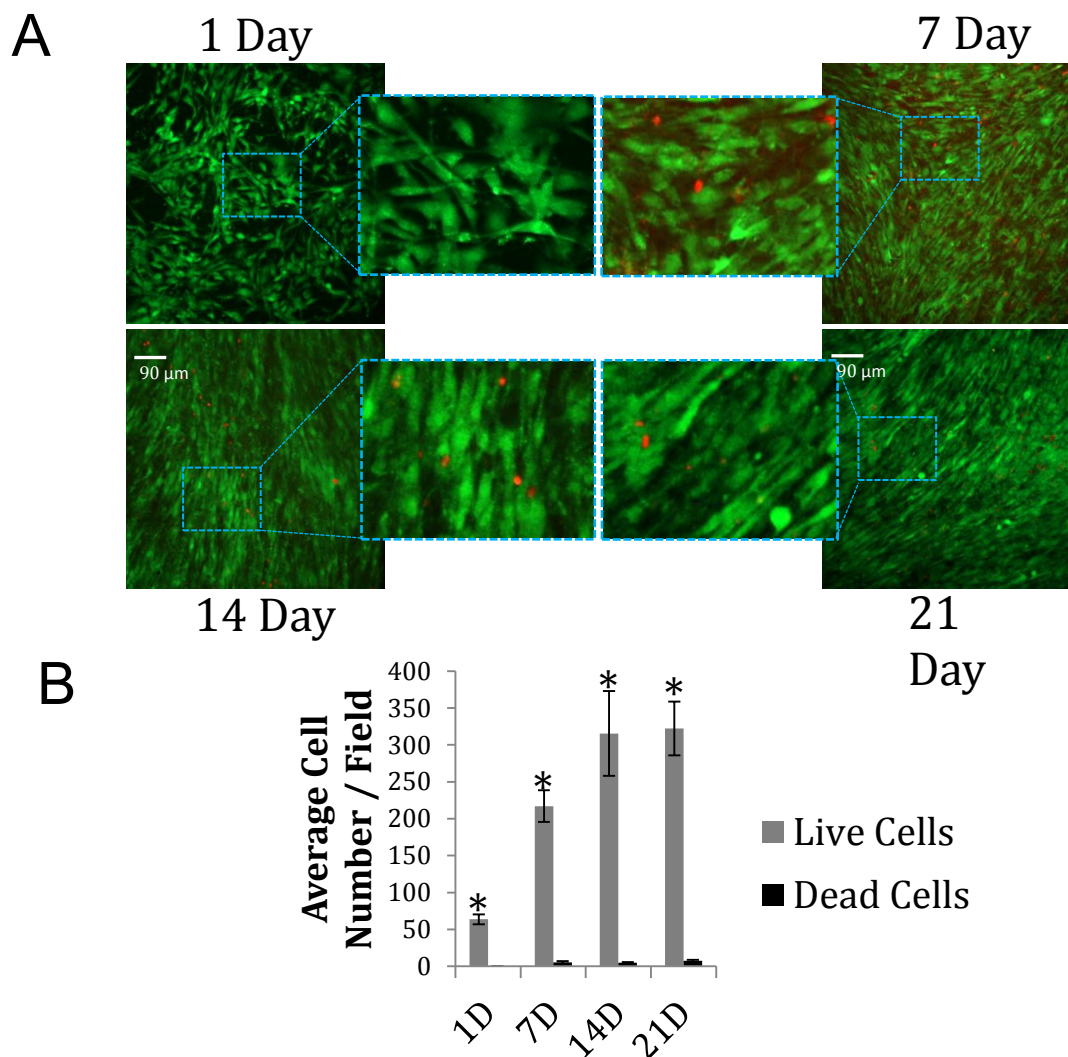
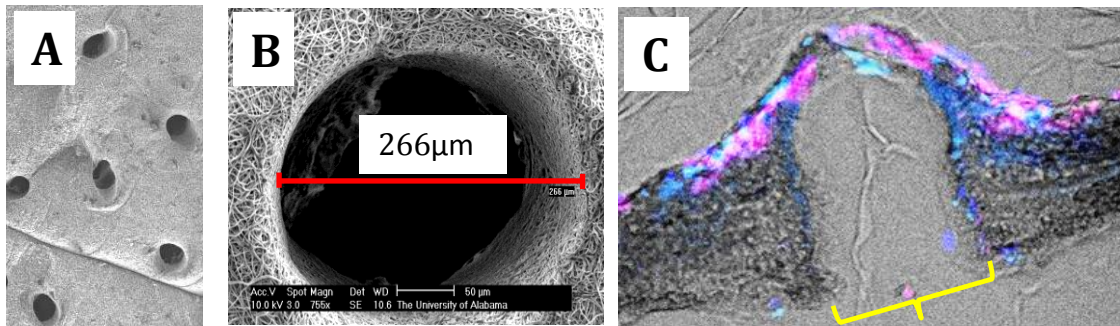


Figure 2: Fibroblast viability on 70:30 col/PCL scaffolds. A) Human fibroblasts (lacking GFP expression) grown on scaffolds for 1, 7, 14, or 21 days were stained for either living (green) or dead (red) cells. Scale bar = 90 μ m. B) Values represent means and standard error of the means measured for 4 distinct fields, detecting the amount of living and dead cells at each time point. Student t-tests were used to compare the number of live cells versus the number of dead cells. * represents significant difference ($p < 0.01$) relative to the dead cell number of the same day.

Note: From “Microporous Dermal-Like Electrospun Scaffolds Promote Accelerated Skin Regeneration” by P.P. Bonvallet, B.K. Culpepper, J.L. Bain, M.J. Schultz, S.J. Thomas, S.L. Bellis, 2014, Tissue Engineering Part A, Epub ahead of print. Copyright 2014 by Bonvallet et al. Reprinted with permission.

scaffolds with 250 μm pores



scaffolds with 160 μm pores

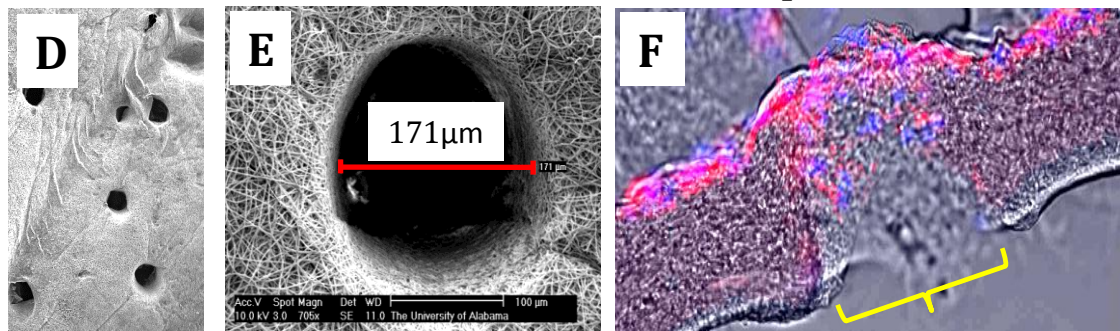


Figure 3: Infiltrating fibroblasts fill 160 μm , but not 250 μm , pores with matrix. A&B) SEM images of scaffolds with 250 μm pores. C) Human dermal fibroblasts were pre-loaded with red fluorescent nanocrystals, and seeded onto porous scaffolds. Samples were counterstained with Hoescht. Fluorescent images were overlaid with phase contrast images to show the scaffold area. D&E) SEM images of scaffolds with 160 μm pores. F) Fibroblasts loaded with red nanocrystals migrated into the 160 μm pores and deposited matrix. Samples were counterstained with Hoescht. Yellow brackets indicate a pore.

Note: From “Microporous Dermal-Like Electrospun Scaffolds Promote Accelerated Skin Regeneration” by P.P. Bonvallet, B.K. Culpepper, J.L. Bain, M.J. Schultz, S.J. Thomas, S.L. Bellis, 2014, Tissue Engineering Part A, Epub ahead of print. Copyright 2014 by Bonvallet et al. Reprinted with permission.

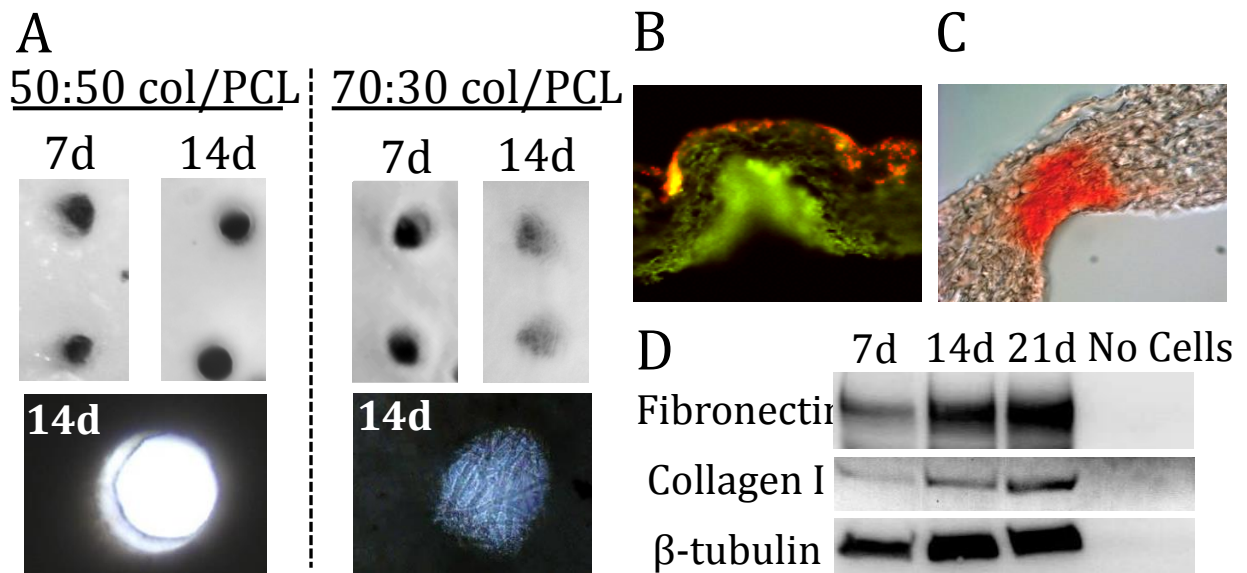


Figure 4: Extracellular matrix is deposited into the pores of 70:30 col/PCL scaffolds, but not 50:50 col/PCL scaffolds. A) Top view images of matrix deposition within pores at 7 and 14 days. Magnified images of 14-day samples reveal a fibrous matrix within pores of 70:30 col/PCL scaffolds. B) Fibronectin deposition within 70:30 col/PCL scaffolds with 160 μm pores was detected by immunofluorescent staining (green). Red staining reflects fibroblasts pre-loaded with red nanocrystals. C) Picrosirius Red was used to stain collagen in 70:30 col/PCL scaffolds with 160 μm pores. D) Immunoblotting for fibronectin, collagen I and β -tubulin was performed on homogenates prepared from microporous 70:30 col/PCL scaffolds with adherent fibroblasts grown for 7, 14 or 21 days. The “no cells” negative control homogenate was prepared from scaffolds that were not seeded with fibroblasts.

Note: From “Microporous Dermal-Like Electrospun Scaffolds Promote Accelerated Skin Regeneration” by P.P. Bonvallet, B.K. Culpepper, J.L. Bain, M.J. Schultz, S.J. Thomas, S.L. Bellis, 2014, Tissue Engineering Part A, Epub ahead of print. Copyright 2014 by Bonvallet et al. Reprinted with permission.

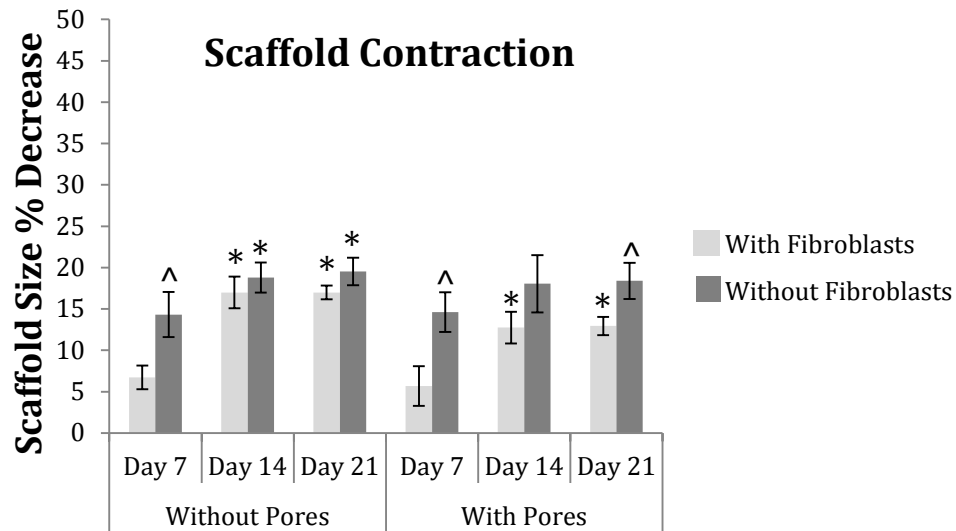


Figure 5: Contraction of 70:30 col/PCL scaffolds with or without 160 μ m pores and fibroblasts. Scaffolds were seeded with fibroblasts and scaffold diameters were measured at varying time intervals to quantify contraction. The same experiment was also performed without seeded fibroblasts. Values represent means and standard deviation for 5 scaffolds per group and two independent experiments were performed. Student t-tests were used to compare the percent change in scaffold contraction of the various groups. * represents significant difference ($p<0.01$) relative to 7 day sample of the same group. ^ represents significant difference ($p<0.05$) compared with scaffolds with fibroblasts for the same time point.

Note: From “Microporous Dermal-Like Electrospun Scaffolds Promote Accelerated Skin Regeneration” by P.P. Bonvallet, B.K. Culpepper, J.L. Bain, M.J. Schultz, S.J. Thomas, S.L. Bellis, 2014, Tissue Engineering Part A, Epub ahead of print. Copyright 2014 by Bonvallet et al. Reprinted with permission.

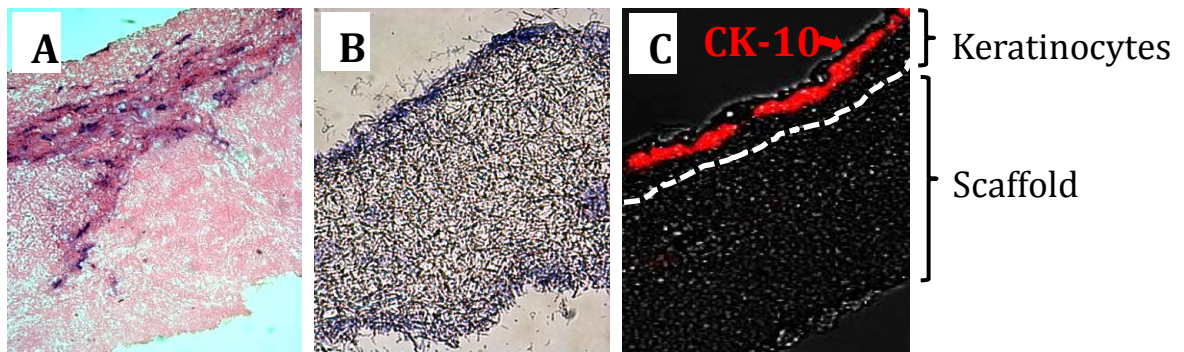


Figure 6: Keratinocytes proliferate and form a stratified epidermal layer on the surface of fibroblast-remodeled scaffolds. A) Fibroblast-remodeled 70:30 col/PCL scaffolds with 160 μm pores were seeded with keratinocytes and allowed to grow at the air-liquid interface for 10 days. Samples were stained with H&E to reveal the epidermal layer. B) 70:30 col/PCL microporous scaffolds lacking fibroblasts were seeded with keratinocytes and grown at the air-liquid interface for 10 days. H&E staining showed that keratinocytes do not stratify on the surface of scaffolds without embedded fibroblasts. C) Fibroblast-remodeled scaffolds with an overlying keratinocyte layer were immunostained for CK-10 (red), a marker for terminally differentiated keratinocytes.

Note: From “Microporous Dermal-Like Electrospun Scaffolds Promote Accelerated Skin Regeneration” by P.P. Bonvallet, B.K. Culpepper, J.L. Bain, M.J. Schultz, S.J. Thomas, S.L. Bellis, 2014, Tissue Engineering Part A, Epub ahead of print. Copyright 2014 by Bonvallet et al. Reprinted with permission.

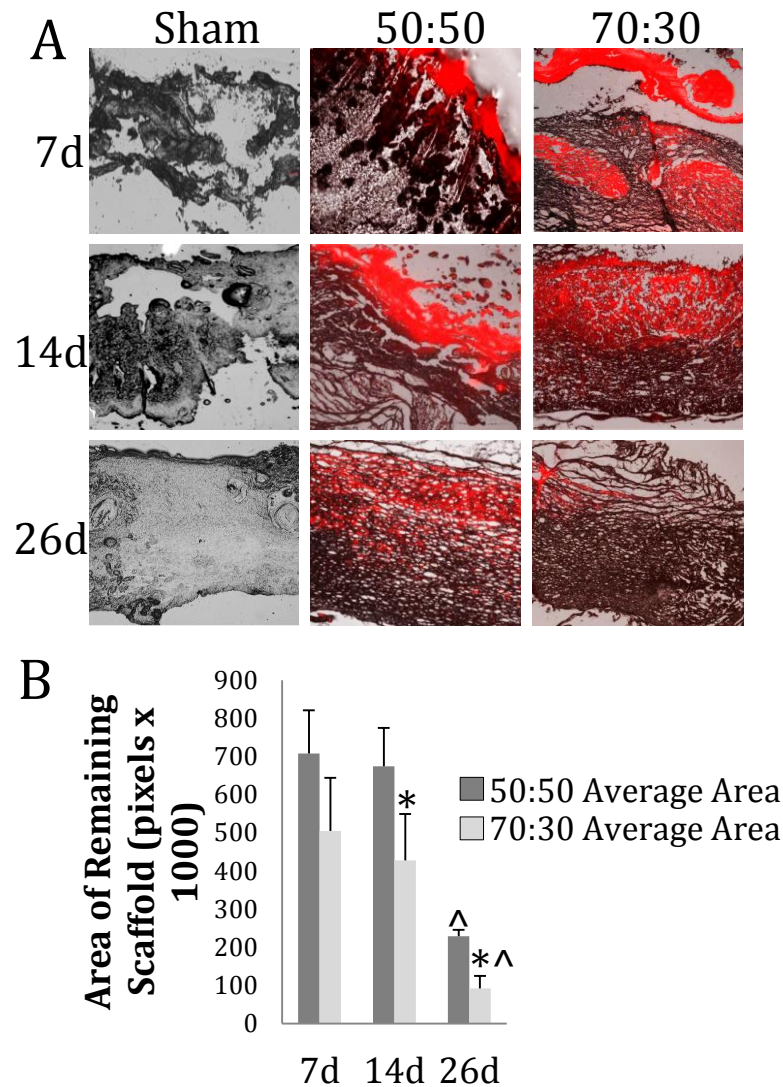


Figure 7: 70:30 col/PCL scaffolds degrade more rapidly than 50:50 col/PCL scaffolds. A) Scaffolds were stained a fluorescent red with DiI and implanted into rat full thickness skin wound defects. At 7, 14, and 26 days, tissue was harvested, sectioned and imaged to assess degradation (n=5). B) Area of remaining fluorescent scaffold was analyzed using NIS Elements software. Student t-tests were used to compare the area of remaining scaffold of the various groups for all time points. * = significantly different ($p < 0.05$) than 50:50 scaffolds of the same day. ^ = significantly different ($p < 0.05$) than 7 and 14 days of the same group.

Note: From “Microporous Dermal-Like Electrospun Scaffolds Promote Accelerated Skin Regeneration” by P.P. Bonvallet, B.K. Culpepper, J.L. Bain, M.J. Schultz, S.J. Thomas, S.L. Bellis, 2014, Tissue Engineering Part A, Epub ahead of print. Copyright 2014 by Bonvallet et al. Reprinted with permission.

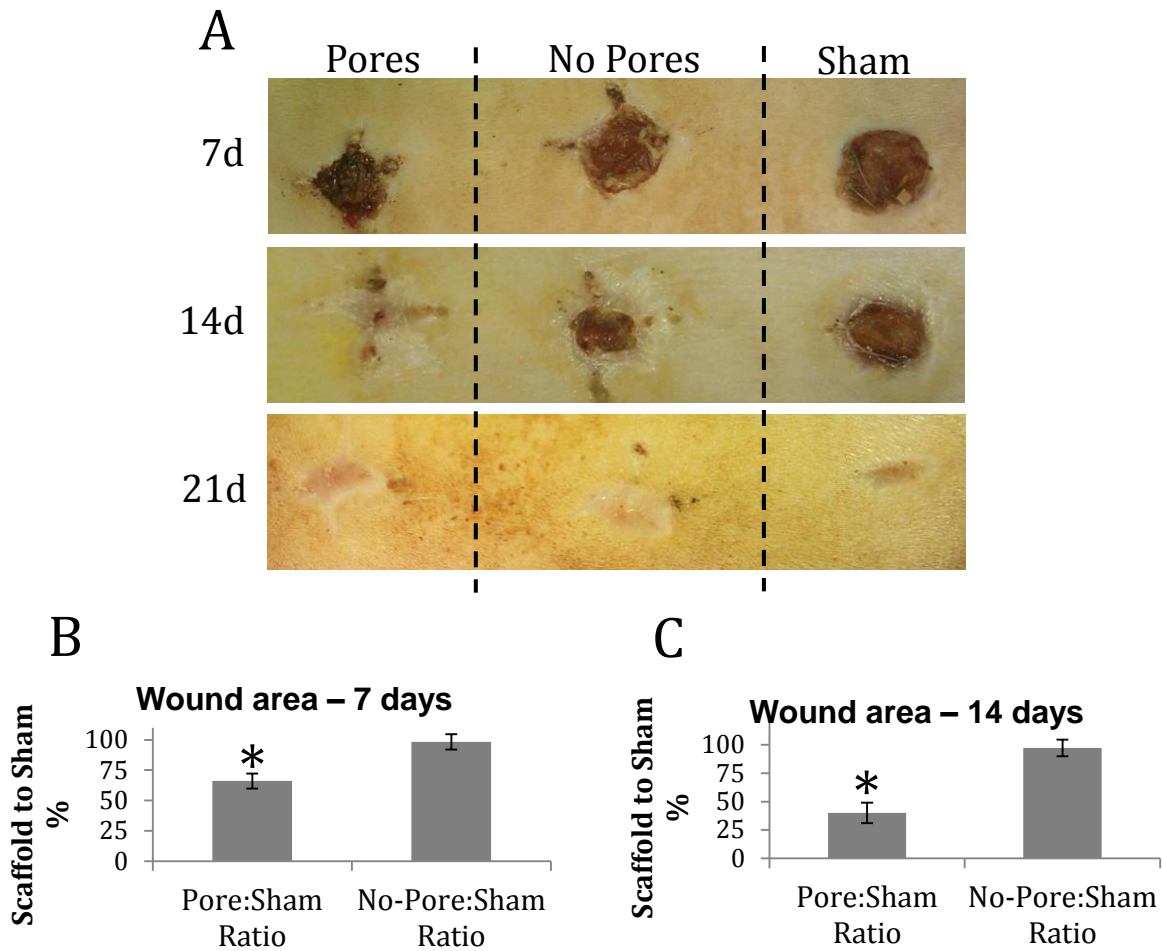


Figure 8: More rapid wound closure is observed for critical size defects implanted with porous scaffolds. A) Three side-by-side full thickness wounds were created in the backskin of a rat. One wound was implanted with 70:30 col/PCL scaffolds with 160 μm pores (“Pores”), another wound was implanted with 70:30 col/PCL scaffolds lacking pores (“No Pores”), and the third wound was covered with gauze (“Sham”). Shown in the figure are representative images of the backskin of individual rats imaged at 7, 14 or 21 days following implantation. B&C) The area of unhealed wound at 7 and 14 days was measured with image J software and values for the wounds implanted with scaffolds were normalized to the area of the sham for each animal ($n = 5$ animals). Student t-tests were used to compare pores:sham ratio with no pores:sham ratio. * = significant difference ($p < 0.05$) relative to no pores:sham group.

Note: From “Microporous Dermal-Like Electrospun Scaffolds Promote Accelerated Skin Regeneration” by P.P. Bonvallet, B.K. Culpepper, J.L. Bain, M.J. Schultz, S.J. Thomas, S.L. Bellis, 2014, Tissue Engineering Part A, Epub ahead of print. Copyright 2014 by Bonvallet et al. Reprinted with permission.

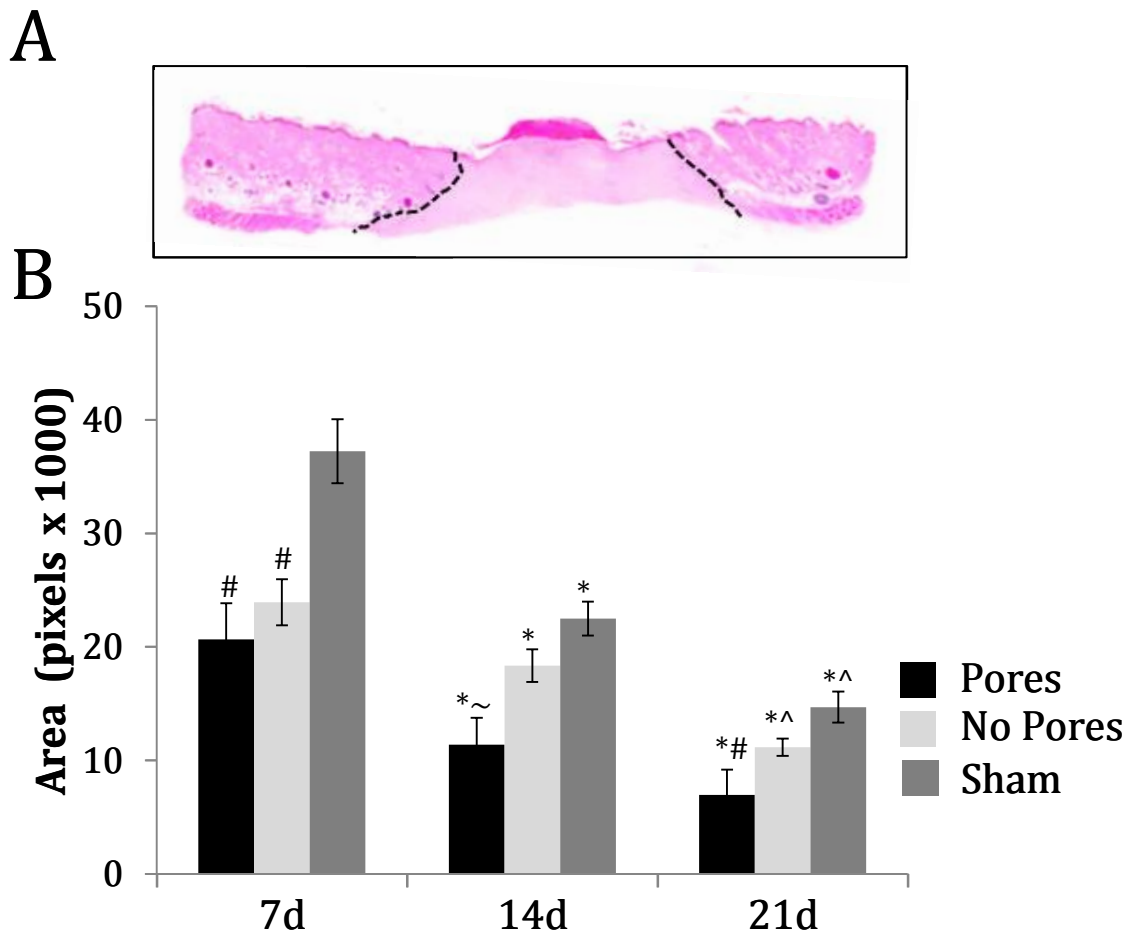


Figure 9: Scaffolds with micropores promote more effective tissue regeneration. A) Cross-section of rat skin tissue undergoing the wound healing process. Black lines designate areas of abnormal tissue morphology. B) Graph depicts average abnormal tissue areas for scaffolds with or without micropores or sham wounds. * represents significant difference ($p < 0.01$) compared to day 7 of the respective group; ^ represents significant difference ($p < 0.05$) relative to day 14 of the respective group; # represents significant difference ($p < 0.02$) relative to sham of the same day; ~ represents significant difference ($p < 0.05$) relative to sham and no pore samples of the same day. Error bars represent standard deviation.

Note: From “Microporous Dermal-Like Electrospun Scaffolds Promote Accelerated Skin Regeneration” by P.P. Bonvallet, B.K. Culpepper, J.L. Bain, M.J. Schultz, S.J. Thomas, S.L. Bellis, 2014, Tissue Engineering Part A, Epub ahead of print. Copyright 2014 by Bonvallet et al. Reprinted with permission.

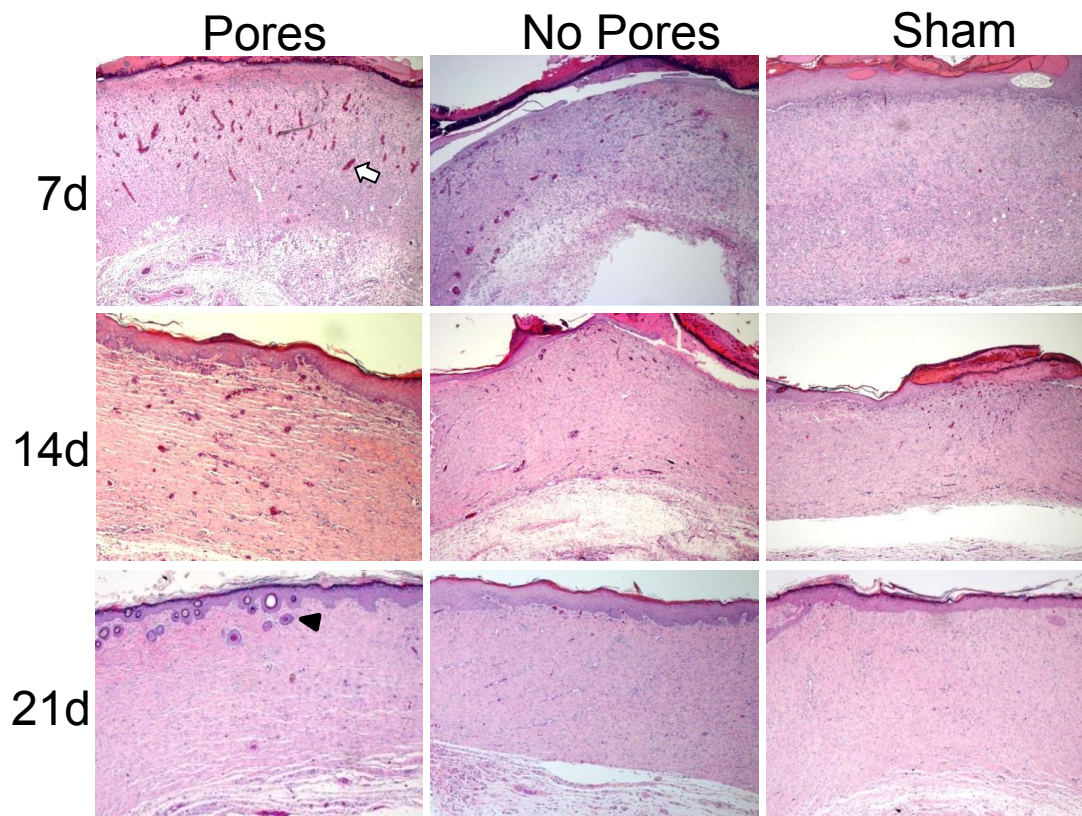


Figure 10: 4x images of wound healing at 7, 14 and 21 days following implantation. Blood vessel formation is apparent in porous and non-porous 70:30 col/PCL scaffolds as early as 7 days (white arrow indicates a representative blood vessel). The epidermis in wounds containing 70:30 col/PCL scaffolds with 160 μm pores forms finger-like projections into the dermis, similar to normal unwounded epidermis. Hair follicle formation can also be seen in wounds containing microporous scaffolds (black arrowhead indicates a representative hair follicle).

Note: From “Microporous Dermal-Like Electrospun Scaffolds Promote Accelerated Skin Regeneration” by P.P. Bonvallet, B.K. Culpepper, J.L. Bain, M.J. Schultz, S.J. Thomas, S.L. Bellis, 2014, Tissue Engineering Part A, Epub ahead of print. Copyright 2014 by Bonvallet et al. Reprinted with permission.

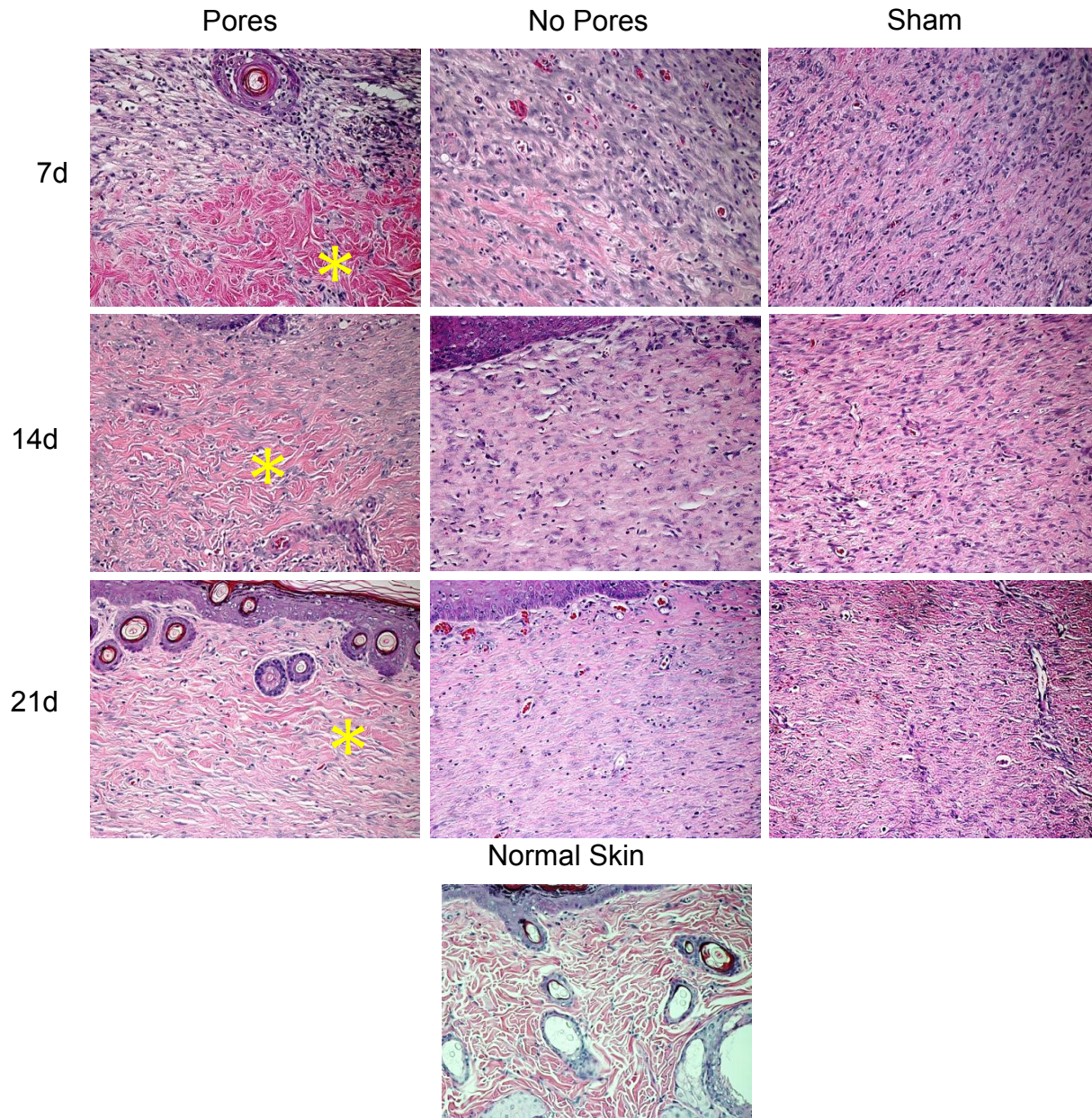


Figure 11: 20x images of wound healing over a 21 day time period show the structure of the matrix. The structure of the matrix within wounds implanted with 70:30 col/PCL scaffolds with 160 μm pores appears more similar to normal skin, evidenced by a loose, wavy matrix (yellow asterisk) and formation of new hair follicles.

Note: From “Microporous Dermal-Like Electrospun Scaffolds Promote Accelerated Skin Regeneration” by P.P. Bonvallet, B.K. Culpepper, J.L. Bain, M.J. Schultz, S.J. Thomas, S.L. Bellis, 2014, Tissue Engineering Part A, Epub ahead of print. Copyright 2014 by Bonvallet et al. Reprinted with permission.

Table 1

Tensile testing of porous and non-porous scaffolds. Stress/strain values were calculated from tensile testing performed on scaffolds. Three different scaffold compositions, with or without pores, were evaluated. Values represent the means and standard deviation from 6 distinct scaffolds per group. * represents $p < .05$ compared to porous scaffolds of the same scaffold formulation.

Scaffold	Tensile Strength (MPa)	Strain
100% PCL - No Pores	4.25 ± 0.96	0.44 ± 0.20 *
100% PCL - Pores	4.32 ± 0.50	0.62 ± 0.03
50/50 col/PCL - No Pores	2.87 ± 0.75	1.09 ± 0.25
50/50 col/PCL - Pores	2.90 ± 0.70	1.30 ± 0.15
70/30 col/PCL - No Pores	2.17 ± 0.33 *	1.14 ± 0.14 *
70/30 col/PCL - Pores	1.40 ± 0.32	0.56 ± 0.16

Note: From “Microporous Dermal-Like Electrospun Scaffolds Promote Accelerated Skin Regeneration” by P.P. Bonvallet, B.K. Culpepper, J.L. Bain, M.J. Schultz, S.J. Thomas, S.L. Bellis, 2014, Tissue Engineering Part A, Epub ahead of print. Copyright 2014 by Bonvallet et al. Reprinted with permission.

Table 2. Number of newly formed hair follicles. The number of hair follicles was counted in different samples over a 21 day time frame. 5 fields were chosen for each specimen and the number of newly formed hair follicles was tallied (n= 5 animals per group).

Days	Pores	No Pores	Sham
7 Day	15	10	0
14 Day	29	13	5
21 Day	56	21	9

Note: From “Microporous Dermal-Like Electrospun Scaffolds Promote Accelerated Skin Regeneration” by P.P. Bonvallet, B.K. Culpepper, J.L. Bain, M.J. Schultz, S.J. Thomas, S.L. Bellis, 2014, Tissue Engineering Part A, Epub ahead of print. Copyright 2014 by Bonvallet et al. Reprinted with permission.

MICROPOROUS DERMAL-MIMETIC ELECTROSPUN SCAFFOLDS PRE-SEEDED
WITH FIBROBLASTS PROMOTE TISSUE REGENERATION IN FULL-
THICKNESS SKIN WOUNDS

by

PAUL P. BONVALLET, MATTHEW J. SCHULTZ, ELIZABETH H. MITCHELL,
JENNIFER L. BAIN, BONNIE K. CULPEPPER, STEVEN J. THOMAS, SUSAN L.
BELLIS

In preparation for Tissue Engineering Part A
Format adapted for dissertation

Abstract

The goal of this study was to assess the skin regenerative properties of microporous electrospun scaffolds pre-seeded with dermal fibroblasts. In previous studies we showed that a 70% collagen I and 30% poly(ϵ -caprolactone) electrospun scaffold (70:30 col/PCL) containing 160 μ m diameter pores had favorable mechanical properties, supported cell infiltration and matrix secretion, and promoted more rapid and effective in vivo skin regeneration when compared to scaffolds lacking micropores. In the current study we tested the hypothesis that regenerative potential of the 70:30 col/PCL microporous scaffolds can be further enhanced by seeding scaffolds with dermal fibroblasts prior to implantation. To address this hypothesis, a Fischer 344 (F344) rat syngeneic model was employed. In vitro studies showed that dermal fibroblasts isolated from F344 rat skin were able to adhere and proliferate on 70:30 col/PCL microporous scaffolds, and the cells also filled the 160 μ m pores with native ECM proteins such as collagen I and fibronectin. Additionally, scaffolds seeded with F344 fibroblasts exhibited a low rate of contraction (~14%) over a 21 day time frame. To assess regenerative potential, scaffolds with or without seeded F344 dermal fibroblasts were implanted into full thickness, critical size defects created in F344 hosts. Specifically, we compared: microporous scaffolds containing fibroblasts seeded for 4 days; scaffolds containing fibroblasts seeded for 1 day; acellular microporous scaffolds; and a sham wound (no scaffold). Scaffolds containing fibroblasts seeded for 4 days had the best response of all treatment groups with respect to accelerated wound healing, a more normal-appearing dermal matrix structure, and hair follicle regeneration. Collectively, these results suggest

that microporous electrospun scaffolds pre-seeded with fibroblasts promote greater wound-healing than microporous scaffolds alone.

Introduction

Skin tissue serves numerous functions such as forming the first line of defense against invading pathogens, protection from physical insults, storage of water and lipids, and touch and pain sensation. The gold standard therapy for severely damaged skin is autografting; however, this is only an option if the patient has sufficient unwounded skin tissue for transplantation [1]. The limited amount of available donor autograft tissue, secondary wound site creation, and uneven appearance of the regenerated skin due to meshing of the donor tissue are undesirable features of autografting, prompting the need for alternative approaches. Alternative therapies include allografts and xenografts [2, 3], but these also have limitations such as graft contraction, weak mechanical properties, rejection, and scar formation [4, 5]. For these reasons, numerous groups are engineering graft materials that can substitute for the current therapies [6-8].

Engineered scaffolds typically consist of synthetic polymers such as poly (ϵ -caprolactone) (PCL), natural biochemical compounds, or a combination of both. Synthetic polymers are used in grafts because they are FDA approved, biodegradable, and have favorable mechanical characteristics [9]. Natural materials such as collagen, hyaluronan, and elastin are used because they promote cell attachment and survival, and mimic the ECM environment native to human skin. However, scaffolds derived from natural ECM molecules often have low mechanical strength and fast degradation rates. Therefore, many groups combine natural and synthetic materials to create scaffolds that have cell instructive biochemical elements as well as suitable mechanical properties.

While many technologies for generating composite scaffolds are currently being investigated, electrospinning represents a promising approach. Electrospun scaffolds have a high surface to volume ratio, which promotes cell adhesion, interconnected pores that facilitate nutrient transport and waste removal, and nanofibers that resemble native ECM [10, 11].

For skin regeneration, electrospun materials have one major shortfall; nanopores spanning the scaffold are too small to allow efficient fibroblast migration throughout the entirety of the scaffold [12]. Many groups are investigating ways to increase the pore size of electrospun scaffolds by using methods such as inclusion of sacrificial particles or fibers, or through changes in the electrospinning apparatus and/or protocol [13, 14].

While some of these approaches have been successful, disadvantages include the difficulty in achieving reproducible pore size and distribution, the need for complicated or expensive experimental set-ups, and the possibility of residual cytotoxic material from sacrificial elements. To address this issue, our group has investigated a cost-effective and simple approach for increasing scaffold pore size [15]. Specifically, micropores were created mechanically in electrospun scaffolds using acupuncture needles. This method generates pores of well-defined microscale diameter, and can be applied to any type of electrospun formulation.

Our prior studies focused on developing a skin regenerative scaffold with optimal biochemical composition, mechanical properties, biodegradability, and pore diameter for cell infiltration. We examined multiple scaffold compositions and determined that a combination of 70% collagen I and 30% PCL (70:30 col/PCL) yielded a substrate that supported dermal fibroblast attachment and proliferation, while still maintaining

appropriate mechanical properties for skin tissue regeneration [15]. Additionally, it was found that the introduction of 160 μm pores into the 70:30 col/PCL scaffolds enhanced fibroblast infiltration, as well as fibroblast-mediated filling of the micropores with native ECM molecules. To evaluate regenerative potential of the 70:30 scaffolds with 160 μm pores, scaffolds were implanted into full-thickness skin defects. When compared with scaffolds lacking micropores or sham wounds, the 70:30 scaffolds with 160 μm pores expedited the wound healing process, assisted in re-epithelialization and follicle regeneration, and promoted the formation of dermal tissue with a basket-weave matrix architecture, resembling normal, unwounded skin.

A wealth of recent literature has stressed the importance of pre-seeding skin or stem cells on a scaffold prior to implantation in order to, “jump start,” the ECM remodeling process and rate of implant integration [16-19]. The goal of the current study was to determine whether 70:30 col/PCL microporous scaffolds with pre-seeded dermal fibroblasts have a greater regenerative capacity than acellular microporous scaffolds. A syngeneic Fischer 344 (F344) rat model was used to evaluate the performance of fibroblast-seeded scaffolds. We first conducted in vitro studies to confirm that, as with human dermal fibroblasts, F344 fibroblasts proliferated on 70:30 col/PCL scaffolds with 160 μm pores, and filled the micropores with ECM. Subsequently, scaffolds pre-seeded with F344 fibroblasts for either 1 or 4 days, or alternatively, acellular microporous scaffolds, were implanted into full-thickness critical size skin defects created in F344 hosts. It was found that scaffolds pre-seeded with fibroblasts for 4 days stimulated the greatest degree of skin regeneration, although both of the fibroblast-seeded scaffolds promoted better skin healing than acellular scaffolds or sham wounds.

Materials and Methods

Preparation of electrospun scaffolds

Hexafluoroisopropanol (HFP) (Sigma), an organic solvent, was used to dissolve 70% collagen I and 30% PCL into solution. The collagen I was derived from calf skin (MP Biomedicals) and the 10,000 Da PCL was purchased from Scientific Polymer Products. After the solution was taken up into a 3-cc syringe with a 27-gauge needle, it was ejected at a constant 2 mL/h rate by the use of a syringe pump (Harvard Apparatus). The needle was charged with 20 KV (Gamma High Voltage Research) so that when the solution was ejected, it naturally traveled 20 cm horizontally to a grounded collecting plate. The collecting plate was covered in a thin aluminum sheet and rotated at 20 rpm for even fiber distribution. Scaffolds were then placed in a desiccator for 24 h to remove any residual HFP. A Humboldt Boring Machine (Fisher) was used to punch scaffolds to size. Micropores were created mechanically using 160 μ m acupuncture needles as described in (15).

Fischer 344 cells and cell culture

A syngeneic Fischer 344 (F344) rat model was employed in order to prevent rejection of implanted cells in in vivo studies. Dermal fibroblasts were isolated from Fischer 344 rat skin by the Skin Cell Culture Core Facility at the University of Alabama at Birmingham (UAB). F344 cells were cultured in Dulbecco's modified Eagle's medium that was supplemented with 10% fetal bovine serum (FBS) and 1% penicillin/streptomycin/amphotericin solution (Invitrogen). All studies were performed with fibroblasts from passages 3-5.

Cell viability and proliferation on scaffolds

F344 fibroblasts were allowed to grow on scaffolds for varying time intervals between 1 and 14 days. At each time point, the scaffolds were submerged in a live/dead cell imaging solution (Life Technologies) for 15 min. Live cells were stained green and dead cells red. The scaffolds were then rinsed in phosphate-buffered saline (PBS) and imaged on a Nikon confocal microscope. In order to determine the number of live and dead cells, the Volocity image analysis software program was used to count cells.

Scaffold contraction

F344 fibroblasts were seeded onto microporous electrospun scaffolds and grown in culture for up to 21 days. At each time point, the diameters of 5 separate scaffolds per group were measured with calipers (Fisher). The initial diameter was also measured so that the difference in diameters could be determined, and the percent contraction calculated.

Fibroblast-mediated ECM deposition into scaffold pores

F344 fibroblasts (35,000 cells) were seeded onto 14 mm diameter microporous scaffolds and allowed to grow for up to 14 days. At each time point, matrix deposition was visualized by the use of a phase-contrast dissecting microscope. Also, fibrous collagen was visualized in these scaffolds by using a picosirius red stain kit (Polysciences, Inc.) on scaffolds that had been OTC embedded, vertically cross-sectioned, and fixed in 4% paraformaldehyde. Furthermore, immunoblots were performed to evaluate fibronectin and collagen I. At each time point following cell

seeding, five separate scaffolds were combined together, rinsed in PBS, frozen in liquid nitrogen, and pulverized using a cryo-pulverizer. A 50 mM Tris buffer (pH 7.4) cell lysate solution containing 150 mM NaCl, 1% Triton X-100, 1% deoxycholate, 0.1% SDS, 5 mM EDTA, and 0.5% Igepal was used to lyse cells in scaffolds. Scaffold homogenates were centrifuged at 15,000 g for 20 min, and supernatants collected. Samples were resolved by SDS-PAGE, and transferred to a polyvinylidene fluoride (PVDF) membrane. Membranes were blocked in 5% milk, incubated with primary antibodies against fibronectin and collagen I (Abcam) and then with secondary antibody. A BioRad ChemiDoc imaging system was used for imaging.

Scaffold implantation into full-thickness skin defects

All animal procedures were performed with approval from the Institutional Animal Care and Use Committee (IACUC) at UAB. Four 15-mm-diameter full-thickness skin defects were created side-by-side in the back skin of F344 rats (n=5). One of the wounds was implanted with a 70:30 col/PCL microporous scaffold lacking any cells; a second defect was implanted with a 70:30 col/PCL microporous scaffold seeded with fibroblasts for 4 days, and a third defect was implanted with a 70:30 col/PCL microporous scaffold seeded with fibroblasts for 1 day. Scaffolds were sutured into place. The fourth wound was left open to heal on its own (sham). At 7, 14, and 21 days, the tissues containing scaffolds were harvested, paraffin embedded, sectioned, and H&E stained. Whole field images were taken with a Nikon microscope and the abnormal tissue area, as well as the basket-weave matrix resembling native skin tissue, were measured with Image J analysis software. Representative images were also taken in order to

demonstrate wound healing characteristics such as re-epithelialization, hair follicle development, and blood vessel formation.

Results

Viability of fibroblasts grown on scaffolds.

To determine whether cells were able to adhere to, and survive on, the scaffolds, we performed live/dead cell staining on scaffolds cultured with F344 fibroblasts for 1, 4, 7, or 14 days. As shown in Fig 1A, the number of viable cells appeared to increase over the 14 day interval, consistent with active cell proliferation, and by 14 days the cells were confluent. Quantification of the staining (Fig 1B) confirmed an increase in viable cell number from 1 to 14 days, and also indicated that cell death was minimal.

Fibroblast-seeded scaffolds have low contraction rates.

Contraction is normal in the wound healing process; however, if excessive contraction of the scaffold occurs, pain, scarring and immobility can result, causing sub-optimal healing [20]. Accordingly, we examined the degree of contraction exhibited by microporous scaffolds seeded with F344 fibroblasts for varying time intervals (Fig 2). We observed an 11.3% decrease in scaffold size at 24 hours after seeding with fibroblasts. By 4 days, the amount of scaffold contraction leveled off at around 14%. These in vitro contraction rates cannot be directly compared to scaffold contraction within the wound bed; however, we believe that 14% contraction is an acceptable value, given that many current commercial products can have contraction rates up to 50% [21, 22].

Infiltrating fibroblasts deposit ECM into scaffold micropores.

F344 fibroblasts were seeded onto microporous scaffolds and allowed to grow and secrete matrix for up to 14 days. At 3, 7, 10, and 14 days post cell-seeding, 20X top view images were taken to assess fibrous matrix deposition. It is apparent from the images in Fig 3 that ECM deposition occurred gradually, with a small amount of pore filling observed within 3 days, and complete pore filling by 14 days.

To further characterize matrix deposition, scaffolds were stained with picrosirius red to detect fibrillar forms of collagen. Collagen deposition is crucial for the wound healing process. As shown in Fig 4A, picrosirius red staining was enriched within the region of the micropore, suggesting that fibroblasts were filling the pores with collagen fibers (note that the electropun fibers also have some staining due to the blended collagen/PCL composition). We also evaluated deposition of fibronectin within scaffolds, as fibronectin is one of the critical ECM molecules within provisional wound healing matrices. To quantify fibronectin deposition, scaffolds seeded with fibroblasts for varying time intervals were homogenized and fibronectin was detected by immunoblotting (Fig 4B). The amount of fibronectin appeared to increase over time. Immunoblotting was similarly performed for collagen I, and it was found that collagen I deposition also accumulated from day 1 to day 14.

Scaffolds pre-seeded with fibroblasts facilitate regeneration of more normal appearing skin tissue than acellular scaffolds.

Having shown that the scaffolds provided good support for fibroblast growth and ECM deposition, our next objective was to assess the capacity of scaffolds to promote wound healing when implanted into full-thickness critical size skin defects. We hypothesized that fibroblast-containing scaffolds with matrix-filled pores would enhance

wound healing when compared with acellular microporous scaffolds. Given that maximal pore filling was observed by approximately 10 days after cell seeding, our initial plan was to implant scaffolds cultured with fibroblasts for 10 days. However, after 10 days of culture, the scaffold handling properties had diminished greatly, and the scaffolds were too fragile to suture into place. Therefore, we adjusted our seeding time points to 1 and 4 days. Notably, some degree of matrix deposition is observed within pores by 3 days after seeding (Fig 3).

Scaffolds cultured with F344 fibroblasts for 1 or 4 days were implanted into 15 mm-diameter full thickness defects created in the backskin of F344 rats. Scaffolds lacking seeded fibroblasts were also implanted into defects to assess the importance of cellular factors, including secreted ECM, in the wound healing response. Additionally, we created sham wounds (no scaffold) as a control. At 7, 14, and 21 days after implantation, the scaffolds and surrounding tissues were harvested, paraffin embedded, sectioned, and stained with H&E. A dense matrix was observed within the wound area, consistent with scar-like tissue formation. To quantify the amount of this tissue present in the various samples, the junction between the abnormal tissue and the normal-appearing skin was designated with black dotted lines (Fig 5A), and the relative area of abnormal tissue was assessed using Image J software. These studies (Fig 5B) showed that scaffolds seeded with cells for 4 days prior to implantation elicited a smaller amount of abnormal tissue than all other treatment groups, at all three time points. It was also apparent that both of the scaffolds seeded with cells evoked less abnormal tissue formation than microporous scaffolds without pre-seeded cells. Sham wounds had the highest amount of abnormal tissue at all time points.

Another notable feature observed in higher magnification images of the regenerated tissue was the architecture of the matrix. The dermal matrix of normal skin has a basket weave structure, represented by a loose wavy appearance. This structure was observed in many of the samples. The area of matrix with a basket weave appearance, relative to areas of abnormal, dense matrix, was measured as indicated in Fig 6A. These studies suggested that the amount of basket-weave matrix was greatest in the wounds containing scaffolds seeded with fibroblasts for 4 days (Fig 6B), followed by scaffolds seeded with cells for 1 day. Acellular scaffolds had less basket-weave matrix than either of the cell-loaded scaffold samples, and all scaffolds elicited a better response than the sham wounds. In addition to a more normal matrix architecture, other features of wound healing appeared to be enhanced in defects implanted with fibroblast-seeded scaffolds. As shown in Fig 7, scaffolds pre-seeded with fibroblasts appeared to stimulate greater follicle regeneration than acellular scaffolds or sham wounds.

Discussion

Commercial skin graft materials have evolved over time into more complex products; however, an ideal scaffold has yet to be developed. Current synthetic scaffolds, along with allograft or xenograft tissues, can elicit adverse clinical outcomes such as graft rejection, scar development, limited wound closure, bleeding, and infection [5]. Therefore, many investigators are focused on engineering a scaffold that can address these shortcomings. An optimal scaffold will incorporate appropriate mechanical properties, an architecture similar to native skin tissue, and degradation characteristics that support initial tissue regeneration, but degrade as more developed tissue forms [23].

Electrospinning is a technology that has existed for decades; however, it is increasingly being used in the tissue engineering field. Our group has adopted electrospinning to create regenerative scaffolds because of this method's simplicity, cost effectiveness, and capacity to produce nanofibrous scaffolds that mimic the topography of native skin tissue [24, 25]. In order to address the problem of small pore sizes inherent in electrospun scaffolds, we used microneedles to mechanically create 160 μm pores throughout the thickness of the scaffolds. Our goal was to create spaces that would foster fibroblast migration and fibroblast-mediated secretion of native ECM.

In these studies, we blended 70% col I and 30% PCL in order to develop a composite nanofibrous mesh that would support cell attachment, migration, and proliferation, and as reported previously [15], degrade with appropriate temporal kinetics. In addition, the 70:30 col/PCL microporous scaffolds seeded with fibroblasts exhibited minimal contraction over a 21-day interval. The inclusion of 160 μm pores throughout the thickness of the scaffolds facilitated the fibroblast-mediated deposition of ECM molecules including collagen I and fibronectin, resulting in a remodeled scaffold more similar to native dermal matrix. These results are consistent with our prior investigation, which compared scaffolds with varying collagen/PCL ratios and pore sizes, and determined that 70:30 col/PCL scaffolds with 160 μm pores offered the best balance between suitable mechanical characteristics, biodegradability, and cell-supportive biochemistry.

Recent reports have suggested that pre-seeding scaffolds with fibroblasts, keratinocytes, stem cells, or a combination of these has a beneficial role in wound healing [18, 26-28]. The advantages that pre-seeded cells provide are thought to result from

deposition of ECM proteins, as well as secreted factors such as cytokines and growth factors. Regenerated tissues within wounds implanted with cell-seeded scaffolds are reported to have a reduced concentration of dense collagen I, faster re-epithelialization, enhanced angiogenesis, and a higher degree of proliferative cells [28-30]. All of these factors have an influence on the wound healing rate, and also aid in reducing scar formation. In light of these findings, the objective of the current study was to determine whether pre-seeding 70:30 col/PCL microporous scaffolds with cells prior to implantation would enhance the wound healing response.

To test this hypothesis, acellular scaffolds, or scaffolds seeded with fibroblasts for either 1 or 4 days, were grafted into full thickness critical size skin defects. It was found that fibroblast-seeded scaffolds stimulated more rapid and effective wound healing than acellular scaffolds. Moreover, scaffolds cultured with fibroblasts for 4 days elicited enhanced skin repair relative to scaffolds cultured with fibroblasts for only 1 day. When clinicians assess skin wound healing from biopsies, they typically screen for a newly formed basket-weave matrix in the dermal layer, because this architecture mimics native unwounded skin tissue. By quantifying the area of basket-weave matrix in our samples, we determined the greatest to least amount of basket-weave matrix in the wounds was as follows: 4 day pre-seeded scaffolds > 1 day pre-seeded scaffolds > acellular porous scaffolds > sham. Although the mechanism underlying the enhanced response to scaffolds cultured with cells for 4 days, rather than 1 day, is currently unknown, we hypothesize that the longer culture interval allowed greater deposition of ECM as well as the possible accumulation of secreted cytokines and growth factors.

In conclusion, 70:30 col/PCL scaffolds with 160 μm pores support fibroblast survival, proliferation, and ECM deposition. Furthermore, the pre-seeding of these scaffolds with dermal fibroblasts prior to implantation stimulated the formation of more normal-appearing regenerated tissue within full-thickness skin defects.

References

1. Sahin I, Alhan D, Nisanci M, Ozer F, Eski M, Isik S. Auto-/homografting can work well even if both autograft and allograft are meshed in 4:1 ratio. *Ulus Travma Acil Cerrahi Derg*; 20:33. 2014.
2. Calota DR, Nitescu C, Florescu IP, Lascar I. Surgical management of extensive burns treatment using allografts. *J Med Life*; 5:486. 2012.
3. Chiu T, Burd A. "Xenograft" dressing in the treatment of burns. *Clin Dermatol*; 23:419. 2005.
4. Chern PL, Baum CL, Arpey CJ. Biologic dressings: current applications and limitations in dermatologic surgery. *Dermatol Surg*; 35:891. 2009.
5. Priya SG, Jungvid H, Kumar A. Skin tissue engineering for tissue repair and regeneration. *Tissue Eng Part B Rev*; 14:105. 2008.
6. Supp DM, Boyce ST. Engineered skin substitutes: practices and potentials. *Clin Dermatol*; 23:403. 2005.
7. Ravichandran R, Sundarrajan S, Venugopal JR, Mukherjee S, Ramakrishna S. Advances in polymeric systems for tissue engineering and biomedical applications. *Macromol Biosci*; 12:286. 2012.
8. Rnjak-Kovacina J, Wise SG, Li Z, Maitz PK, Young CJ, Wang Y, Weiss AS. Electrospun synthetic human elastin:collagen composite scaffolds for dermal tissue engineering. *Acta Biomater*; 8:3714. 2012.
9. Mogosanu GD, Grumezescu AM. Natural and synthetic polymers for wounds and burns dressing. *Int J Pharm*; 463:127. 2014.
10. Suganya S, Venugopal J, Ramakrishna S, Lakshmi BS, Dev VRG. Naturally derived biofunctional nanofibrous scaffold for skin tissue regeneration. *Int J Biol Macromol*; 68:135. 2014.
11. Jayarama Reddy V, Radhakrishnan S, Ravichandran R, Mukherjee S, Balamurugan R, Sundarrajan S, Ramakrishna S. Nanofibrous structured

- biomimetic strategies for skin tissue regeneration. *Wound Repair Regen*; 21:1. 2013.
12. Rnjak-Kovacina J, Weiss AS. Increasing the pore size of electrospun scaffolds. *Tissue Eng Part B Rev*; 17:365. 2011.
 13. Kim TG, Chung HJ, Park TG. Macroporous and nanofibrous hyaluronic acid/collagen hybrid scaffold fabricated by concurrent electrospinning and deposition/leaching of salt particles. *Acta Biomater*; 4:1611. 2008.
 14. Blakeney BA, Tambralli A, Anderson JM, Andukuri A, Lim DJ, Dean DR, Jun HW. Cell infiltration and growth in a low density, uncompressed three-dimensional electrospun nanofibrous scaffold. *Biomaterials*; 32:1583. 2011.
 15. Bonvallet PP, Culpepper BK, Bain JL, Schultz MJ, Thomas SJ, Bellis SL. Microporous Dermal-Like Electrospun Scaffolds Promote Accelerated Skin Regeneration. *Tissue Eng Part A*; Epub ahead of print 2014.
 16. You HJ, Han SK. Cell Therapy for Wound Healing. *J Korean Med Sci*; 29:311. 2014.
 17. Fang T, Lineaweaver WC, Sailes FC, Kisner C, Zhang F. Clinical Application of Cultured Epithelial Autografts on Acellular Dermal Matrices in the Treatment of Extended Burn Injuries; Epub ahead of print *Ann Plast Surg*. 2013.
 18. Pezeshki-Modaress M, Rajabi-Zeleti S, Zandi M, Mirzadeh H, Sodeifi N, Nekookar A, Aghdami N. Cell-loaded gelatin/chitosan scaffolds fabricated by salt-leaching/lyophilization for skin tissue engineering: In vitro and in vivo study. *J Biomed Mater Res A*. Epub ahead of print. 2013.
 19. Barker DA, Bowers DT, Hughley B, Chance EW, Klembczyk KJ, Brayman KL, Park SS, Botchwey EA. Multilayer cell-seeded polymer nanofiber constructs for soft-tissue reconstruction. *JAMA Otolaryngol Head Neck Surg*; 139:914. 2013.
 20. Harrison CA, MacNeil S. The mechanism of skin graft contraction: an update on current research and potential future therapies. *Burns*; 34:153. 2008.
 21. Stephenson AJ, Griffiths RW, La Hausse-Brown TP. Patterns of contraction in human full thickness skin grafts. *Br J Plast Surg*; 53:397. 2000.
 22. Harrison CA, Gossiel F, Layton CM, Bullock AJ, Johnson T, Blumsohn A, MacNeil S. Use of an in vitro model of tissue-engineered skin to investigate the mechanism of skin graft contraction. *Tissue Eng*; 12:3119. 2006.
 23. Yildirim L, Thanh NT, Seifalian AM. Skin regeneration scaffolds: a multimodal bottom-up approach. *Trends Biotechnol*; 30:638. 2012.

24. Kumbar SG, James R, Nukavarapu SP, Laurencin CT. Electrospun nanofiber scaffolds: engineering soft tissues. *Biomed Mater*; 3:034002. 2008.
25. Pham QP, Sharma U, Mikos AG. Electrospinning of polymeric nanofibers for tissue engineering applications: a review. *Tissue Eng*; 12:1197. 2006.
26. Deepa R, Paul W, Anilkumar TV, Sharma CP. Differential Healing of Full Thickness Rabbit Skin Wound by Fibroblast Loaded Chitosan Sponge. *J Biomed Mater Res A*; 3:261. 2013.
27. Zeinali R, Biazar E, Keshel SH, Tavirani MR, Asadipour K. Regeneration of full-thickness skin defects using umbilical cord blood stem cells loaded into modified porous scaffolds. *ASAIO J*; 60:106. 2014.
28. Revi D, Paul W, Tv A, Sharma CP. Chitosan Scaffold Co cultured with Keratinocyte and Fibroblast Heals Full Thickness Skin Wounds in Rabbit. *J Biomed Mater Res A*. Epub ahead of print. 2013.
29. Velnar T, Bailey T, Smrko V. The wound healing process: an overview of the cellular and molecular mechanisms. *J Int Med Res*; 37:1528. 2009.
30. Suh EJ, Remillard MY, Legesse-Miller A, Johnson EL, Lemons JM, Chapman TR, Forman JJ, Kojima M, Silberman ES, Collier HA. A microRNA network regulates proliferative timing and extracellular matrix synthesis during cellular quiescence in fibroblasts. *Genome Biol*; 13:R121. 2012.

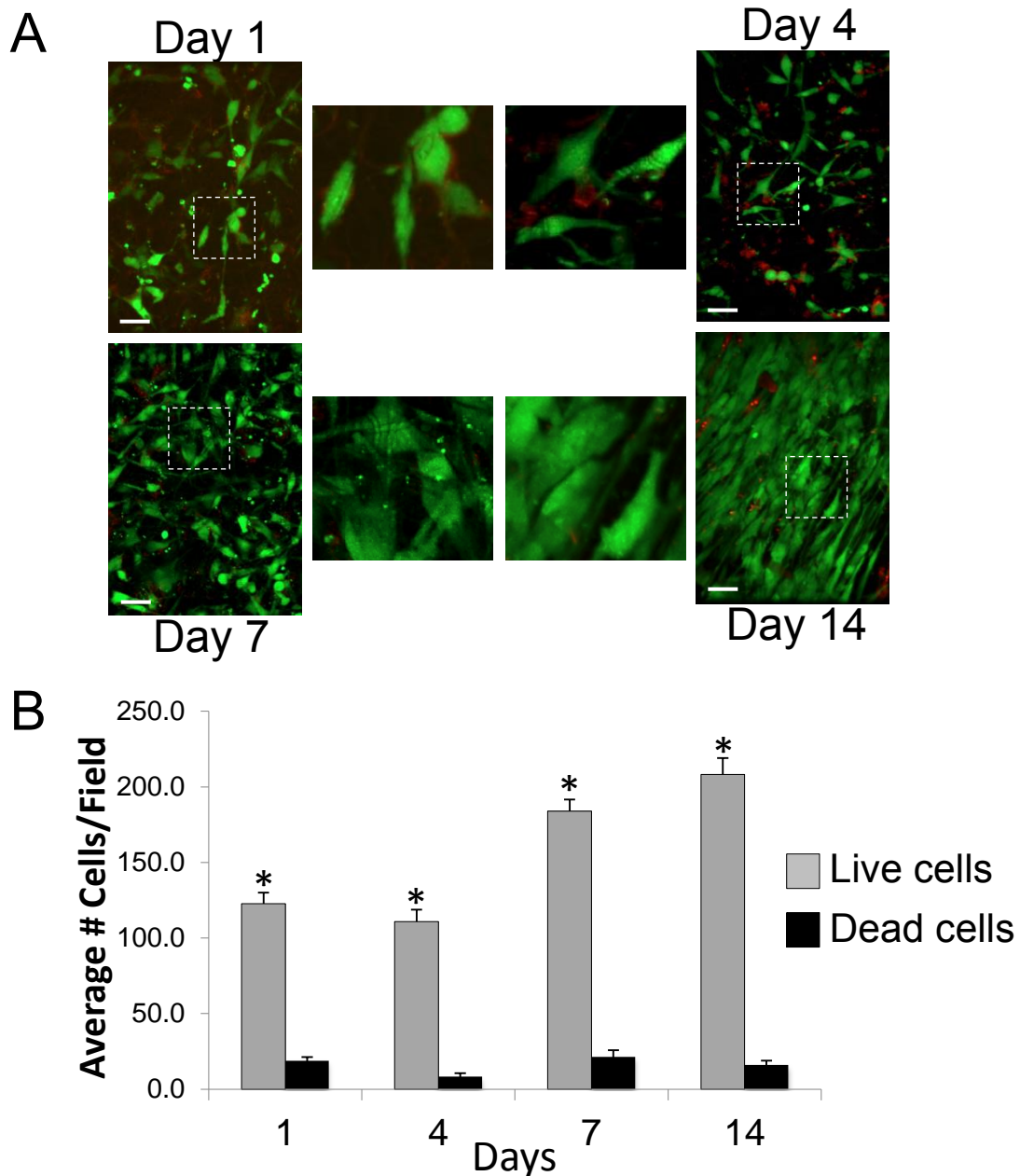


Fig 1. Fibroblast viability on 70:30 col/PCL scaffolds. (A) F344 fibroblasts grown on scaffolds for 1, 4, 7, and 14 days were stained for either living (green) or dead (red) cells. Scale bar = 40 μ m. (B) Values represent means and standard error of the means measured for three distinct fields, detecting the amount of living and dead cells at each time point. A student's t-test was used to compare live versus dead cells at each time point. *Represents $p < 0.01$.

Note: From "Microporous Dermal-Mimetic Electrospun Scaffolds Pre-Seeded with Fibroblasts Promote Tissue Regeneration in Full-Thickness Skin Wounds" by P.P. Bonvallet, M.J. Schultz, E.H. Mitchell, J.L. Bain, B.K. Culpepper, S.J. Thomas, S.L. Bellis. Manuscript in preparation.

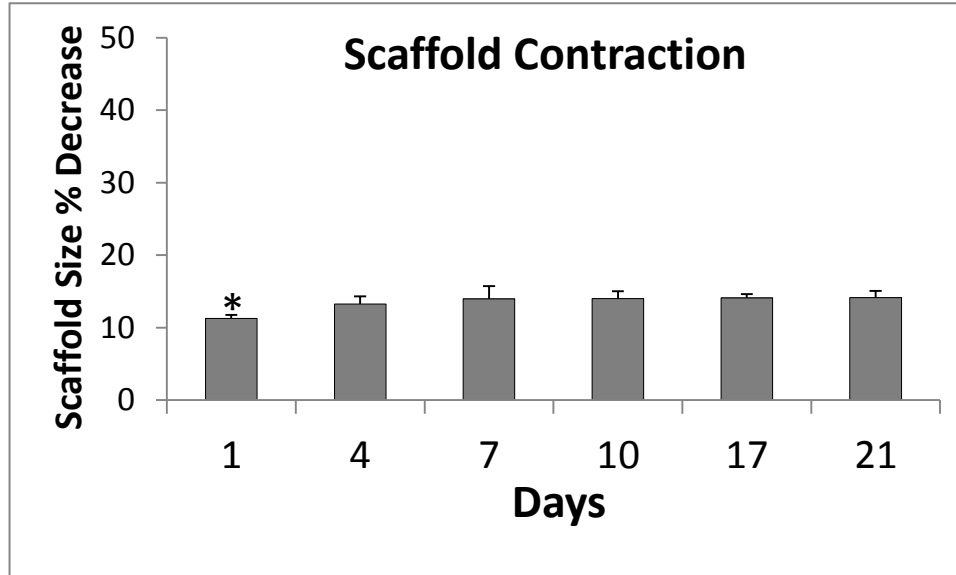


Fig 2. Contraction of porous 70:30 col/PCL scaffolds containing seeded fibroblasts. Scaffold diameters were measured at each time interval to quantify contraction (plotted as percent decrease in scaffold diameter). Values represent means and standard deviation for five scaffolds per time point. Two independent experiments were performed. A one way Anova was performed to compare the percent change in scaffold contraction of the various groups. *Represents significant difference ($p < 0.01$) relative to all other groups.

Note: From “Microporous Dermal-Mimetic Electrospun Scaffolds Pre-Seeded with Fibroblasts Promote Tissue Regeneration in Full-Thickness Skin Wounds” by P.P. Bonvallet, M.J. Schultz, E.H. Mitchell, J.L. Bain, B.K. Culpepper, S.J. Thomas, S.L. Bellis. Manuscript in preparation.

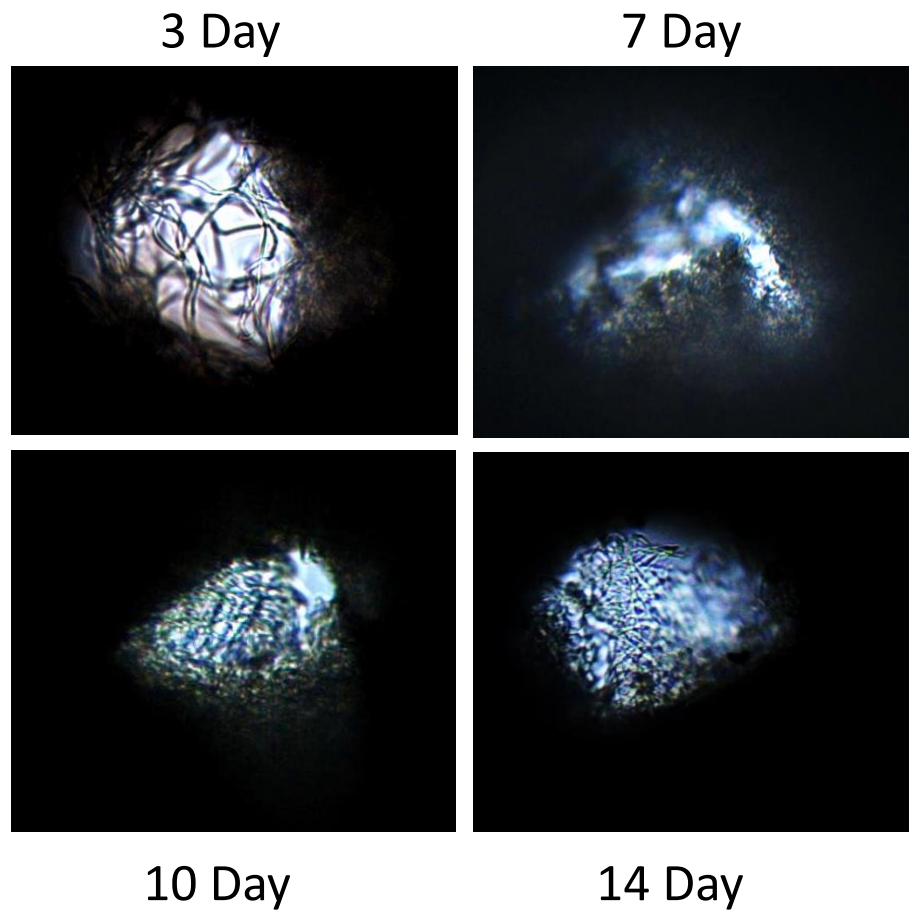


Fig 3. Extracellular matrix is deposited into the 160 μm pores of 70:30 col/PCL scaffolds. Top-down phase-contrast images of pores at 3, 7, 10, and 14 days following cell seeding reveal fibrous matrix deposition over time.

Note: From “Microporous Dermal-Mimetic Electrospun Scaffolds Pre-Seeded with Fibroblasts Promote Tissue Regeneration in Full-Thickness Skin Wounds” by P.P. Bonvallet, M.J. Schultz, E.H. Mitchell, J.L. Bain, B.K. Culpepper, S.J. Thomas, S.L. Bellis. Manuscript in preparation.

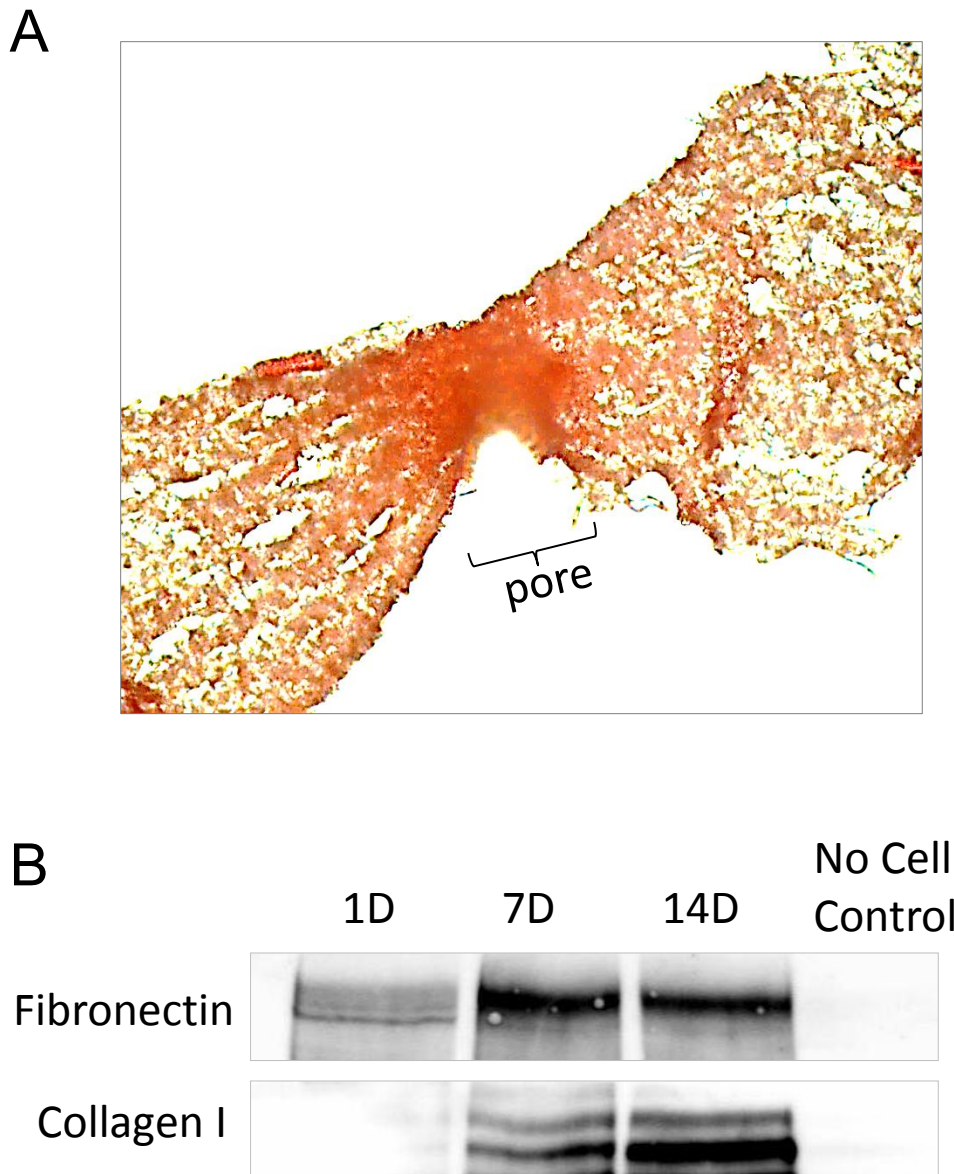
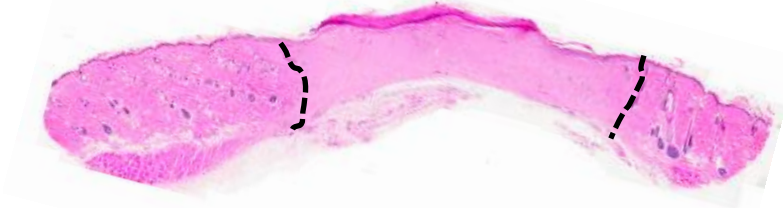


Fig 4. Collagen and fibronectin are deposited into 160 μ m pores within scaffolds. (A) A Picrosirius Red stain was used to detect fibrous collagen in 70:30 col/PCL scaffolds. (B) Immunoblotting for collagen I and fibronectin was performed on homogenates prepared from porous scaffolds with adherent fibroblasts grown for 1, 7, and 14 days. The no cell negative control was prepared from scaffolds that were not seeded with fibroblasts.

Note: From “Microporous Dermal-Mimetic Electrospun Scaffolds Pre-Seeded with Fibroblasts Promote Tissue Regeneration in Full-Thickness Skin Wounds” by P.P. Bonvallet, M.J. Schultz, E.H. Mitchell, J.L. Bain, B.K. Culpepper, S.J. Thomas, S.L. Bellis. Manuscript in preparation.

A



B

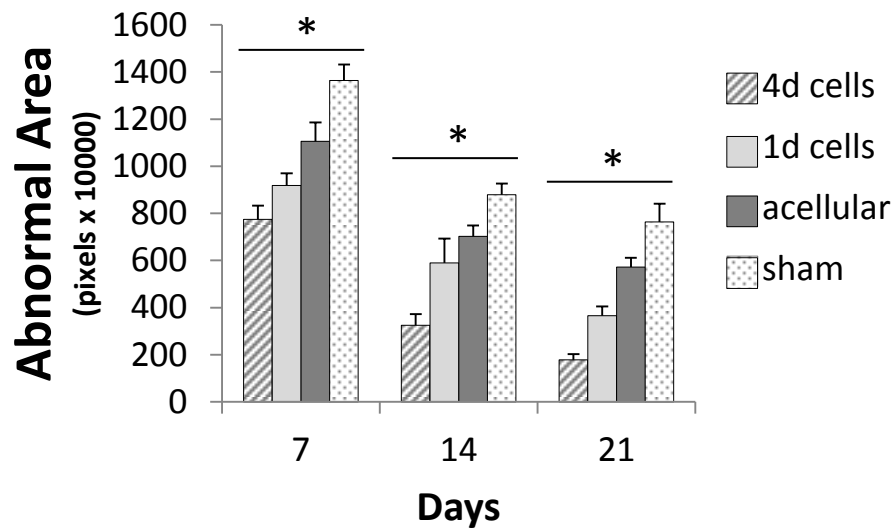


Fig 5. Pre-seeded scaffolds promote more effective tissue regeneration. (A) A cross-section of rat skin tissue undergoing the wound-healing process. Black dashed lines designate junctions between abnormal tissue and normal skin morphology. (B) Graph depicts average abnormal tissue areas ($n=5$) of harvested tissues containing porous scaffolds seeded for 4 days with fibroblasts, porous scaffolds seeded for 1 day, acellular porous scaffolds, and sham wounds. A repeated measure Anova was performed to compare significance between treatment groups. *Represents $p<0.01$ for all treatment groups that are significantly different from each other within the same time point. Also, all treatment groups significantly decreased over time ($p<0.001$).

Note: From “Microporous Dermal-Mimetic Electrospun Scaffolds Pre-Seeded with Fibroblasts Promote Tissue Regeneration in Full-Thickness Skin Wounds” by P.P. Bonvallet, M.J. Schultz, E.H. Mitchell, J.L. Bain, B.K. Culpepper, S.J. Thomas, S.L. Bellis. Manuscript in preparation.

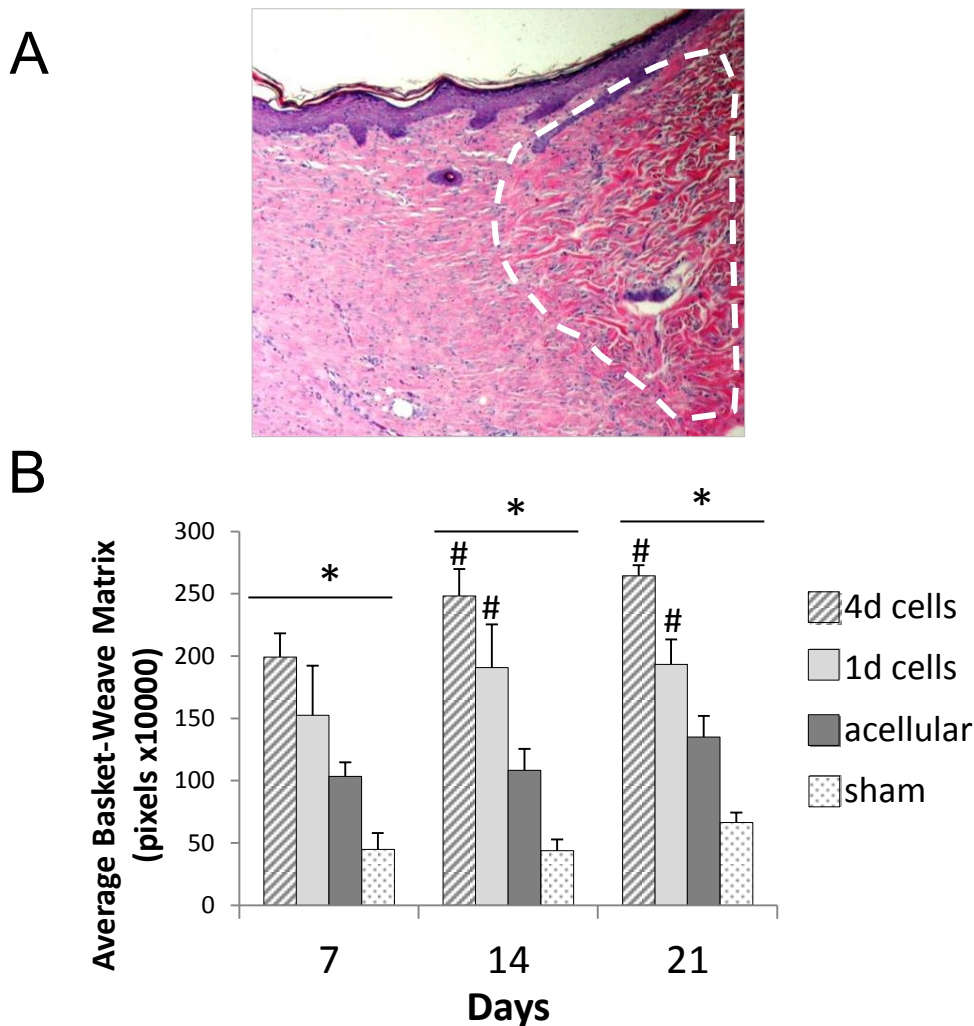


Fig 6. Scaffolds pre-seeded with fibroblasts promote formation of ECM with a high degree of basket-weave structure, resembling unwounded skin tissue. (A) A cross-section of rat skin tissue containing basket-weave matrix in the dermis. White dashed line designates area of basket-weave matrix. (B) Graph depicts average basket-weave area (n=5) of harvested tissues containing porous scaffolds seeded for 4 days with fibroblasts, porous scaffolds seeded for 1 day, acellular porous scaffolds, and sham wounds. A repeated measure Anova was performed to compare significance between treatment groups. *Represents $p < 0.01$ for all treatment groups that are significantly different from each other within the same time point. #Represents treatment groups significantly different than the 1 day time point.

Note: From “Microporous Dermal-Mimetic Electrospun Scaffolds Pre-Seeded with Fibroblasts Promote Tissue Regeneration in Full-Thickness Skin Wounds” by P.P. Bonvallet, M.J. Schultz, E.H. Mitchell, J.L. Bain, B.K. Culpepper, S.J. Thomas, S.L. Bellis. Manuscript in preparation.

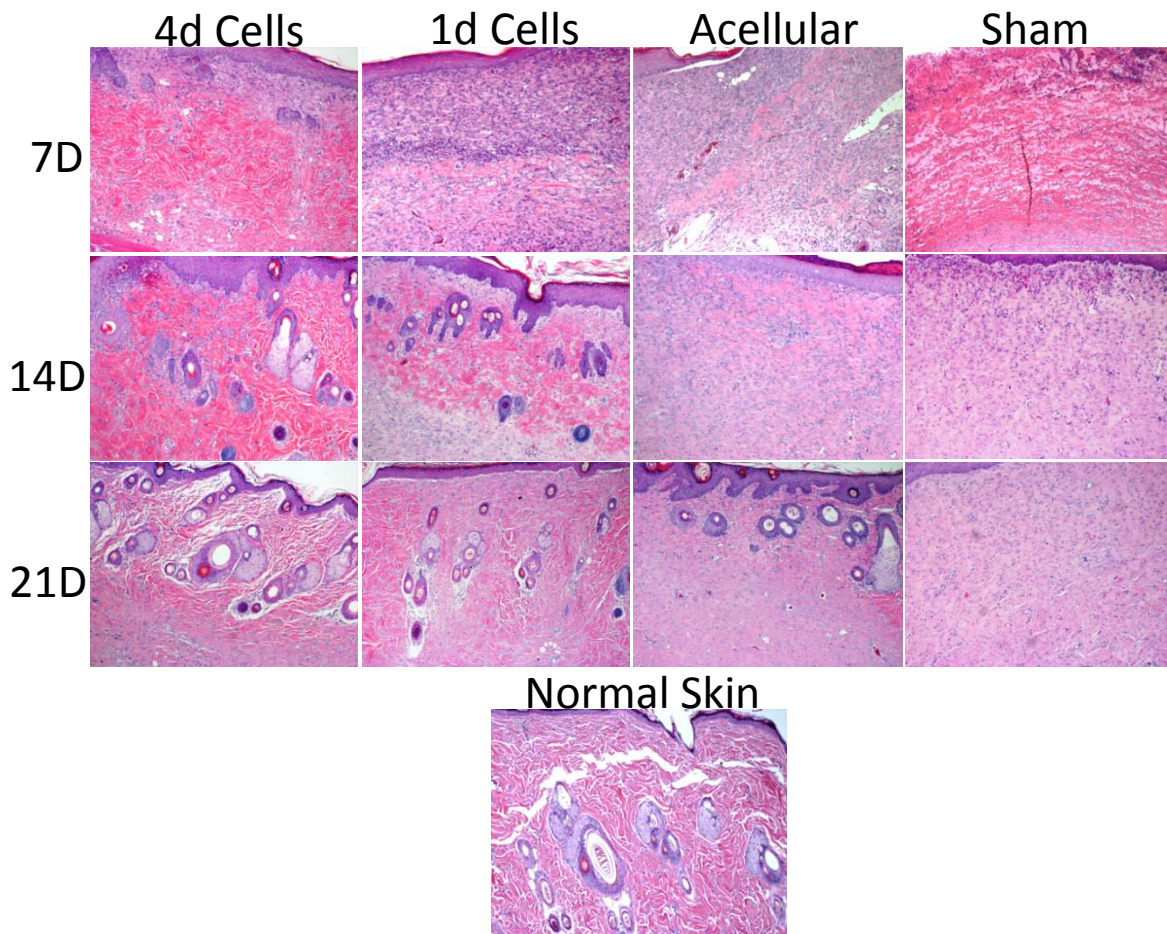


Fig 7. Images (10X) of wound healing over a 21-day time period show the structure of the matrix in each treatment group. The matrix in wounds containing scaffolds pre-seeded with fibroblasts appears more normal to skin tissue with loose, wavy basket-weave matrix and the formation of hair follicles.

Note: From “Microporous Dermal-Mimetic Electrospun Scaffolds Pre-Seeded with Fibroblasts Promote Tissue Regeneration in Full-Thickness Skin Wounds” by P.P. Bonvallet, M.J. Schultz, E.H. Mitchell, J.L. Bain, B.K. Culpepper, S.J. Thomas, S.L. Bellis. Manuscript in preparation.

CONCLUSIONS

It is a common misconception that skin tissue is a simple organ because it is viewed as a basic covering for underlying organs. Rather, it is a complex organ constructed of multiple cell types, proteins, growth factors, cytokines, hair follicles, and glands. It has many complex layers that all have many roles. It serves numerous functions such as a protection and barrier function, reservoir for the storage of lipids and water, sensation due to nerve endings, prevention of water loss, and regulation of body temperature [88]. When skin is severely damaged, it is crucial to seek medical attention because mortality can result if left untreated.

The current therapies that surgeons use cover the wound and assist in healing; however, they leave a lot to be desired because downfalls such as scar formation, limited take rates, infection, and rejection [89] are a major issue when it comes to wound repair. Because skin tissue is composed of so many elements and serves an array of functions, engineering an effective substitute is a difficult task.

To address the overwhelming need for a safe and effective skin grafting material, a major goal in the tissue engineering field has been to develop an advanced biomaterial that is capable of supporting cellular responses consistent with new skin tissue growth. The major constituent of most commercially available products along with those in the research phase is collagen I. Collagen I composes approximately 80% of skin tissue and therefore is the logical substrate for grafting [27]. Collagen scaffolds can be prepared in a variety ways. In this study we wanted to avoid the use of cross-linking reagents due to their toxic effect on cells, their uncontrollable degree of cross-linking, and their effect on

degradation in vivo. We also wanted to avoid any techniques that would compromise or denature the structure of collagen. For these reasons we chose electrospinning to create our scaffolds. These nanofibrous meshes have interconnected pores and a high surface to volume ratio, naturally mimicking the architecture of extracellular matrix [73]. The ease of fabrication of these scaffolds also makes this an appealing technique.

The initial objective of this study was to establish a method for creating electrospun scaffolds with fibroblasts embedded throughout. It is well cited in the literature that fibroblasts have a very difficult time infiltrating throughout the thickness of these scaffolds due to the nanopore sizes created during the electrospinning process [90, 91]. We found that when fibroblasts were seeded on the surface of electrospun scaffolds, which were created using a normal set up, there was very little to no cell migration throughout these scaffolds. The only cells that were visualized were on the outer surface of the scaffolds where they were originally seeded. They were spread across the entire top surface; however, there was no apparent cell infiltration into the scaffold. This led us to investigate numerous variations on the electrospinning process. We next attempted an electrospinning and electrospraying method. This involves electrospinning scaffolding material out of one needle and electrospraying a solution of fibroblasts out of another needle at the same time (Fig 1). This method had very limited success as well due to the cell solution and fiber solution repelling each other because they were both negatively charged, causing an uneven mixing of the two. We next attempted a layer-by-layer method in which we electrospun a layer of the scaffold solution followed by electrospraying a cell solution layer on top of that. This was repeated numerous times to create a multiple layered scaffold with cells throughout. The success of these scaffolds

was limited due to the high potential for contamination along with the limited viability of cells. We believe the high voltage had a detrimental effect on the cells; therefore, limiting cell survival, spreading, and proliferation throughout the scaffolds. Because of the challenges that we faced with changing normal electrospinning protocols, we decided that we would modify the scaffold post-electrospinning. These alternative protocols all require complicated equipment set ups and are difficult to generate reproducible scaffolds with good fidelity. Accordingly, these alternative scaffolds will be difficult to scale up for mass manufacturing.

Normal electrospinning parameters were established so that the fibers were approximately 180 nm in diameter, which approximates the size of a native collagen fiber. Briefly, collagen I and PCL were mixed into solution with the organic solvent hexafluoroisopropanol and taken up into a syringe with a 27 gauge blunt tip needle. The solution was charged with 20 KV and ejected out of the syringe at 2 ml per hour from a syringe pump. The tip of the needle was set up 20 cm horizontally from a grounded collecting plate which was covered in a thin sheet of aluminum in order to collect the nanofibrous mesh. The collecting plate was rotated at 20 rpm in order to ensure even fiber distribution throughout.

The approach we used to increase porosity within these electrospun scaffolds was a simple, yet effective method. We adopted technology used in dermatology. A device, called the Derma Stamp (Alibaba.com), is used to create micro punctures in the skin in order to induce collagen and ECM deposition in order to eliminate wrinkles and stretch marks. Given that this was an effective method for creating micropunctures in objects with even spacing and pore diameters, we determined that this would be an effective

method for creating pores throughout our scaffolds. Also, we chose this method because of the feasibility of scaling this method up for manufacturing purposes. On a large scale, sheets of electrospun scaffold can be pressed with a large press, inducing larger pores throughout the entire scaffold (Fig 2).

Initially, we examined a variety of different pore sizes and the fibroblast responses in order to maximize the amount of migration, proliferation, and ECM secretion. Pores should be larger than the size of fibroblasts, but not so large that fibroblasts would have a difficult time secreting ECM to completely fill the pores. Fibroblasts are anywhere from less than 10 μm to 100 μm in size [92]; therefore, we determined that pores should be bigger than 100 μm in diameter. We also came upon the conclusion that 250 μm pores were too large because fibroblasts were not able to secrete sufficient matrix to completely fill these pores.

In order to assess fibroblast response to matrices, we first had to develop a protocol for staining cells, ECM, and scaffolds. Electrospun scaffolds composed of col I and PCL presented many challenges when it came to staining. Initially, we attempted paraffin embedding the scaffolds in order to section and stain. The downfalls of paraffin embedding are the heat and xylene used in the staining process. Both of these factors break down PCL, thus degrading the scaffold. Alternatively, the scaffolds were embedded in optimal cutting temperature (OTC) compound and frozen. Next, cells had to be stained in order to be visualized. We attempted many different methods such as using Cell Tracker dyes and antibodies. These methods were ineffective in overcoming the bright autofluorescence of the scaffolds. To address these issues, we determined that red nanocrystals and also forcing the expression of green fluorescent protein (GFP) in

fibroblasts was the most effective method for visualizing the cells on scaffolds. We also faced difficulties when it came to staining of the ECM; however, we discovered that using specific antibodies along with a picrosirius red stain, a fibrous collagen stain, were the most effective methods for staining ECM.

The fibroblast response was evaluated upon scaffolds containing a variety of different size diameter pores. We evaluated fibroblast migration amongst the pores to validate that the fibroblasts were indeed migrating into the pores. We also visualized matrix deposition by the use of images taken at various time points. We also stained for various ECM proteins such as collagen and fibronectin by the use of antibodies. Finally, the ECM deposition was verified by immunoblotting. After many experiments we determined the optimal pore size to be 160 μm in diameter.

After optimizing scaffold electrospinning protocols, staining methods, and pore size, we examined fibroblast response to various ratios of col I:PCL. In order to do that, 100% col I, 100% PCL, 80% col I/20% PCL, 70% col I/30% PCL, 60% col I/40% PCL, and 50% col I/50% PCL scaffolds were constructed. Fibroblast response was observed when seeded on the surface and allowed to grow for given time points. We also assessed scaffold contraction and tensile strength of the scaffolds. We determined that 100% collagen scaffolds did not have appropriate tensile strengths and degraded much too fast to be a therapeutic graft. 100% PCL scaffolds did support fibroblast growth; however, proliferation and spreading of the cells was not ideal. 70% col I/30% PCL scaffolds had tensile strengths of approximately 1-2 MPa, which is at the lower end of the native skin tissue tensile strength, but is stronger than many current clinical therapies [93]. Also, 70% col I/30% PCL scaffolds had minimal contraction as seen from our contraction

studies where the maximal amount of contraction exhibited was approximately 18% over a 21 day time period. We came to the conclusion that 70% col I/30% PCL scaffolds yielded the best balance in terms of mechanical properties while still allowing fibroblasts to adhere, spread, and proliferate.

Scaffold degradation in vivo is an important aspect that should be considered when engineering matrices. Scaffolds should remain in the wound bed long enough to stimulate regeneration and over time the scaffold should degrade, allowing the body to take over the process. Ideally, the scaffold should completely degrade within 3-4 weeks [94]; therefore, scaffolds should be engineered accordingly. In order to test our scaffolds, we created full-thickness wounds in the back-skin of rats and implanted different ratio collagen I to PCL scaffolds in the wounds. Prior to implantation, we stained the scaffolds with a fluorescent red dye in order to track the scaffold degradation over time. The results from these experiments revealed that a ratio of 70% collagen I:30% PCL resulted in degradation rates within that 3-4 week range, an optimal time frame for degradation in vivo.

Various groups have reported the necessity of having a high degree of porosity within scaffolds to allow for blood and cell infiltration as well as angiogenesis when used clinically or implanted into animal models [95, 96]. We hypothesized that introducing micropores into electrospun scaffolds would elicit improved wound healing responses and reduced scar formation when used in vivo. To assess wound healing in vivo, we compared porous scaffolds to non-porous scaffolds. Both scaffolds contained 70% col I and 30% PCL. In the back-skin of rats we created 3 full-thickness skin wound defects. In those wounds we sutured into place the 2 scaffolds and left one wound (sham) to heal on

its own for comparison purposes. At each time point pictures were taken to assess wound closure, infection, and general skin healing. After pictures were taken, the skin tissue was harvested, formalin fixed, sectioned and H&E stained in order to assess both dermal and epidermal healing. From the images taken at each time point, we observed porous scaffolds had a 33% faster wound closure rate than both non-porous scaffolds and shams at 7 days. By 14 days, porous scaffolds had a 60% faster wound closure rate than both non-porous and sham wounds. Interestingly, we observed that non-porous and sham wounds had no significant difference in their wound closure rate.

H&E staining allowed us to visualize blood vessel formation, matrix structure, hair follicle formation, and epidermal stratification. In the skin tissue sections, we observed that the porous matrices allowed for faster vessel infiltration into the wound bed. We believe this vessel infiltration helped accelerated the wound healing response. In porous scaffolds we also observed a high degree of basket-weave matrix in the dermal tissue as opposed to the non-porous scaffolds and sham wounds. When measuring the abnormal appearing tissue after various time points, we were able to evaluate tissue response to scaffolds. There was a significantly larger degree of more abnormal appearing tissue in wounds that contained non-porous scaffolds and sham wounds compared to wounds containing porous scaffolds. As expected, wounds with non-porous scaffolds had significantly more normal appearing tissue than the sham wounds. In this case, we believe the abnormal resultant tissue to be the precursors of scar tissue formation. We can conclude from these experiments that by simply increasing porosity within scaffolds, skin tissue regeneration is greatly accelerated and improved, leaving a much healthier normal appearing dermis.

The final goal of this thesis was to evaluate how pre-seeded scaffolds affect the wound healing response when implanted into the back-skin of rats. Various groups have shown the importance and added benefit that pre-seeding cells in scaffolds can have [80-82]. Pre-seeding scaffolds has advantageous effects in the wound healing process. Pre-seeding has been shown to assist in the increase in vasculature and decrease in scar tissue formation. We believe this occurs because of fibroblast ECM deposition and growth factor and cytokine secretion. Having growth factors and cytokines already present in the wound bed can have advantageous effects due to their chemoattractant and instructive properties. We believe these factors all have a role in accelerating the wound healing process, allowing for the formation of more normal, healthy skin tissue. To examine this in our model, we pre-seeded porous electrospun scaffolds with Fischer 344 (F344) fibroblasts prior to implanting them into full-thickness rat skin wound defects. Fischer rats are a syngeneic model, meaning that all of the F344 rats have the same genetic background. For this reason, cells can be taken from one rat and placed in another without eliciting an immune response. Initially, we allowed fibroblasts to grow on porous scaffolds for 10 days prior to implantation. Results were inconclusive from this experiment because the scaffolds became weak and difficult to suture into place. Because of this, surgical glue was used, which we believe to have interfered with the wound healing response. For this reason, we next implanted scaffolds with fibroblasts pre-seeded for both 1 and 4 days along with a porous scaffold that contained no fibroblasts and a sham wound for comparison. After a range of time points, we harvested, paraffin embedded, and H&E stained the tissues to evaluate skin regeneration responses. Again, we measured the amount of abnormal tissue in the wound bed, which we believe to be

preliminary scar tissue formation. Our data show that the longer scaffolds are pre-seeded with fibroblasts, the amount of more normal appearing tissue was increased. Both the 1 and 4 day pre-seeded scaffolds had a better healing response than the porous scaffold containing no cells. Most interesting was the newly formed matrix in the scaffolds pre-seeded with fibroblasts. We observed a high degree of basket-weave matrix in these scaffolds. There was also a large presence of blood vessels and hair follicle formation. These tissues that contained pre-seeded scaffolds resembled normal uninjured skin tissue. We conclude from these experiments that scaffolds pre-seeded with fibroblasts do in fact greatly assist in the regeneration of normal healthy skin tissue.

Currently, there are FDA approved therapies that contain allogeneic fibroblasts or keratinocytes. Apligraf and Orcel both contain fibroblasts and keratinocytes derived from neonatal foreskin [97]. Dermagraft is a polygalactin mesh that contains allogeneic fibroblasts [98]. These scaffolds are cryopreserved in order to maintain cell viability. There have been limited successes with these scaffolds; however, shortcomings exist due to their scaffolding material and cryopreservation process. Gels, collagen sponges, and polygalactin meshes have inadequate mechanical properties, degradation rates, and porosity. Therefore, we believe by combining a biomimetic scaffold resembling native skin tissue along with pre-seeded cells, a scaffold capable of rapid, healthy skin tissue regeneration is possible.

Based on our findings presented in this thesis, we postulate that matrices composed of PCL and collagen I containing 160 μm pores are promising materials for regenerating tissue for patients who undergo severe skin trauma. The base electrospun scaffolds alone have advantageous properties because they can easily be tailored to

incorporate features as researchers understand more about the skin wound healing response and elements that effect it. Moreover, we believe that these scaffolds in combination with fibroblasts pre-seeded prior to surgery have a synergic effect. By providing an ideal wound healing environment along with cells that secrete ECM, growth factors, and cytokines, we believe that the scaffolds presented in this thesis have the potential to revolutionize the standard clinical therapy.

Future studies are crucial to this research in order to advance these scaffold to clinical trials. Because of the high degree of tailorability of these scaffolds, our scaffolds are amenable for incorporating additional biological cues. Hyaluronan for example, has been shown to play roles in cell migration and proliferation which ultimately results in tissue ingrowth. It is also very hydrophilic which would keep the wound bed moist to assist in healing by reducing fibrosis [99]. Elastin is another component of skin that typically isn't distributed properly in scar tissue. It increases the tensile strength of skin and gives it elasticity [100]. The incorporation of growth factors such as FGF-2 and VEGF would enhance scaffolds by signaling for fibroblast recruitment and proliferation as well as controlling for blood vessel formation [5]. Also, in vivo studies are needed to test the mechanism behind scaffolds containing pre-seeded fibroblasts having a better wound healing response than those that lack seeded cells. The reasons for this could be 2 fold. It could be due to the role of the fibroblasts secreting matrix into these scaffolds and turning the scaffold into a material that more closely mimics the body. It could also be due to the role of growth factor and cytokine secretion, from fibroblasts, into the wound bed. These factors have strong chemotactic properties for recruiting other cells such as platelets, other fibroblasts, keratinocytes, and immune cells. They are also

chemoinstructive, meaning that they have roles in regulating the various stages of the wound healing process. Finally, it is crucial to this research to assess the long term effects of these scaffolds when implanted. It would be beneficial to harvest tissues after longer time points in order to assess scar formation, dermal matrix construction, and epidermal stratification.

In summary, we have constructed microporous electrospun scaffolds that support rapid and effective skin tissue regeneration. These scaffolds also are a great in vitro model for examining cellular response to dermal matrices. Our results demonstrate that the base scaffold, collagen I and PCL, is a promising biodegradable biomaterial with favorable mechanical properties for skin regeneration applications. Ultimately, we believe this work reveals that we have not only engineered a scaffold that creates a favorable environment for skin cells in vitro, but we have also established that our porous electrospun matrices accelerate the wound healing process and simultaneously create skin tissue that appears to resemble unwounded skin tissue when implanted in vivo.

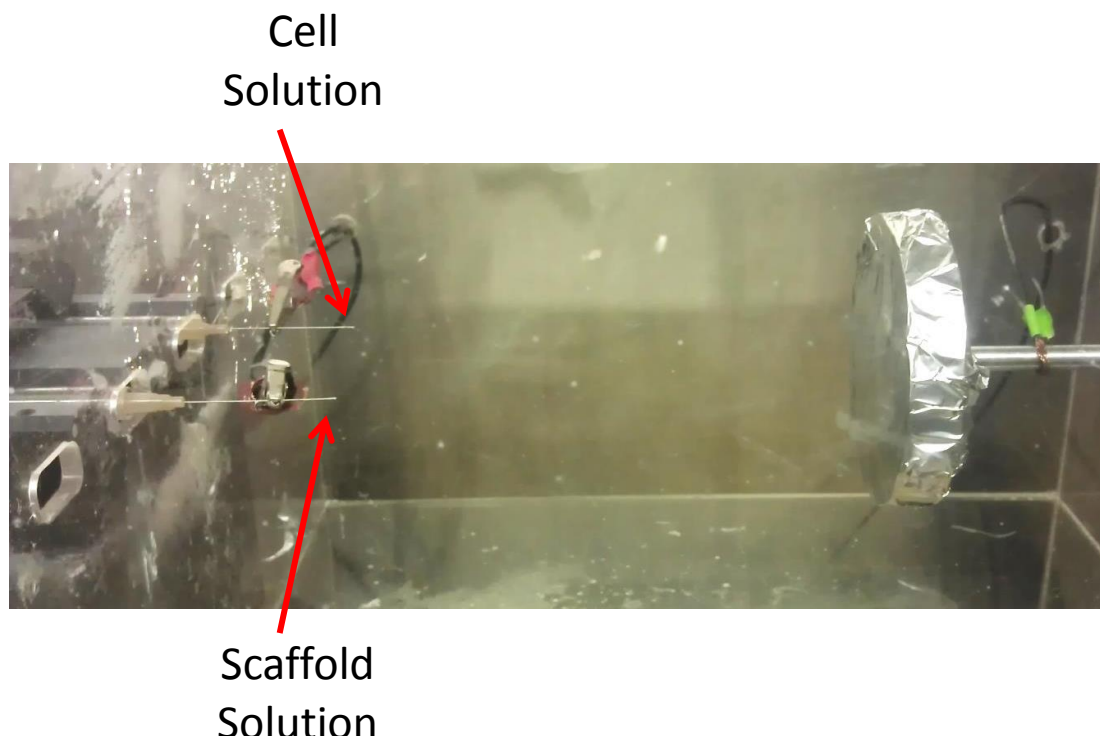


Fig 1. Electrospinning and electrospraying. In this method, 2 syringes were used. One syringe contained a solution of cells and the other contained a solution of scaffolding material.

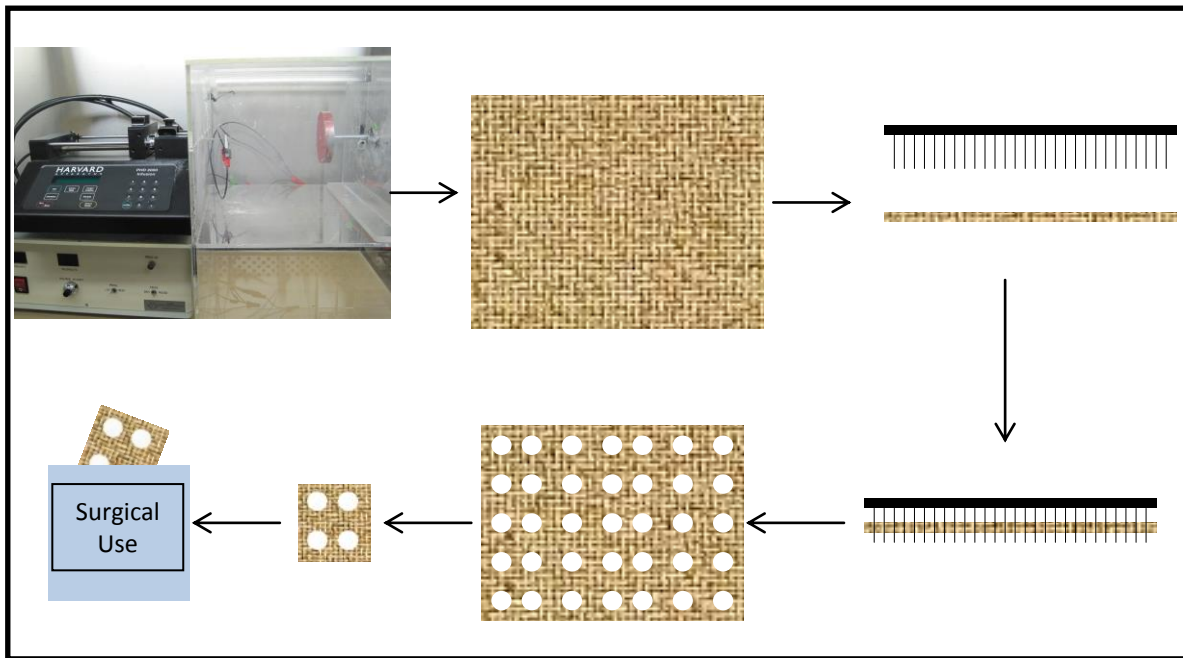


Fig 2. Mechanical press for creating large pores. A large press containing numerous evenly spaced microneedles can be used to create many pores throughout electrospun scaffolds. This process can be scaled up on a large scale for manufacturing purposes.

GENERAL LIST OF REFERENCES

1. Kirschner N, Houdek P, Fromm M, Moll I, Brandner JM. Tight junctions form a barrier in human epidermis. *European Journal of Cell Biology*; 89:839. 2010.
2. Kirschner N, Rosenthal R, Furuse M, Moll I, Fromm M, Brandner JM. Contribution of Tight Junction Proteins to Ion, Macromolecule, and Water Barrier in Keratinocytes. *J Invest Dermatol*; 133:1161. 2013.
3. Simpson CL, Patel DM, Green KJ. Deconstructing the skin: cytoarchitectural determinants of epidermal morphogenesis. *Nat Rev Mol Cell Biol*; 12:565. 2011.
4. Breitkreutz D, Koxholt I, Thiemann K, Nischt R. Skin basement membrane: the foundation of epidermal integrity--BM functions and diverse roles of bridging molecules nidogen and perlecan. *Biomed Res Int*; 2013:179784. 2013.
5. Schultz GS, Wysocki A. Interactions between extracellular matrix and growth factors in wound healing. *Wound Repair Regen*; 17:153. 2009.
6. Bissell MJ, Hall HG, Parry G. How does the extracellular matrix direct gene expression? *J Theor Biol*; 99:31. 1982.
7. Bornstein P. Cell-matrix interactions: the view from the outside. *Methods Cell Biol*; 69:7. 2002.
8. Santos M, Paramio JM, Bravo A, Ramirez A, Jorcano JL. The expression of keratin k10 in the basal layer of the epidermis inhibits cell proliferation and prevents skin tumorigenesis. *J Biol Chem*; 277:19122. 2002.
9. Blanpain C, Fuchs E. Epidermal homeostasis: a balancing act of stem cells in the skin. *Nat Rev Mol Cell Biol*; 10:207. 2009.
10. Kormos B, Belso N, Bebes A, Szabad G, Bacsa S, Szell M, Kemeny L, Bata-Csorgo Z. In vitro dedifferentiation of melanocytes from adult epidermis. *PLoS One*; 6:e17197. 2011.
11. Cichorek M, Wachulska M, Stasiewicz A, Tyminska A. Skin melanocytes: biology and development. *Postepy Dermatol Alergol*; 30:30. 2013.
12. Morrison KM, Miesegaes GR, Lumpkin EA, Maricich SM. Mammalian Merkel cells are descended from the epidermal lineage. *Developmental Biology*; 336:76. 2009.
13. Maricich SM, Wellnitz SA, Nelson AM, Lesniak DR, Gerling GJ, Lumpkin EA, Zoghbi HY. Merkel Cells Are Essential for Light-Touch Responses. *Science*; 324:1580. 2009.
14. Igyártó BZ, Kaplan DH. Antigen presentation by Langerhans cells. *Current Opinion in Immunology*; 25:115. 2013.

15. Merad M, Ginhoux F, Collin M. Origin, homeostasis and function of Langerhans cells and other langerin-expressing dendritic cells. *Nat Rev Immunol*; 8:935. 2008.
16. da Rocha-Azevedo B, Grinnell F. Fibroblast morphogenesis on 3D collagen matrices: the balance between cell clustering and cell migration. *Exp Cell Res*; 319:2440. 2013.
17. Bainbridge P. Wound healing and the role of fibroblasts. *J Wound Care*; 22:407. 2013.
18. Harrison CA, MacNeil S. The mechanism of skin graft contraction: An update on current research and potential future therapies. *Burns*; 34:153. 2008.
19. Javierre E, Moreo P, Doblaré M, García-Aznar JM. Numerical modeling of a mechano-chemical theory for wound contraction analysis. *International Journal of Solids and Structures*; 46:3597. 2009.
20. Jeon YK, Jang YH, Yoo DR, Kim SN, Lee SK, Nam MJ. Mesenchymal stem cells' interaction with skin: wound-healing effect on fibroblast cells and skin tissue. *Wound Repair Regen*; 18:655. 2010.
21. Maxson S, Lopez EA, Yoo D, Danilkovitch-Miagkova A, Leroux MA. Concise review: role of mesenchymal stem cells in wound repair. *Stem Cells Transl Med*; 1:142. 2012.
22. Mansilla E, Spretz R, Larsen G, Nunez L, Drago H, Sturla F, Marin GH, Roque G, Martire K, Diaz Aquino V, Bossi S, Gardiner C, Lamonega R, Lauzada N, Cordone J, Raimondi JC, Tau JM, Biasi NR, Marini JE, Patel AN, Ichim TE, Riordan N, Maceira A. Outstanding survival and regeneration process by the use of intelligent acellular dermal matrices and mesenchymal stem cells in a burn pig model. *Transplant Proc*; 42:4275. 2010.
23. Chen L, Tredget EE, Wu PY, Wu Y. Paracrine factors of mesenchymal stem cells recruit macrophages and endothelial lineage cells and enhance wound healing. *PLoS One*; 3:e1886. 2008.
24. Davies LC, Jenkins SJ, Allen JE, Taylor PR. Tissue-resident macrophages. *Nat Immunol*; 14:986. 2013.
25. Rodero MP, Khosrotehrani K. Skin wound healing modulation by macrophages. *Int J Clin Exp Pathol*; 3:643. 2010.
26. Khan R, Khan MH. Use of collagen as a biomaterial: An update. *J Indian Soc Periodontol*; 17:539. 2013.
27. Cheng W, Yan-Hua R, Fang-Gang N, Guo-An Z. The content and ratio of type I and III collagen in skin differ with age and injury. *African Journal of Biotechnology*; 10:2524. 2011.

28. Stoffels JM, Zhao C, Baron W. Fibronectin in tissue regeneration: timely disassembly of the scaffold is necessary to complete the build. *Cell Mol Life Sci*; 70:4243. 2013.
29. Almine JF, Wise SG, Weiss AS. Elastin signaling in wound repair. *Birth Defects Res C Embryo Today*; 96:248. 2012.
30. Pasquali-Ronchetti I, Baccarani-Contri M. Elastic fiber during development and aging. *Microsc Res Tech*; 38:428. 1997.
31. Ruoslahti E. RGD and other recognition sequences for integrins. *Annu Rev Cell Dev Biol*; 12:697. 1996.
32. Schwartz I, Seger D, Shaltiel S. Vitronectin. *Int J Biochem Cell Biol*; 31:539. 1999.
33. Durbeej M. Laminins. *Cell Tissue Res*; 339:259. 2010.
34. Jiang D, Liang J, Noble PW. Hyaluronan in tissue injury and repair. *Annu Rev Cell Dev Biol*; 23:435. 2007.
35. Voigt J, Driver VR. Hyaluronic acid derivatives and their healing effect on burns, epithelial surgical wounds, and chronic wounds: a systematic review and meta-analysis of randomized controlled trials. *Wound Repair Regen*; 20:317. 2012.
36. Nyman E, Huss F, Nyman T, Junker J, Kratz G. Hyaluronic acid, an important factor in the wound healing properties of amniotic fluid: in vitro studies of re-epithelialisation in human skin wounds. *J Plast Surg Hand Surg*; 47:89. 2013.
37. Werner S, Krieg T, Smola H. Keratinocyte-fibroblast interactions in wound healing. *J Invest Dermatol*; 127:998. 2007.
38. Ghahary A, Ghaffari A. Role of keratinocyte-fibroblast cross-talk in development of hypertrophic scar. *Wound Repair Regen*; 15 Suppl 1:S46. 2007.
39. Menon SN, Flegg JA, McCue SW, Schugart RC, Dawson RA, McElwain DL. Modelling the interaction of keratinocytes and fibroblasts during normal and abnormal wound healing processes. *Proc Biol Sci*; 279:3329. 2012.
40. Andreadis ST, Hamoen KE, Yarmush ML, Morgan JR. Keratinocyte growth factor induces hyperproliferation and delays differentiation in a skin equivalent model system. *FASEB J*; 15:898. 2001.
41. Wong VW, Gurtner GC, Longaker MT. Wound healing: a paradigm for regeneration. *Mayo Clin Proc*; 88:1022. 2013.
42. Stadelmann WK, Digenis AG, Tobin GR. Physiology and healing dynamics of chronic cutaneous wounds. *Am J Surg*; 176:26S. 1998.

43. Romer J, Lund LR, Eriksen J, Pyke C, Kristensen P, Dano K. The receptor for urokinase-type plasminogen activator is expressed by keratinocytes at the leading edge during re-epithelialization of mouse skin wounds. *J Invest Dermatol*; 102:519. 1994.
44. Peacock EE, Jr. Healing and control of healing--introduction. *World J Surg*; 4:269. 1980.
45. Singer AJ, Clark RA. Cutaneous wound healing. *N Engl J Med*; 341:738. 1999.
46. Peck MD. Epidemiology of burns throughout the world. Part I: Distribution and risk factors. *Burns*; 37:1087. 2011.
47. Machens HG, Berger AC, Mailaender P. Bioartificial skin. *Cells Tissues Organs*; 167:88. 2000.
48. O'Loughlin A, McIntosh C, Dinneen SF, O'Brien T. Review paper: basic concepts to novel therapies: a review of the diabetic foot. *Int J Low Extrem Wounds*; 9:90. 2010.
49. Orgill DP, Ogawa R. Current methods of burn reconstruction. *Plast Reconstr Surg*; 131:827e. 2013.
50. Wainwright DJ, Bury SB. Acellular dermal matrix in the management of the burn patient. *Aesthet Surg J*; 31:13S. 2011.
51. Juhasz I, Kiss B, Lukacs L, Erdei I, Peter Z, Remenyik E. Long-term followup of dermal substitution with acellular dermal implant in burns and postburn scar corrections. *Dermatol Res Pract*; 2010:210150. 2010.
52. Yim H, Cho YS, Seo CH, Lee BC, Ko JH, Kim D, Hur J, Chun W, Kim JH. The use of AlloDerm on major burn patients: AlloDerm prevents post-burn joint contracture. *Burns*; 36:322. 2010.
53. Marston WA. Dermagraft, a bioengineered human dermal equivalent for the treatment of chronic nonhealing diabetic foot ulcer. *Expert Rev Med Devices*; 1:21. 2004.
54. Gonzalez Alana I, Torrero Lopez JV, Martin Playa P, Gabilondo Zubizarreta FJ. Combined use of negative pressure wound therapy and Integra(R) to treat complex defects in lower extremities after burns. *Ann Burns Fire Disasters*; 26:90. 2013.
55. Zaulyanov L, Kirsner RS. A review of a bi-layered living cell treatment (Apligraf) in the treatment of venous leg ulcers and diabetic foot ulcers. *Clin Interv Aging*; 2:93. 2007.
56. Rennert RC, Sorkin M, Garg RK, Januszyk M, Gurtner GC. Cellular response to a novel fetal acellular collagen matrix: implications for tissue regeneration. *Int J Biomater*; 2013:527957. 2013.

57. Hayn E. Successful treatment of complex traumatic and surgical wounds with a foetal bovine dermal matrix. *Int Wound J*. 2013.
58. Supp DM, Boyce ST. Engineered skin substitutes: practices and potentials. *Clin Dermatol*; 23:403. 2005.
59. Pereira RF, Barrias CC, Granja PL, Bartolo PJ. Advanced biofabrication strategies for skin regeneration and repair. *Nanomedicine (Lond)*; 8:603. 2013.
60. You C, Wang X, Zheng Y, Han C. Three types of dermal grafts in rats: the importance of mechanical property and structural design. *Biomed Eng Online*; 12:125. 2013.
61. Harrison CA, MacNeil S. The mechanism of skin graft contraction: an update on current research and potential future therapies. *Burns*; 34:153. 2008.
62. Rehim SA, Singhal M, Chung KC. Dermal Skin Substitutes for Upper Limb Reconstruction: Current Status, Indications, and Contraindications. *Hand Clin*; 30:239. 2014.
63. Yildirimer L, Thanh NTK, Seifalian AM. Skin regeneration scaffolds: a multimodal bottom-up approach. *Trends in Biotechnology*; 30:638. 2012.
64. Wang X, Liu S, Zhao Q, Li N, Zhang H, Zhang X, Lei X, Zhao H, Deng Z, Qiao J, Cao Y, Ning L, Liu S, Duan E. Three-dimensional hydrogel scaffolds facilitate in vitro self-renewal of human skin-derived precursors. *Acta Biomater*. 2014.
65. Dumville JC, O'Meara S, Deshpande S, Speak K. Hydrogel dressings for healing diabetic foot ulcers. *Cochrane Database Syst Rev*; 7:CD009101. 2013.
66. Zhou M, Ulijn RV, Gough JE. Extracellular matrix formation in self-assembled minimalistic bioactive hydrogels based on aromatic peptide amphiphiles. *J Tissue Eng*; 5:2041731414531593. 2014.
67. Jayarama Reddy V, Radhakrishnan S, Ravichandran R, Mukherjee S, Balamurugan R, Sundarajan S, Ramakrishna S. Nanofibrous structured biomimetic strategies for skin tissue regeneration. *Wound Repair and Regeneration*; 21:1. 2013.
68. Han CM, Zhang LP, Sun JZ, Shi HF, Zhou J, Gao CY. Application of collagen-chitosan/fibrin glue asymmetric scaffolds in skin tissue engineering. *J Zhejiang Univ Sci B*; 11:524. 2010.
69. Lee V, Singh G, Trasatti JP, Bjornsson C, Xu X, Tran TN, Yoo SS, Dai G, Karande P. Design and fabrication of human skin by three-dimensional bioprinting. *Tissue Eng Part C Methods*; 20:473. 2014.

70. Naseri N, Algan C, Jacobs V, John M, Oksman K, Mathew AP. Electrospun chitosan-based nanocomposite mats reinforced with chitin nanocrystals for wound dressing. *Carbohydr Polym*; 109:7. 2014.
71. Lai HJ, Kuan CH, Wu HC, Tsai JC, Chen TM, Hsieh DJ, Wang TW. Tailor Design Electrospun Composite Nanofibers with Staged Release of Multiple Angiogenic Growth Factors for Chronic Wound Healing. *Acta Biomater*. 2014.
72. Ingavle GC, Leach JK. Advancements in Electrospinning of Polymeric Nanofibrous Scaffolds for Tissue Engineering. *Tissue Eng Part B Rev*. 2013.
73. Bhardwaj N, Kundu SC. Electrospinning: a fascinating fiber fabrication technique. *Biotechnol Adv*; 28:325. 2010.
74. Liu W, Thomopoulos S, Xia Y. Electrospun nanofibers for regenerative medicine. *Adv Healthc Mater*; 1:10. 2012.
75. Vasita R, Katti DS. Nanofibers and their applications in tissue engineering. *Int J Nanomedicine*; 1:15. 2006.
76. Phipps MC, Clem WC, Grunda JM, Clines GA, Bellis SL. Increasing the pore sizes of bone-mimetic electrospun scaffolds comprised of polycaprolactone, collagen I and hydroxyapatite to enhance cell infiltration. *Biomaterials*; 33:524. 2012.
77. Rnjak-Kovacina J, Weiss AS. Increasing the pore size of electrospun scaffolds. *Tissue Eng Part B Rev*; 17:365. 2011.
78. Zhu X, Cui W, Li X, Jin Y. Electrospun fibrous mats with high porosity as potential scaffolds for skin tissue engineering. *Biomacromolecules*; 9:1795. 2008.
79. Blakeney BA, Tambralli A, Anderson JM, Andukuri A, Lim DJ, Dean DR, Jun HW. Cell infiltration and growth in a low density, uncompressed three-dimensional electrospun nanofibrous scaffold. *Biomaterials*; 32:1583. 2011.
80. Pezeshki-Modaress M, Rajabi-Zeleti S, Zandi M, Mirzadeh H, Sodeifi N, Nekookar A, Aghdami N. Cell-loaded gelatin/chitosan scaffolds fabricated by salt-leaching/lyophilization for skin tissue engineering: In vitro and in vivo study. *J Biomed Mater Res A*. 2013.
81. Deepa R, Paul W, Anilkumar TV, Sharma CP. Differential Healing of Full Thickness Rabbit Skin Wound by Fibroblast Loaded Chitosan Sponge. *Journal of Biomaterials and Tissue Engineering*; 3:261. 2013.
82. Zeinali R, Biazar E, Keshel SH, Tavirani MR, Asadipour K. Regeneration of full-thickness skin defects using umbilical cord blood stem cells loaded into modified porous scaffolds. *ASAIO J*; 60:106. 2014.

83. Biazar E, Keshel SH. The healing effect of stem cells loaded in nanofibrous scaffolds on full thickness skin defects. *J Biomed Nanotechnol*; 9:1471. 2013.
84. Revi D, Paul W, Tv A, Sharma CP. Chitosan Scaffold Co cultured with Keratinocyte and Fibroblast Heals Full Thickness Skin Wounds in Rabbit. *J Biomed Mater Res A*. 2013.
85. Velnar T, Bailey T, Smrkolj V. The wound healing process: an overview of the cellular and molecular mechanisms. *J Int Med Res*; 37:1528. 2009.
86. Suh EJ, Remillard MY, Legesse-Miller A, Johnson EL, Lemons JM, Chapman TR, Forman JJ, Kojima M, Silberman ES, Collier HA. A microRNA network regulates proliferative timing and extracellular matrix synthesis during cellular quiescence in fibroblasts. *Genome Biol*; 13:R121. 2012.
87. Cen L, Liu W, Cui L, Zhang W, Cao Y. Collagen Tissue Engineering: Development of Novel Biomaterials and Applications. *Pediatr Res*; 63:492. 2008.
88. Montfrans CV, Stok M, Geerkens M. Biology of chronic wounds and new treatment strategies. *Phlebology*; 29:165. 2014.
89. Hanpanich BS. Tissue engineering of skin and soft tissue augmentation, medical view. *J Med Assoc Thai*; 93 Suppl 7:S332. 2010.
90. Zhong S, Zhang Y, Lim CT. Fabrication of large pores in electrospun nanofibrous scaffolds for cellular infiltration: a review. *Tissue Eng Part B Rev*; 18:77. 2012.
91. Martins A, Araujo JV, Reis RL, Neves NM. Electrospun nanostructured scaffolds for tissue engineering applications. *Nanomedicine (Lond)*; 2:929. 2007.
92. Abercrombie M. Fibroblasts. *J Clin Pathol Suppl (R Coll Pathol)*; 12:1. 1978.
93. Zak M, Kuropka P, Kobielarz M, Dudek A, Kaleta-Kuratewicz K, Szotek S. Determination of the mechanical properties of the skin of pig fetuses with respect to its structure. *Acta Bioeng Biomech*; 13:37. 2011.
94. Franco RA, Nguyen TH, Lee BT. Preparation and characterization of electrospun PCL/PLGA membranes and chitosan/gelatin hydrogels for skin bioengineering applications. *J Mater Sci Mater Med*; 22:2207. 2011.
95. Wang X, You C, Hu X, Zheng Y, Li Q, Feng Z, Sun H, Gao C, Han C. The roles of knitted mesh-reinforced collagen-chitosan hybrid scaffold in the one-step repair of full-thickness skin defects in rats. *Acta Biomater*; 9:7822. 2013.
96. Widgerow AD. Bioengineered matrices--part 1: attaining structural success in biologic skin substitutes. *Ann Plast Surg*; 68:568. 2012.

97. O'Donnell TF, Jr., Lau J. A systematic review of randomized controlled trials of wound dressings for chronic venous ulcer. *J Vasc Surg*; 44:1118. 2006.
98. Papanas N, Eleftheriadou I, Tentolouris N, Maltezos E. Advances in the topical treatment of diabetic foot ulcers. *Curr Diabetes Rev*; 8:209. 2012.
99. Li L, Qian Y, Jiang C, Lv Y, Liu W, Zhong L, Cai K, Li S, Yang L. The use of hyaluronan to regulate protein adsorption and cell infiltration in nanofibrous scaffolds. *Biomaterials*; 33:3428. 2012.
100. Rnjak-Kovacina J, Wise SG, Li Z, Maitz PK, Young CJ, Wang Y, Weiss AS. Electrospun synthetic human elastin:collagen composite scaffolds for dermal tissue engineering. *Acta Biomater*; 8:3714. 2012.

APPENDIX A
IACUC APPROVAL



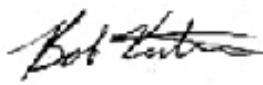
THE UNIVERSITY OF ALABAMA AT BIRMINGHAM

Institutional Animal Care and Use Committee (IACUC)

NOTICE OF APPROVAL

DATE: September 3, 2013

TO: SUSAN L BELLIS, M.D.
MCLM-982A
(205) 934-3441

FROM: 
Robert A. Kesterson, Ph.D., Chair
Institutional Animal Care and Use Committee (IACUC)

SUBJECT: Title: UAB Skin Disease Research Center: Fibroblast-Embedded Electrospun Matrices for Skin Regeneration
Sponsor: National Institute of Arthritis & Musculoskeletal & Skin Diseases/NIH/DHHS
Animal Project_Number: 130909448

As of September 3, 2013 the animal use proposed in the above referenced application is approved. The University of Alabama at Birmingham Institutional Animal Care and Use Committee (IACUC) approves the use of the following species and number of animals:

Species	Use Category	Number In Category
Rats	A	20
Rats	B	70

Animal use must be renewed by August 31, 2014. Approval from the IACUC must be obtained before implementing any changes or modifications in the approved animal use.

Please keep this record for your files, and forward the attached letter to the appropriate granting agency.

Refer to Animal Protocol Number (APN) 130909448 when ordering animals or in any correspondence with the IACUC or Animal Resources Program (ARP) offices regarding this study. If you have concerns or questions regarding this notice, please call the IACUC office at (205) 934-7692.

Institutional Animal Care and Use Committee (IACUC)	Mailing Address:
CH19 Suite 403	CH19 Suite 403
933 19th Street South	1530 3rd Ave S
(205) 934-7692	Birmingham, AL 35294-0019
FAX (205) 934-1188	



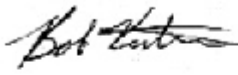
THE UNIVERSITY OF ALABAMA AT BIRMINGHAM

Institutional Animal Care and Use Committee (IACUC)

NOTICE OF APPROVAL

DATE: September 3, 2013

TO: SUSAN L BELLIS, M.D.
MCLM-982A
(205) 934-3441

FROM: 
Robert A. Kesterson, Ph.D., Chair
Institutional Animal Care and Use Committee (IACUC)

SUBJECT: Title: UAB Skin Disease Research Center: Fibroblast-Embedded Electrospun Matrices
for Skin Regeneration
Sponsor: National Institute of Arthritis & Musculoskeletal & Skin Diseases/NIH/DHHS
Animal Project_Number: 130909448

As of September 3, 2013 the animal use proposed in the above referenced application is approved. The University of Alabama at Birmingham Institutional Animal Care and Use Committee (IACUC) approves the use of the following species and number of animals:

Species	Use Category	Number In Category
Rats	A	20
Rats	B	70

Animal use must be renewed by August 31, 2014. Approval from the IACUC must be obtained before implementing any changes or modifications in the approved animal use.

Please keep this record for your files, and forward the attached letter to the appropriate granting agency.

Refer to Animal Protocol Number (APN) 130909448 when ordering animals or in any correspondence with the IACUC or Animal Resources Program (ARP) offices regarding this study. If you have concerns or questions regarding this notice, please call the IACUC office at (205) 934-7692.

Institutional Animal Care and Use Committee (IACUC)
CH19 Suite 403
933 19th Street South
(205) 934-7692
FAX (205) 934-1188

Mailing Address:
CH19 Suite 403
1530 3rd Ave S
Birmingham, AL 35294-0019